

# **A Digital Tool to Analyze and Visualize the Damage of Structures under Compound Flood Hazards**

Tingwei Du

**MSc Thesis in Building Technology**

**Building Technology Graduation Studio**

MSc Architecture, Urbanism & Building Sciences

Title:

**A Digital Tool to Analyse and Visualize the Damage of Structures  
under Compound Flood Hazards**

Author:

**Tingwei Du**

5808138

June 24, 2024

Mentors:

**Simona Bianchi** Structural Design & Mechanics, TU Delft

**Azarakhsh Rafiee** Computational Design & Digital twin, TU Delft

## Acknowledgements

Looking back on my two years of study in Delft, it was filled with challenges and unexpected surprises, which I loved. These experiences have made me realize how fortunate I am to be driven by curiosity. I am immensely grateful for the active support of the AE+T Academy and the daily academic conferences, which kept me immersed in the exploration of new worlds and continuously motivated me to acquire new knowledge over the past two years.

Additionally, the differences between Dutch and Chinese education styles have taught me the importance of education in shaping one's perspective. It's not about good or bad but about being able to objectively assess your strengths and weaknesses, and to store up the energy to make changes. One day, you can look back and see how far you have come from where you started.

The most fortunate aspect of my journey was meeting my favorite teacher, Simona Bianchi, who served as a mentor for Bishop. She not only provided practical academic solutions but also taught me the mindset needed to face problems and demonstrated the working conditions of a good researcher. I am also deeply thankful to my GIS supervisor, Azarakhsh Rafiee, for his patience and concern when I encountered difficulties, for supporting me, and helping me think of solutions during my most challenging moments, as well as providing concrete references and models.

I would like to extend my gratitude to my classmates for their encouragement during group meetings, the exchange of ideas, and the inspiration they provided. There are many more people I would like to thank, but finally, I would like to express my deepest gratitude to my family, friends, Shi Su, and myself, for their support, which has allowed me to keep moving forward.

# Abstract

In response to global climate change and the increasing frequency of extreme natural hazards, an early intervention flood risk assessment methodology has been developed to assess damage at the building component level. This approach allows for the precise identification of vulnerable structural components and localized redesigns, leading to more cost-effective and safer structural solutions. The focus of this paper is on quantifying flood damage to components and visualizing the results, with two main objectives: 1) quantifying the damage and 2) interactive visualization.

Hydrodynamic simulations of compound floods under future climate scenarios are performed to apply the quantitative results at the micro level. Using future climate scenarios obtained by perturbing atmospheric data with a regional climate model, the top 24 hours of flood-driven data are selected to create inundation maps. Vulnerability curves for each material are plotted, taking into account the sensitivity of the component materials to water. Based on the water depth at each point, the failure probability is determined. This method of quantifying component vulnerability provides new insights into micro-level flood damage.

Finally, an integrated BIM-GIS model is constructed, and the damage level and distribution are displayed on the ArcGIS Pro platform. This allows different stakeholders to intuitively obtain damage level information. Users can customize their view, for example, by focusing solely on the damage to first-floor exterior windows or by examining the damage levels of components and buildings under different intensity flood ratings.

Key words –

[Climate change, Compound flood, Flood damage assessment, Hydrodynamic simulation, BIM – GIS integration, 3D visualization]

# Contents

1	Introduction .....	7
1.1	Background.....	7
1.2	Problem statement.....	7
1.3	Scope .....	7
1.1.1	Research question and sub-questions .....	7
1.1.2	Objectives.....	8
1.1.3	Boundary conditions .....	8
1.4	Research methodology.....	9
2	Theoretical background .....	11
2.1	Climate challenge .....	11
2.2	Compound flood(CF) risk.....	13
2.3	Microscale analysis.....	13
3	Literature review.....	14
3.1	Flood analysis and simulation .....	14
3.1.1	Weather scenarios .....	14
3.1.2	Compound flood .....	17
3.1.3	Flood assessment model.....	18
3.2	Damage assessment .....	25
3.2.1	Flood action on buildings .....	26
3.2.2	Damage assessment methods .....	27
3.2.3	Components fragility analysis .....	28
3.2.4	Loss analysis approach.....	33
3.3	Digitalization.....	35
3.3.1	Three methods of BIM-GIS integration.....	35

3.3.2	Methodology of computational analysis .....	38
3.3.3	Interactive map attempts .....	42
4	Case study .....	44
4.1	Methodology and workflow .....	45
4.2	Data preparation .....	46
4.3	Flood simulation .....	52
4.4	Damage assessment .....	58
4.4.1	Fragile curves .....	58
4.4.2	Damage classification.....	58
4.4.3	Overall damage cost.....	59
4.5	3D Visualization .....	60
4.5.1	Building an "integrated model" .....	60
4.5.2	Spatial join.....	61
4.5.3	Colour coded .....	63
4.5.4	Display modes .....	64
4.6	Result and discussion .....	64
5	Conclusion.....	70
5.1	Response to the questions .....	70
5.2	Recommendation for future work .....	71
6	Reflection .....	72
7	Bibliography .....	80
8	Appendix .....	85

# 1 Introduction

## 1.1 Background

At present, when dealing with compound flood disasters, the neglect of the joint effect between multiple hazards often leads to an underestimation of the flood hazard level, which in turn leads to an overestimation of the resilience of the building, and how to accurately predict the resilience of the building's full life cycle is an important means of assisting in the decision-making of the building or its operation and maintenance.

Flood Damage Analysis (FDA) has evolved assessment methods across different spatial scales—macro, meso, and micro. Many studies have utilized flood hazard curves (inundation depth-frequency) linked with building attributes (height, material, age, etc.). While effective for assessing urban or community-scale scenarios, this method lacks the capability to simulate water flow around and within buildings, neglecting the influence of flood velocity and duration on building resilience. Consequently, the unique resilience of each building to flooding remains unaccounted for. Furthermore, the absence of detailed structural information and building location specifics impedes direct application of study results to design, necessitating further analysis for design decisions. These intricacies are crucial in identifying building-specific risk sources.

## 1.2 Problem statement

### **Main problem**

In the Netherlands, the problem of quantifying damage to building structures caused by climate change-induced compound flooding remains unresolved, and it is not possible to visually locate the location of damaged structures and the extent of damage.

### **Sub-problems**

- In a compound flood scenario, these three contributing factors may be affected by the same weather system, causing them to converge in physical space and exacerbating the resulting impacts.
- It is difficult to transfer information directly between Building Information Modeling (BIM) and Geographic Information Systems (GIS), so data must be exchanged using an intermediate format or language.
- Currently, most freely available hydrodynamic models are not open source and the results generated need to be imported into other software for further data analysis.

## 1.3 Scope

### 1.1.1 Research question and sub-questions

#### **Main research question**

How We Built a BIM-GIS Based Viewer to Quantify the Risk of Structures components When Facing Compound Flooding Scenarios?

#### **Sub-questions**

1. How to assess multi-hazards risk for compound flooding in quantitative manner in urban scale, to consider of hazard inter-dependency?
2. How to construct a hydrodynamic model to simulate urban flooding during compound flood outbreaks?
3. What intensity indexes and performance indicators should be used to analyse failure behaviour of structure.
4. How to integrate simulation models in a viewer for their efficient performance on building structures, to interactively display the hazard index of each component?

### 1.1.2 Objectives

#### General objective

A digital assistant tool for structural flood-resistant assessment in the Netherlands' coastal areas.

#### Sub-objectives

- To define the classification of compound disasters and methods for analyzing interactive correlations.
- To define the data types and transmission media for storing BIM and GIS data.
- To establish a comprehensive framework to facilitate effective interaction between the BIM and GIS model into a viewer to visualize the damage state.

#### Final products

A lightweight visualization tool is developed to access the damage of structure component, featuring:

- Camera movement at different object zoom levels, and
- Color-coded building components with different damage costs
- Clicking to select specific components for querying related detailed information.

This allows stakeholders to visually inspect affected components, assisting in decision-making.

### 1.1.3 Boundary conditions

1. The primary emphasis of this study is to evaluate damage at the micro level, where vulnerability pertains to the strength of structural elements and exposure concerns the area susceptible to water contact and sensitivity. However, it's important to note that this study does not assess property, residents, or infrastructure. For further insights into infrastructure and societal calculation methodology, references can be found in (Kelman, 2002) and (Ge et al., 2013).
2. To avoid excessive computational costs caused by too large a volume of data, a stochastic model rather than a physical model was used when analyzing the frequency of flood disasters caused by initiating factors. Therefore, hydraulic conditions such as underground seepage and pipe networks are not considered to ensure the fast operation of the model.
3. In analysing the effects of flooding on building structures, only the effects of flooding on the skin of the building were considered. Scenarios about wall infiltration and water ingress into openings are beyond the scope of this paper.
4. As for damage analysis, only a probabilistic perspective on the overall structural vulnerability was provided. Due to the limitation of level of detail needed, the nature of uncertainties involved, and the

lack of computational resources, finite element analysis of the building structure was not performed to obtain more specific vulnerability results.

## 1.4 Research methodology

Since its introduction in 2014, the significance of coastal complex flooding for sustainable development has gained widespread recognition. The field has experienced significant growth, with a 9.4-fold increase in literature from 2014 to 2022, totaling 364 articles.(Sun et al., 2024) This surge underscores the extensive scope of research dedicated to compound flooding. Figure 1 illustrates the methodological framework of this paper, detailing the problem formulation, vision, research, application, and conclusion.

The literature for the research component of this paper is primarily sourced from Web of Science, Scopus, ResearchGate, Google Scholar, and Elsevier. The research is structured around the following sections:

1. **Compound Flood:** Examines the mechanics of its generation, the triggering factors, the interactions between these factors, and their impact on buildings.
2. **Weather System:** Classifies scenarios under climate change, predicts resulting weather data, and identifies sources of weather data.
3. **Flood Simulation Model:** Compares flood modeling models, and evaluates the amenity and applicability of common simulation software.
4. **Vulnerability Study:** Conducts uncertainty analysis in numerical models, explores vulnerability analysis methods, and establishes damage level classification standards.
5. **BIM-GIS Integrated System:** Focuses on data collection, BIM-GIS interoperability, and data utilization and analysis methods.
6. **3D Visualization:** Provides an overview of digital technology, geoscientific modeling, and a comparative analysis of 3D modeling software.

These six areas can be grouped into three subsections:

1. **Flood Analysis and Simulation** (1, 2, 3)
2. **Damage Assessment** (4)
3. **Visualization** (5, 6)

In each subsection, the existing literature is summarized and compared, and theoretical solutions applicable to this project are presented. This structured approach ensures a comprehensive understanding of complex flooding and its implications, facilitating the development of effective and sustainable solutions. (Fig. 1)

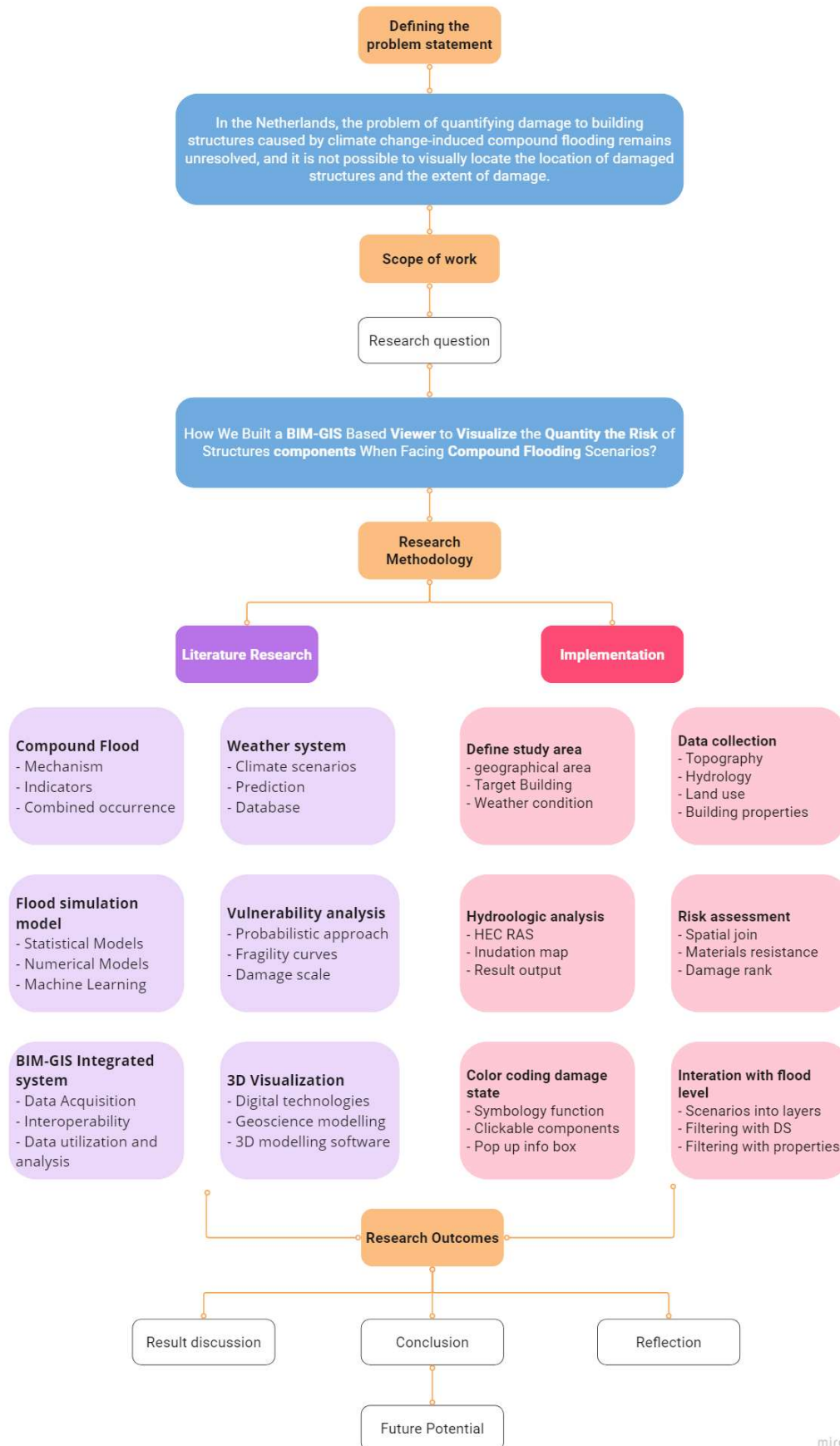


Figure 1: Research methodology diagram

## 2 Theoretical background

### 2.1 Climate challenge

A significant portion of the global population resides in low-lying coastal regions, where population density, infrastructure, and economic activity are concentrated, rendering them highly susceptible to flooding (Vousdoukas et al., 2018). Sea level rise (SLR) in the coming years, attributed to factors such as thermal expansion and the melting of continental glaciers and polar ice caps, will elevate both mean and extreme sea levels, thereby escalating the risk of compound flood events (Bevacqua et al., 2019). This phenomenon, driven by various meteorological processes, is anticipated to amplify future compound flood hazards. While studies have demonstrated this trend along the European coast, comprehensive data for most of the world's low-lying coastal areas are currently unavailable (Bevacqua et al., 2019). Climate change projections indicate an increase in meteorological events that drive compound coastal flooding (Fig. 2). Exceptionally, the projected population growth in coastal areas makes an integrated assessment of the meteorological drivers affecting compound floods and their response to climate change imminent.

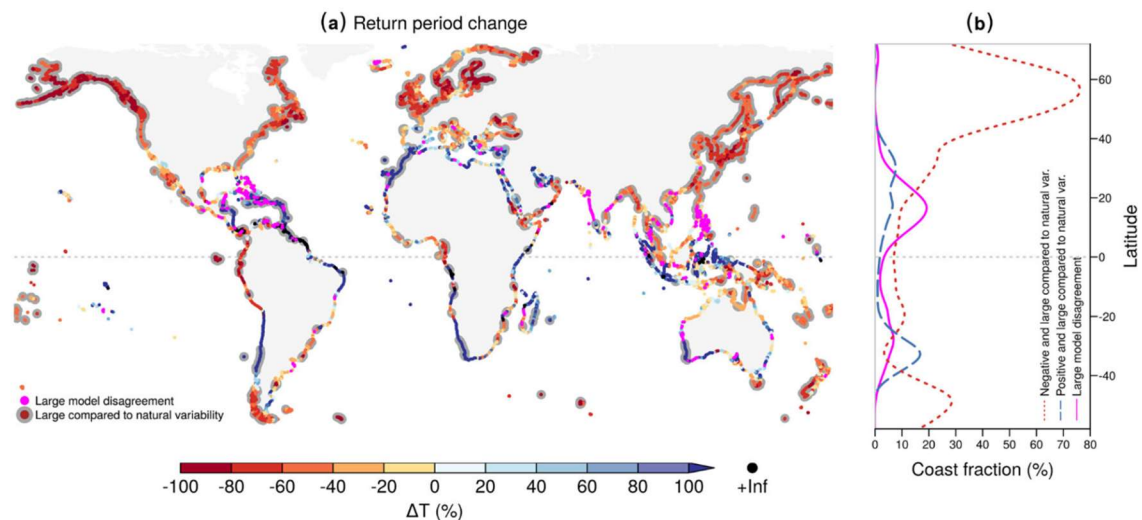
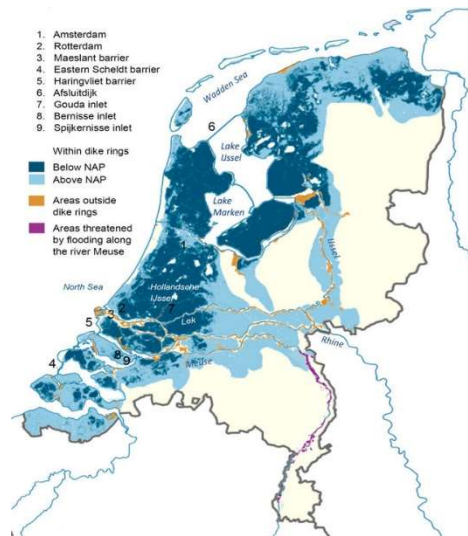


Figure 2: Future changes in the return periods of concurrent meteorological drivers of compound flood. (Bevacqua et al., 2019)

According to the latest projections of the Royal Netherlands Meteorological Office (van den Hurk et al., 2016), the upper limit of sea level rise in 2100 is 100 cm. The urban area of the flood-prone areas of the Dutch delta increased approximately sixfold during the 20th century, and by 2100 the urban area of the flood-prone areas will increase further to 125%, with a potential depth of inundation typically exceeding 2.5 m. The flood-prone areas of the Dutch delta will increase by a factor of 2.5 m, with a potential depth of inundation typically exceeding 2.5 m. More meteorological events that drive compound coastal flooding are projected under climate change. (Fig. 3)



**Figure 3:** Map of the Netherlands showing flood prone zones (blue shadings) and features of the water management system (adapted from PBL61). N.A.P. is the Amsterdam Ordnance Level which is the reference plane for sea level height in the Netherlands.(van den Hurk et al., 2016)

In the context of future climate warming, the probability of compound coastal floods (CF) is expected to increase significantly, particularly in specific regions such as the west coast of the United Kingdom, northern France, the eastern and southern coasts of the North Sea, and the eastern part of the Black Sea (see Figure 3A). By the end of the 21st century, the proportion of coastline with a return period of less than 6 years is expected to rise from the current 3% to 11%. Hotspot areas where the return period will be below this value include the Bristol Channel, the coasts of Devon and Cornwall in the United Kingdom, and the North Sea coasts of the Netherlands and Germany (see Figure 4B).(Bevacqua et al., 2019)

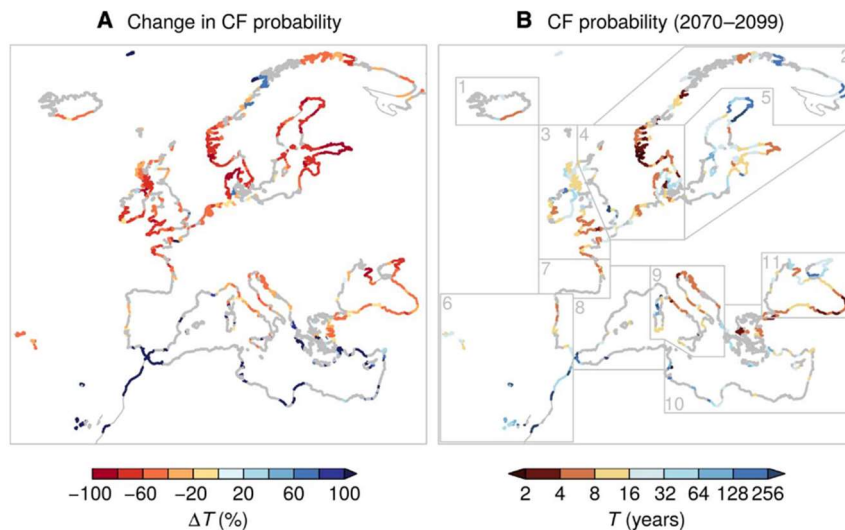


**Figure 4:** Future probability of potential compound flooding (CF). (A) Multimodel mean of projected change (%) of CF return periods, between future (2070–2099) and present (1970–2004) climate. (B) Return periods for the future (2070–2099). Gray points indicate locations where only four or fewer of six models agree on the sign of the return period change (three or less of five models in the Black Sea). Areas of gray points in (A) and (B) are slightly different, as the former are computed taking into account the past period (1970–2004) and the latter the period (1980–2004) (see delta change approach in Materials and Methods). (Bevacqua et al., 2019)

## 2.2 Compound flood(CF) risk

Complex flooding is usually a multi-hazard issue, characterized by the convergence of various hazard drivers, including heavy rainfall, river discharge, and storm surges. Compound floods can arise from the simultaneous presence of three indicators, none of which are extreme individually but combine to amplify the risk. Focusing solely on the likelihood of extreme scenarios for one factor is likely to underestimate the flood risk.(Eilander et al., 2020; Santiago-Collazo et al., 2019) Moreover, these hazards may stem from the same weather system, making them statistically interdependent, physically superimposed, and concentrated in the same geographical area, like large waves coupled with elevated sea levels leading to coastal flooding, or increased river flow coinciding with high sea levels resulting in river flooding. To accurately assess the probability of flooding, it's essential to understand not just the high and extreme values of each variable, but also the likelihood of their simultaneous occurrence. When the compounding occurrence is eliminated for inland water levels below the warning level of +7 cm NAP, there's a potential reduction in the probability of reaching the specified inland water level by up to a factor of 2. (Couasnon et al., 2020)

Correlations between coastal zones and flood drivers have been found globally. For example, the dependence of storm surges and precipitation has been found in the cases of Australia and the United States (Hatzikyriakou & Lin, 2018)A correlation between storm surge and flow was demonstrated in the Netherlands(Klerk et al., 2015; Leal et al., 2021; Ridder et al., 2018; van den Hurk et al., 2015), Italy (Taramelli et al., 2022), and the United Kingdom (Amirebrahimi et al., 2015; Hawkes, 2008). Watershed studies have also shown that ignoring the dependence between the three underestimates the return period of floods.

## 2.3 Microscale analysis

Flood damage analysis (FDA) is typically developed for three main scales of analysis; macro (Fig. 5A), meso (Fig. 5B), and micro (Fig. 5C) (Apel et al., 2008). The internationally recognized standard approach for Flood Damage Assessment (FDA) involves the utilization of "damage curves." (Merz et al., 2010)

The first two method (macro, meso) evaluates damage by categorizing buildings based on properties such as type, age, height, and building material, alongside flood characteristic curves encompassing inundation depth, duration, water flow velocity, return period, and weighting factors. Building damage ratings across various time dimensions are then derived. The efficacy of this approach has been validated in extensive applications covering a significant number of buildings.(Merz et al., 2010) However, this kind of method target broad-scale applications, offering less detailed outputs without assessing damage to individual buildings. In contrast, micro analysis focuses on smaller spatial areas and adopts an object-oriented approach to evaluate damage to individual buildings or small groups of buildings. This analytical technique can provide further information on the details and position of damage at the building level. These details are particularly important in the early stages of design to determine the structure of the building and to improve the structural design to reinforce key components.

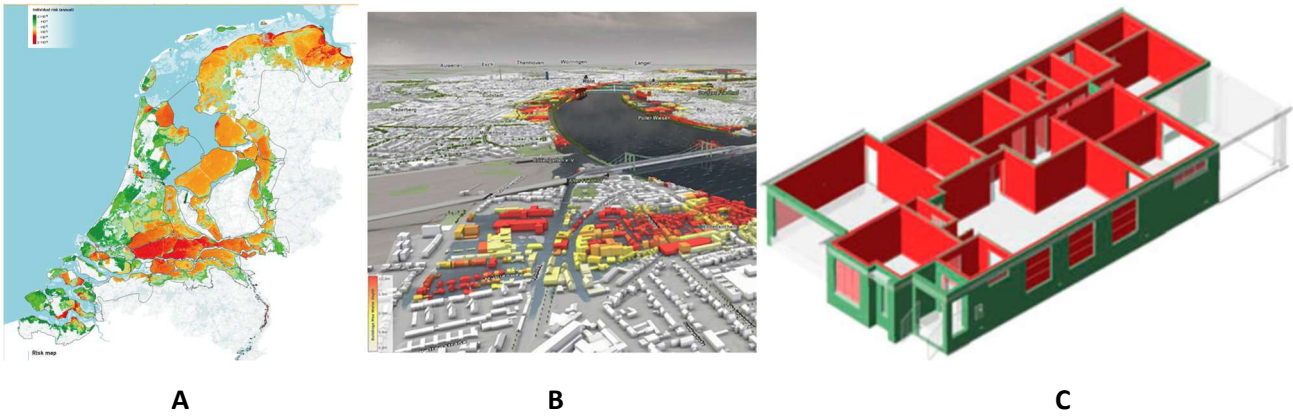


**Figure 5: Three main scales of analysis. (A)** The risk map shows the current individual risk (IR) in 2015 in The Netherlands (Vergouwe & Sarink, 2016) **(B)** The risk map generated by VISDOM simulation software in German. (<https://www.vrvis.at/produkte-loesungen/visdom>) **(C)** The colour coded damage map calculated by ANSYS FEA and visualised in ESRI ArcScene. (Amirebrahimi et al., 2015)

## 3 Literature review

### 3.1 Flood analysis and simulation

Coastal areas are increasingly threatened by flooding due to extreme weather driven by climate change. The compounding effects of ocean levels, rainfall, and rivers subject coastal cities to complex interactions of causative factors. This section explores the combined effects of these multiple factors under specific climate scenarios. Additionally, it compares and analyzes the scope of application of models used for assessing disasters and the software used for simulating these disasters, providing scientific guidance for subsequent applications.

#### 3.1.1 Weather scenarios

The latest climate scenario, the KNMI'23 Climate Scenario, was released in 2023, replacing the KNMI'14 Climate Scenario. The four KNMI'23 scenarios describe possible tipping points for climate change in the Netherlands:

- **Hd:** High emission levels and a "dry" scenario with slightly wet winters and significantly dry summers.
- **Hn:** High emission levels and a "wet" scenario with significantly wetter winters and slightly drier summers.
- **Ld:** Low emission levels and a "dry" scenario with slightly wet winters and significantly dry summers.
- **Ln:** Low emission levels and a "wet" scenario with significantly wetter winters and slightly drier summers.

These four new scenarios outline the future climate of the Netherlands. They form the basis for research into the effects of climate change and adaptation to this change.

Season	Variable	Indicator	Climate in 1991-2020 = reference period	2050 (2036-2065)				2100 (2086-2115)				
				Ld	Ln	Hd	Hn	Ld	Ln	Hd	Hn	
		Global temperature rise compared to 1991-2020		+0.8°C	+0.8°C	+1.5°C	+1.5°C	+0.8°C	+0.8°C	+0.9°C	+4.0°C	
		Global temperature rise compared to 1850-1900		+1.7°C	+1.7°C	+2.4°C	+2.4°C	+1.7°C	+1.7°C	+4.9°C	+4.9°C	
Year	Sea level along the Dutch coastline	average level	0 cm <sup>1</sup>	+24 (16-34) cm	+24 (16-34) cm	+27 (19-38) cm	+27 (19-38) cm	+44 (26-73) cm	+44 (26-73) cm	+82 (59-124) cm	+82 (59-124) cm	
		rate of change	3 mm/year <sup>1</sup>	+3 (1-6) mm/year	+3 (1-6) mm/year	+5 (4-8) mm/year	+5 (4-8) mm/year	-1 (-4-4) mm/year	-1 (-4-4) mm/year	+11 (6-23) mm/year	+11 (6-23) mm/year	
	Temperature	average	10.5°C	+0.9°C	+0.9°C	+1.6°C	+1.6°C	+1.5°C	+0.9°C	+0.9°C	+4.4°C	
	Precipitation	amount	851 mm	0%	+3%	-2%	+3%	0%	+3%	-3%	+8%	
	Solar radiation	average	120 W/m <sup>2</sup>	+5.8 W/m <sup>2</sup>	+4.8 W/m <sup>2</sup>	+5.4 W/m <sup>2</sup>	+2.5 W/m <sup>2</sup>	+5.8 W/m <sup>2</sup>	+4.8 W/m <sup>2</sup>	+7.1 W/m <sup>2</sup>	+1.3 W/m <sup>2</sup>	
	Humidity	average relative humidity <sup>2</sup>	82%	-1%	-1%	-1%	0%	-1%	-1%	-1%	+1%	
	Evaporation	potential evaporation (Makkink)	603 mm	+7%	+6%	+9%	+6%	+7%	+6%	+17%	+11%	
	Wind	average wind speed	4.8 m/s	-0.1 m/s	-0.1 m/s	0.0 m/s	0.0 m/s	-0.1 m/s	-0.1 m/s	-0.1 m/s	-0.1 m/s	
	Winter	Temperature	average	3.9°C	+0.7°C	+0.7°C	+1.2°C	+1.3°C	+0.7°C	+0.7°C	+3.7°C	+3.9°C
			average daily maximum	6.3°C	+0.7°C	+0.7°C	+1.1°C	+1.2°C	+0.7°C	+0.7°C	+3.5°C	+3.6°C
average daily minimum			1.4°C	+0.7°C	+0.7°C	+1.2°C	+1.4°C	+0.7°C	+0.7°C	+4.0°C	+4.2°C	
Precipitation			amount	218 mm	+4%	+5%	+4%	+7%	+4%	+5%	+14%	+24%
number of wet days (0.1 mm)		57 days	0.0 days	0.0 days	0.0 days	-0.6 days	0.0 days	0.0 days	0.0 days	+1.1 days		
days with >= 10 mm		5.4 days	-0.4 days	+0.5 days	+0.5 days	-0.8 days	+0.4 days	+0.5 days	+1.6 days	+2.5 days		
10-day total precipitation exceeded once every 10 years		109 mm <sup>1</sup>	-2%	+2%	0%	+2%	-2%	+2%	+8%	+15%		
Solar radiation		average	34 W/m <sup>2</sup>	+1.2 W/m <sup>2</sup>	+1.5 W/m <sup>2</sup>	+0.8 W/m <sup>2</sup>	+0.4 W/m <sup>2</sup>	+1.2 W/m <sup>2</sup>	+1.5 W/m <sup>2</sup>	-0.7 W/m <sup>2</sup>	-1.5 W/m <sup>2</sup>	
Humidity		average relative humidity <sup>2</sup>	87%	0%	0%	+1%	+1%	0%	0%	+1%	+2%	
Wind		average wind speed	5.6 m/s	-0.1 m/s	-0.1 m/s	0.0 m/s	+0.1 m/s	-0.1 m/s	-0.1 m/s	+0.1 m/s	+0.2 m/s	
	days with wind direction between north and west	13 days	+0.1 days	-0.8 days	0.0 days	+0.1 days	+0.1 days	-0.8 days	-1.7 days	-1.0 days		

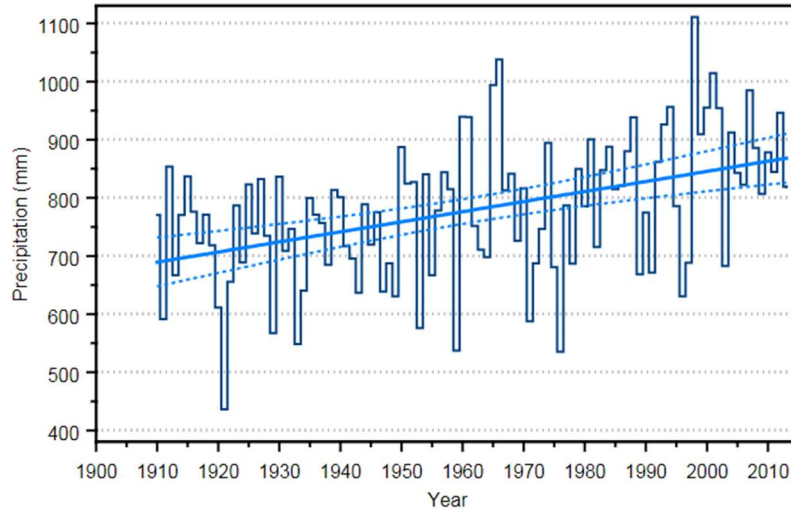
Season	Variable	Indicator	Climate in 1991-2020 = reference period	2050 (2036-2065)				2100 (2086-2115)				
				Ld	Ln	Hd	Hn	Ld	Ln	Hd	Hn	
Spring	Temperature	average	9.6°C	+0.8°C	+0.7°C	+1.3°C	+1.1°C	+0.8°C	+0.7°C	+3.6°C	+3.3°C	
		average daily maximum	13.7°C	+0.9°C	+0.8°C	+1.2°C	+1.0°C	+0.9°C	+0.8°C	+3.3°C	+2.9°C	
		average daily minimum	5.5°C	+0.7°C	+0.7°C	+1.4°C	+1.3°C	+0.7°C	+0.7°C	+3.9°C	+3.7°C	
	Precipitation	amount	153 mm	+1%	+3%	0%	+4%	+1%	+3%	+4%	+10%	
	Solar radiation	average	161 W/m <sup>2</sup>	+6.6 W/m <sup>2</sup>	+5.2 W/m <sup>2</sup>	+3.2 W/m <sup>2</sup>	+0.8 W/m <sup>2</sup>	+6.6 W/m <sup>2</sup>	+5.2 W/m <sup>2</sup>	-0.2 W/m <sup>2</sup>	-4.8 W/m <sup>2</sup>	
	Humidity	average relative humidity <sup>2</sup>	78%	-1%	-1%	0%	0%	-1%	-1%	+1%	+2%	
	Evaporation	potential evaporation (Makkink)	190 mm	+6%	+5%	+6%	+4%	+6%	+5%	+10%	+6%	
	Drought	maximum precipitation deficit April and May	76 mm	+11%	+6%	+15%	+5%	+11%	+6%	+21%	+8%	
	Summer	Wind	average wind speed	4.7 m/s	-0.1 m/s	-0.1 m/s	0.0 m/s	0.0 m/s	-0.1 m/s	-0.1 m/s	+0.1 m/s	0.0 m/s
			Temperature	average	17.3°C	+1.2°C	+1.1°C	+2.1°C	+1.7°C	+1.2°C	+1.1°C	+5.1°C
average daily maximum		21.7°C	+1.4°C	+1.2°C	+2.2°C	+1.7°C	+1.4°C	+1.2°C	+5.4°C	+4.7°C		
average daily minimum		12.9°C	+1.0°C	+1.0°C	+1.9°C	+1.8°C	+1.0°C	+1.0°C	+5.0°C	+4.9°C		
Precipitation		amount	235 mm	-8%	-2%	-13%	-5%	-8%	-2%	-29%	-12%	
		1-day total precipitation exceeded once every 10 years <sup>4</sup>	63 mm <sup>1</sup>	+4 (1-6)%	+5 (2-7)%	+6 (2-9)%	+9 (5-14)%	+4 (1-6)%	+5 (2-7)%	+15 (5-26)%	+26 (12-41)%	
		hourly precipitation exceeded once per year <sup>5</sup>	16 mm <sup>1</sup>	+4 (2-6)%	+6 (3-8)%	+6 (2-9)%	+11 (6-16)%	+4 (2-6)%	+6 (3-8)%	+15 (5-26)%	+31 (17-46)%	
Solar radiation		average	206 W/m <sup>2</sup>	+12 W/m <sup>2</sup>	+9.1 W/m <sup>2</sup>	+14 W/m <sup>2</sup>	+7.4 W/m <sup>2</sup>	+12 W/m <sup>2</sup>	+9.1 W/m <sup>2</sup>	+24 W/m <sup>2</sup>	+11 W/m <sup>2</sup>	
Humidity		average relative humidity <sup>2</sup>	77%	-2%	-1%	-2%	-1%	-2%	-1%	-4%	-1%	
Evaporation		potential evaporation (Makkink)	286 mm	+8%	+6%	+11%	+7%	+8%	+6%	+22%	+14%	
Drought	maximum precipitation deficit for April-September	160 mm	+22%	+13%	+35%	+15%	+22%	+13%	+79%	+37%		
	maximum precipitation deficit for April-September exceeded once every 10 years	265 mm	+16%	+9%	+30%	+16%	+16%	+9%	+63%	+30%		
Wind	average wind speed	4.2 m/s	-0.1 m/s	-0.1 m/s	-0.1 m/s	-0.1 m/s	-0.1 m/s	-0.1 m/s	-0.2 m/s	-0.2 m/s		
Autumn	Temperature	average	11.2°C	+1.0°C	+0.9°C	+1.8°C	+1.6°C	+1.0°C	+0.9°C	+5.0°C	+4.8°C	
		average daily maximum	14.5°C	+1.1°C	+1.1°C	+1.9°C	+1.6°C	+1.1°C	+1.1°C	+5.1°C	+4.6°C	
		average daily minimum	7.8°C	+0.9°C	+0.9°C	+1.8°C	+1.7°C	+0.9°C	+0.9°C	+5.1°C	+5.1°C	
	Precipitation	amount	245 mm	+4%	+5%	+1%	+4%	+4%	+5%	+1%	+13%	
Solar radiation	average	77 W/m <sup>2</sup>	+3.7 W/m <sup>2</sup>	+3.5 W/m <sup>2</sup>	+3.7 W/m <sup>2</sup>	+1.4 W/m <sup>2</sup>	+3.7 W/m <sup>2</sup>	+3.5 W/m <sup>2</sup>	+5.4 W/m <sup>2</sup>	+1.0 W/m <sup>2</sup>		
Humidity	average relative humidity <sup>2</sup>	85%	-1%	0%	-1%	0%	-1%	0%	-1%	0%		
Wind	average wind speed	4.7 m/s	-0.1 m/s	-0.1 m/s	-0.1 m/s	0.0 m/s	-0.1 m/s	-0.1 m/s	-0.2 m/s	-0.1 m/s		

Figure 6: KNMI'23 scenario table with country averages(KNMI'23 climate scenarios)

Observed trends and future scenarios per variable:

i. Precipitation:

The annual average precipitation is calculated based on long-term time series from 102 stations in the Netherlands, starting from 1910. For each series, the monthly totals were calculated. The monthly precipitation totals from the 102 stations were then averaged to calculate the annual average precipitation total for the Netherlands. Figure 7 shows the linear trend line of the annual average precipitation in the Netherlands. From the figure, it can be seen that the total increase from 1910 to 2013 is 178.6 millimetres, which represents a 25.5% increase.



**Figure 7:** Annual precipitation in the Netherlands 1910-2013 (mean of 102 stations). The straight line represent a linear regression fit. The dashed lines give the 95% confidence bands. (van den Hurk et al., 2016)

From the resampling of RACMO2, we can make predictions of precipitation for future scenarios. Figure 8 shows the observed precipitation increase in winter and summer for different scenarios. and the average increase for the four future scenarios.

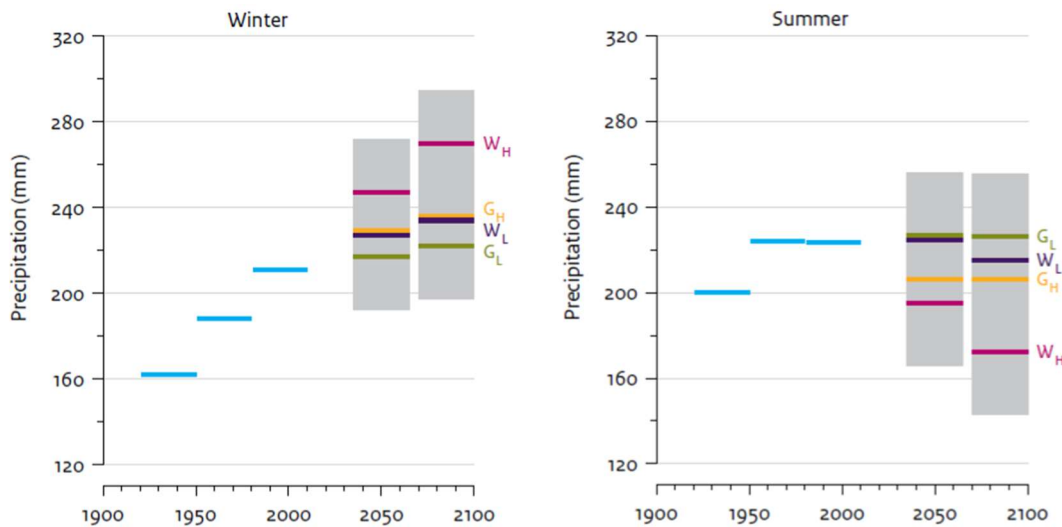


**Figure 8:** Winter and summer precipitation in De Bilt (Netherlands). Observations (three 30-year averages, in blue), 44 scenarios (2050 and 2085, in four colours) and natural variations for 30-year averages (in grey) are shown(van den Hurk et al., 2016)

ii. Sea level rise

Sea level, as a variable arising from global climate change, was modeled and analyzed by KNMI'14 using the CMIP5 model to derive the following scenarios and temporal ranges of change (Table 1), and trends, with upper and lower bounds, which correspond to the uncertainty ranges of 5 to 95% of sea level rise estimated by the model simulations.

after rounding to 0.1m precision.

KNMI'14 scenario	Low (2050)	Low (2085)	High (2050)	High (2085)
$dT_{glob}$	+1.0°C	+1.5°C	+2.0°C	+3.5°C
Global mean	15 to 30 cm	30 to 60 cm	20 to 35 cm	45 to 75 cm
North Sea	15 to 30 cm	25 to 60 cm	20 to 40 cm	45 to 80 cm

**Table 1:** KNMI'14 Sea-level scenario ranges for Global and North Sea

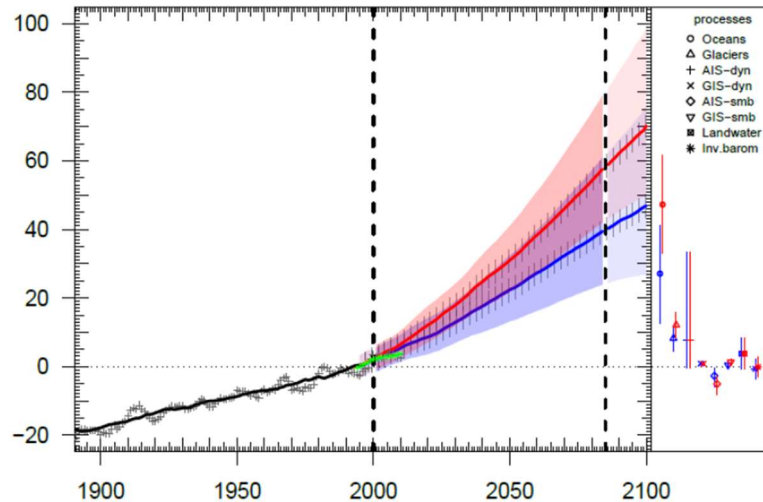


**Figure 9:** KNMI'14 scenarios for North Sea area mean sea-level rise and its likely range (shading), relative to 1986-2005 mean. The vertical axis denotes the 30-year running mean sea-level change in cm, while the horizontal axis denotes time. Observational data consists of the average of 6 stations in The Netherlands. The green symbols indicate the 5-year running means obtained from satellite altimetry (1993-2013) over the North Atlantic, with respect to 1993-1998. (source observations: Permanent Service for Mean Sea Level, <http://www.psmsl.org>). (van den Hurk et al., 2016)

In conclusion, changes in precipitation and sea level due to global climate change vary with different climate scenarios. Bart predicted future rainfall scenarios by resampling historical data using RACMO2, while sea level rise was projected for various temporal scenarios with different temperatures through CMIP5 modeling. This section aims to incorporate different future climate scenarios into data collection efforts and provide guidance for responding appropriately to these changes.

### 3.1.2 Compound flood

#### Mechanism

Based on the concept of compound events proposed by the IPCC, this is defined as "a compound event is a combination of multiple drivers or hazards that together trigger social or environmental risks." Coastal compound flooding is one of the typical compound events, caused by a combination of multiple flood drivers. (Figure 10) These flood drivers include rainfall, runoff, sea level, and storm surges. Since a single factor cannot capture all the relevant conditions leading to a hazard, researchers are dedicated to studying the risk of flood formation under different combinations. The extreme values of compound flooding are mainly divided into three types:

1. **Coastal urban areas:** Heavy rainfall and storm surges occur simultaneously, causing flooding through their combined effects or exacerbating the flood depth of either factor. (Bevacqua et al., 2019; Ridder et al., 2018; Santos et al., 2021)
2. **Coastal river areas:** River discharge and storm surges occur simultaneously, leading to riverbank overflow and increased flood depth. (Heinrich et al., 2023; Khanal et al., 2019; Klerk et al., 2015; Zellou & Rahali, 2019; Zheng et al., 2013)

3. **Compound flooding caused by the simultaneous or sequential occurrence of rainfall, storm surges, and river discharge.**(Svensson & Jones, 2004a, 2004b)

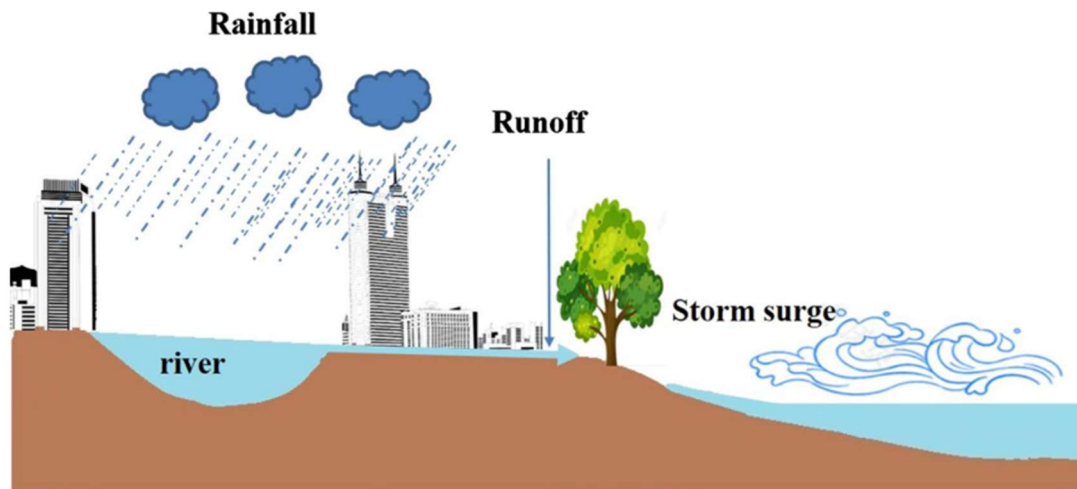


**Figure 10:** Mechanism of compound flood in coastal area.(Xu et al., 2022)

### 3.1.3 Flood assessment model

The correlation, joint probability, and combined effects of multiple drivers on flooding have ignited exploration within the scientific community to evaluate compound floods. In recent years, three primary perspectives have zeroed in on compounding mechanisms in coastal areas. These encompass: 1. Statistical models (Stochastic model), which demonstrates the interdependence between flood drivers and establishing their joint distribution. 2. Numerical models (Mechanistic model), which simulate the physical process of composite flood formation. 3. Empirical models, leveraging the statistical relationship between rainfall inputs and observed runoff outputs for flood prediction.

The Alois Tilloy (Tilloy et al., 2019) study delineated three primary modeling approaches for assessing the interrelationships between single hazards (Fig. 11): stochastic, empirical, and mechanistic. A database comprising 146 references related to multi-hazard interrelationships was compiled to exemplify the quantitative methods applied across various categories of hazards (in terms of interrelation types: Independence, changing conditions, triggering, compound, mutually exclusive, and in terms of disaster types: earthquakes, hurricanes, floods, etc.). The table below (Table 2) summarizes the advantages, disadvantages, practicality, and application cases of the three quantification methods.

The focus of the study is on hydrologic hazards. Copula (31%) and physical models (30%) emerged as the most prevalent methodologies due to their capacity to generate results for diverse scenarios and draw inferences beyond observed data. However, there are distinctions between them. In the absence of prior knowledge on the hazards under study, it is necessary to fit several copula models with varying levels of complexity to the data and compare them. Utilizing a copula that fails to adequately capture the dependence structure between two variables can result in either underestimation or overestimation of their joint probability. On the other hand, physical models are characterized by higher computational costs and demand larger volumes of data. (Mazas & Hamm, 2017)

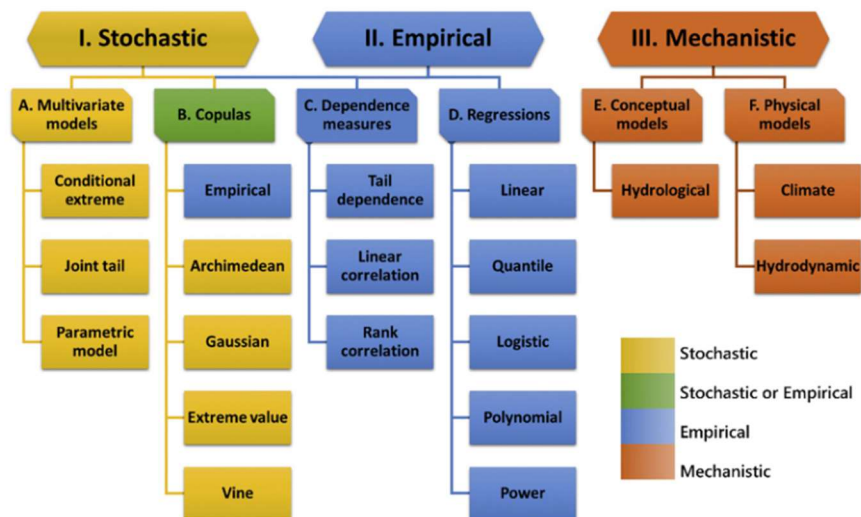


**Figure 11:** Natural hazard interrelationship models: three different modelling approaches (I. stochastic, II. empirical, and III. mechanistic), six families (A. multivariate, B. copula, C. dependence measures, D. regressions, E. conceptual models and F. physical models) and 19 modelling methods. This classification is based on a review of 70 references from 1980 to 2018 (see Supplementary Material Table B1). (Tilloy et al., 2019)

	Stochastic	Empirical	Mechanistic (conceptual/physical)
<b>Applicable type</b>	Compound Hazards estimation of joint probabilities of exceedance and return periods	Triggering Hazards Geophysical hazards	Compound Hazards Hydrodynamic models are the most prevalent (e.g., river flooding, coastal flooding, compound flooding, tsunami).
<b>Examples</b>	Quantitative multi-hazard risk assessment with vulnerability surface and hazard joint return period (Ming et al., 2014)	Dependence between sea surge, river flow and precipitation in south and west Britain (Svensson & Jones, 2004)	Conceptual: A Review on Hydrological Models (Devia et al., 2015) Physical: Investigating compound flooding in an estuary using hydrodynamic modelling: a case study from the Shoalhaven River, Australia (Kumbier et al., 2018)

**Table 2:** Application scenarios of three quantitative models

### 3.1.3.1 Statistical models

Statistical modelling is based on the dependence between drivers and their joint distribution. (Figure 12) The commonly used statistical methods are the threshold excess method, point process method, conditional method, Kendall rank correlation coefficient method, tail correlation coefficient method, and copula function method, etc. In order to obtain the characteristics of the flooding factors in time and space, the common methods for the dependence between drivers and their joint distribution are explained below, respectively.

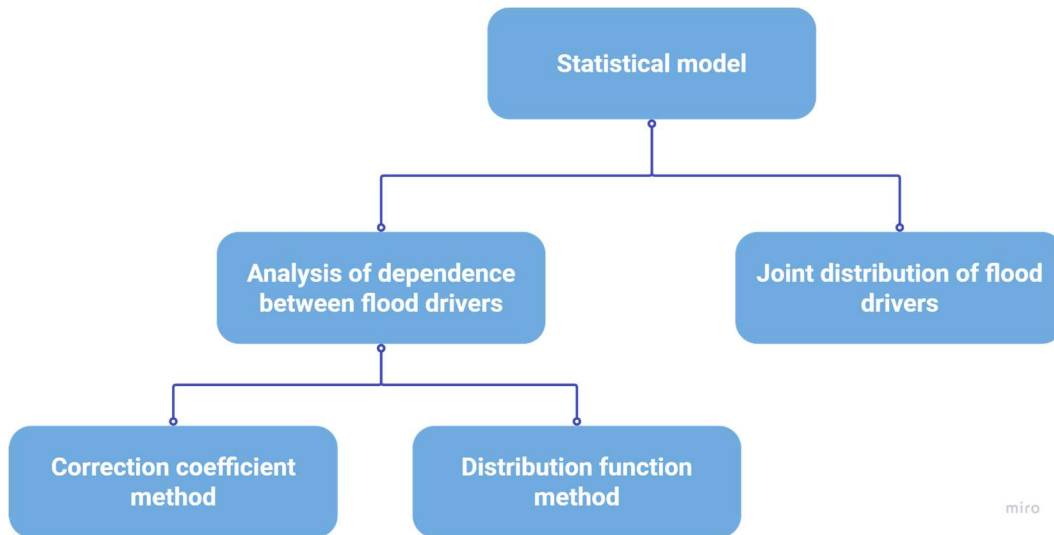


**Figure 12:** Framework of models of Statistic Model

#### i. Depending between flood drivers

The severity of flooding caused by multiple drivers occurring simultaneously is greater than flooding caused by a single factor. Therefore, in order to properly assess compound flood impacts, the dependencies between flood factors need to be quantified. In general, (Xu et al., 2022) , the methods for calculating dependencies can be categorized into two types:

1. Correlation coefficient method. The correlation coefficient is calculated directly from the data.
2. Distribution function method. This method requires determining the distribution function of individual factors and then calculating the dependencies.

#### ii. Joint distribution of flood drivers

The significance of studying the joint distribution, also known as the multifunctional distribution, is to study the joint risk of time, determine the reproduction period and provide conditions for the boundary numerical physics model. Methods for calculating the joint distribution are: the copula function method, the Moran method, and the joint distribution method composed of specific marginal distributions.

Stochastic models have been particularly used to model compound hazards as they provide the joint probabilities of multi hazard occurring at the same time as well as the return period. These quantities are commonly required by engineers and decision makers.

However, due to the uncertainty of its distribution function and the uncertainty of its parameters will affect the results of hydrological frequency calculation, thus affecting the calculation of the probability of disaster occurrence, and thus affecting the engineering design and disaster prevention and control. Uncertainty in statistical modeling needs to be further studied.

### 3.1.3.2 Numerical models

The main idea of numerical modeling is to simulate the complex physical movement of water bodies by calculating physical equations. Due to its complexity, composite flood modeling usually contains multiple models, namely: hydraulic, hydrologic, ocean circulation, etc. Figure 13 shows the relationship between the parameters of the three models, the software and the interaction.

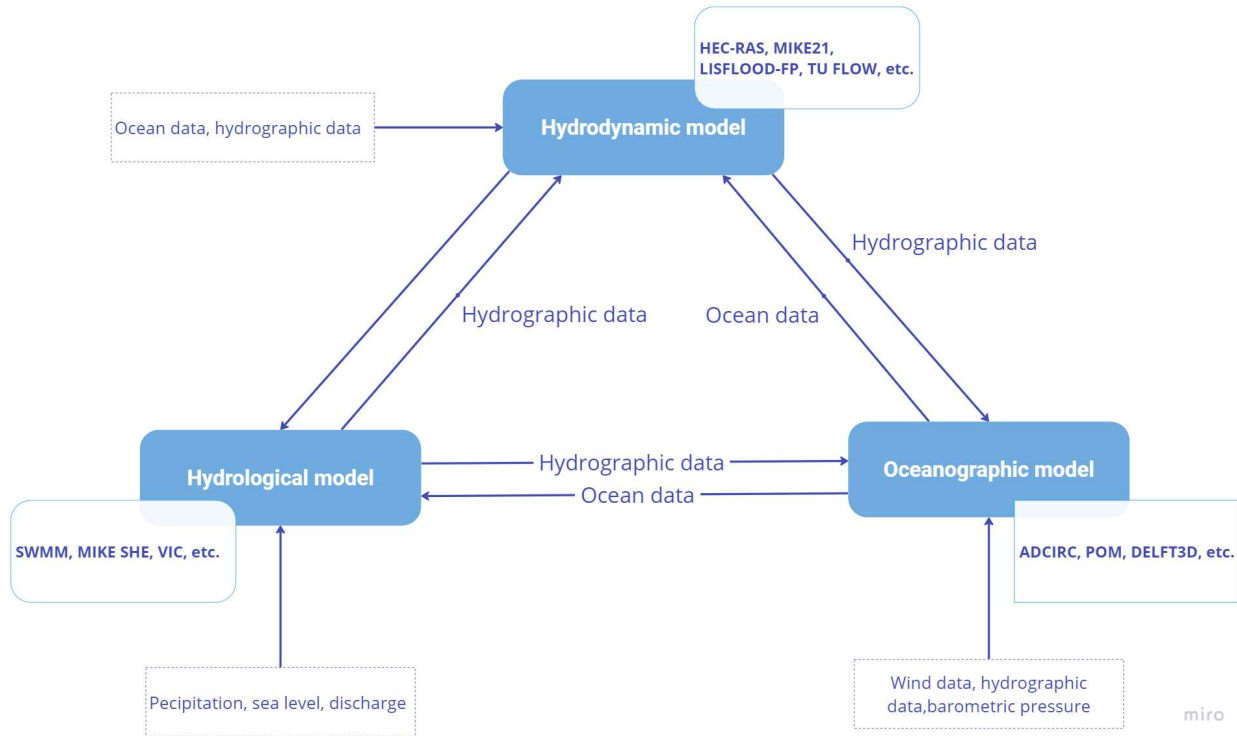


**Figure 13:** Three types of unidirectional compound flood simulation, and their relationships

In flood assessment studies, different models are mostly coupled to construct a composite flood modeling framework. The model coupling can be divided into different kinds of model-oriented, hydrologically-dominated coupling model, hydrodynamics-dominated coupling model, Oceanography-dominated coupling model. Table 3 illustrates the scope of these coupled model.

Coupled model categories	Function	input	output
Hydrological-dominated model	Simulate the final inundation map	Observed or simulated hydrological and oceanographic dataset	Inundation extents
Hydrodynamics-dominated model	simulate the entire process from precipitation runoff to inundation	Observed data or model-generated sea level	Inundation extents
Oceanographic-dominated model	simulate marine processes	simulated or observed data of hydrological processes(rainfall, runoff)	flood water levels and velocities

**Table 3:** Comparison of three coupled model

In the case study, the following Table 4 was summarized and the key points of each composite model were recognized in the literature reflection:

1. In Hydrological model, if the interactions between storm surge and runoff is ignored, it will lead to inaccurate outcomes.
2. Similarly, Hydrodynamic model could simply implement the data gained from hydrodynamic and oceanographic models, which make the process simple and direct. However, it may cause underestimation of the final simulation result, resulting in inaccurate outcomes.
3. As for Oceanographic coupled model, if underestimate the interaction between rainfall, river flooding and marine process can also lead to wrong result.

<b>Case Studies</b>	<b>Categories</b>	<b>Models</b>	<b>Indicators</b>	<b>Subjects</b>
Developing a hybrid modeling and multivariate analysis framework for storm surge and runoff interactions in urban coastal flooding(Hasan Tanim & Goharian, 2020)	Hydrology-dominated model	Delft3D -SWAN, SWMM	Storm surge, runoff	Duration, depth
Hydrodynamic Simulation of an Irregularly Meandering Gravel-Bed River: Comparison of MIKE 21 FM and Delft3D Flow models(Parsapour-moghaddam et al., 2018)	Hydrodynamics-dominated model	Delft3D-Flow, MIKE 21FM	discharge	depth-averaged velocities
Investigating compound flooding in an estuary using hydrodynamic modelling: a case study from the Shoalhaven River, Australia(Kumbier et al., 2018)	Hydrodynamics-dominated model	Delft3D	rainfall, storm surges	flood extents and inundation depths
Simulating storm surge waves for structural vulnerability estimation and flood hazard mapping(Hatzikyriakou & Lin, 2017)	Hydrodynamics-dominated model	ADCIRC ? SWAN and BOUSS1D	storm surge	Inundation area, wave and velocity
A study on compound flood prediction and inundation simulation under future scenarios in a coastal city(Zhong et al., 2024)	Hydrodynamics-dominated model	Delft3D-FLOW, HEC-RAS	rainfall, storm surges, river level	Inundation area, depth
A full-scale fluvial flood modelling framework based on a high-performance integrated	Hydrodynamics-dominated model	HiPIMS	rainfall	Inundation

hydrodynamic modelling system (HiPIMS)(Xia et al., 2019)				
More meteorological events that drive compound coastal flooding are projected under climate change(Bevacqua et al., 2020)	Oceanography-dominated model	D-FLOW	Rainfall, waves, sea level, storm surge	Sea level
Storm surge and extreme river discharge: a compound event analysis using ensemble impact modelling(Khanal et al., 2019)	Hydrodynamics-dominated model	WAQUA/DSCMv5 SPHY, HBV96	Storm surge, discharge	Water level
The role of atmospheric rivers in compound events consisting of heavy precipitation and high storm surges along the Dutch coast(Ridder et al., 2018)	Oceanography-dominated model	WAQUA/DSCMv5	water levels, precipitation	Atmospheric river
Developing a modelling framework to simulate compound flooding: when storm surge interacts with riverine flow(Loveland et al., 2021)	Oceanography-dominated model	HEC-RAS, ADCIRC	Storm surge, river discharge	Water level

**Table 4:** Case studies of coupling flood model research

### 3.1.3.3 Empirical models

Empirical models are based on statistical relationships between rainfall and runoff. Future flood conditions can be simulated with a small number of data inputs and are commonly used for flood forecasting and urban drainage design. Types of empirical models include data-driven methods such as regression models, artificial neural networks, various machine learning algorithms, and the Soil Conservation Service Curve Number (SCS-CN) method.(Kumar et al., 2023)

Among empirical models, flood modeling using artificial intelligence (AI) and machine learning (ML) is a relatively new field that has the potential to revolutionize the way floods are predicted and managed (Hou et al., 2021). Artificial intelligence and machine learning algorithms are used to analyze large amounts of data, including meteorological, hydrological, and topographical data, to improve the accuracy and reliability of flood models.

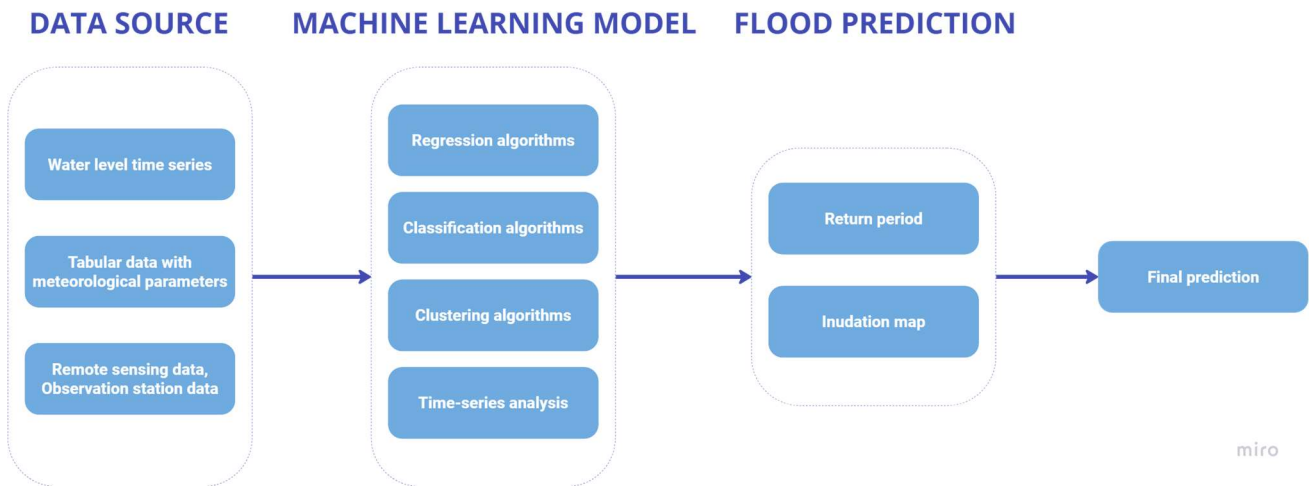


**Figure 14:** Process for flood prediction using ML methods

The whole process involves three main phases (Fig 14) : data collection, selection of appropriate machine learning models, flood forecasting, prediction and risk mapping. The first step collects various data including water level time series, remotely sensed data and tabular data. The second step selects the machine learning model selection based on the data characteristics and prediction problem. Regression techniques can be used to estimate flood levels using historical data. In the third step, a classification algorithm is used to categorize the flood risk based on climate, topography, and previous historical flood data, and to create a flood risk heat map.

### 3.1.3.4 Summary

Model Type	Description	Pros	Cons
<b>Statistical models</b>	provide a simplified representation of the hydrological cycle	<ul style="list-style-type: none"> <li>• Ease of Use: Simple to understand and apply.</li> <li>• Minimal Input Requirements: Require only a few parameters.</li> <li>• Practical Application: Useful for small to medium-sized catchments with a well-understood hydrological context.</li> </ul>	<ul style="list-style-type: none"> <li>• Simplification: May not accurately represent complex physical processes involved in runoff generation.</li> <li>• Limitations in Scenario Analysis: Limited ability to simulate the effects of land use change and climate change.</li> <li>• Applicability: Less effective for larger or more complex catchments.</li> </ul>
<b>Numerical models</b>	simulate runoff and flooding by representing the physical processes involved	<ul style="list-style-type: none"> <li>• Accuracy: Can accurately represent complex hydrological processes.</li> </ul>	<ul style="list-style-type: none"> <li>• Data Intensive: Require extensive and detailed input data.</li> </ul>

	<ul style="list-style-type: none"> <li>• Versatility: Useful for predicting runoff from large catchments and simulating detailed scenarios.</li> <li>• Comprehensive: Capable of addressing the impacts of various changes, including land use and climate change.</li> </ul>	<ul style="list-style-type: none"> <li>• Complexity: Can be complex and time-consuming to set up and run.</li> <li>• Sensitivity: May be sensitive to errors in input data, impacting the reliability of results.</li> </ul>
<p><b>Empirical models</b> based on statistical relationships between rainfall inputs and observed runoff outputs. They rely on historical data to establish these relationships and make predictions.</p>	<ul style="list-style-type: none"> <li>• Simplicity and Efficiency: Easy to use and interpret.</li> <li>• Minimal Data Requirements: Require only historical rainfall and runoff data.</li> <li>• Practical Uses: Effective for flood forecasting, urban drainage design, and water resources planning.</li> </ul>	<ul style="list-style-type: none"> <li>• Simplification: Do not accurately represent the physical processes involved in runoff generation.</li> <li>• Limited Flexibility: Limited ability to simulate the effects of land use change and climate change.</li> <li>• <input type="checkbox"/> Historical Dependence: May not perform well outside the range of historical data used to develop the model.</li> </ul>

**Table 5:** Comparison of three flood analysis model, including its pros and cons.

As shown in the table 5, each model has its own scope of application: Conceptual Models are ideal for smaller catchments with well-understood hydrological processes but may not handle complex or changing conditions well; Physical Process-Based Models offer detailed and accurate simulations for large catchments and complex scenarios but require extensive data and computational resources; Empirical Models provide efficient and practical solutions for planning and forecasting based on historical data but may lack accuracy in novel or evolving situations.

Given the lightweight computational approach utilized in this paper and the requirement for integration with a BIM-GIS framework, it is crucial to provide sufficient geographic, hydrological, and architectural information inputs. A digital model based on physical processes is preferred because it can offer the necessary accuracy to ensure reliable structural analysis at the micro level. Moreover, if the simulation software is open-source, it allows for the incorporation of physical parameters into the GIS file, thereby enhancing the informativeness of the visualization.

### 3.2 Damage assessment

The uniqueness of buildings is often overlooked in current flood damage assessments, resulting in macro and meso damage evaluations that are inadequate for informing structural design decisions. This section aims to

address this research gap by developing an assessment model capable of micro-analysis of building components. The model will consider the effects of flood hydrodynamics on the building and encode the damage rating. To achieve this goal, the following research tasks are necessary:

1. **Impacts of Flood Action on Buildings:** Investigate how different flood dynamics, such as water depth, velocity, and duration, directly affect various building components.
2. **Fragility Curves for Building Components:** Create vulnerability curves for each building component based on different materials, which will quantify the relationship between flood exposure and damage.
3. **Damage Grading Model:** Develop a model to group various components based on similar fragilities and expected loss.

This research will enable a more accurate and detailed evaluation of flood damage at the micro level, ultimately improving the robustness of building design against flood risks.

### 3.2.1 Flood action on buildings

The damage to building components is caused by the action of floods. Flood actions may include hydrostatic, hydrodynamic, waves, buoyancy, debris, erosion, and nonphysical (Kelman & Spence, 2004). Given the focus of this study on coastal areas and to maintain consistency with data from compound flood research, we mainly discuss hydrostatic pressure here.

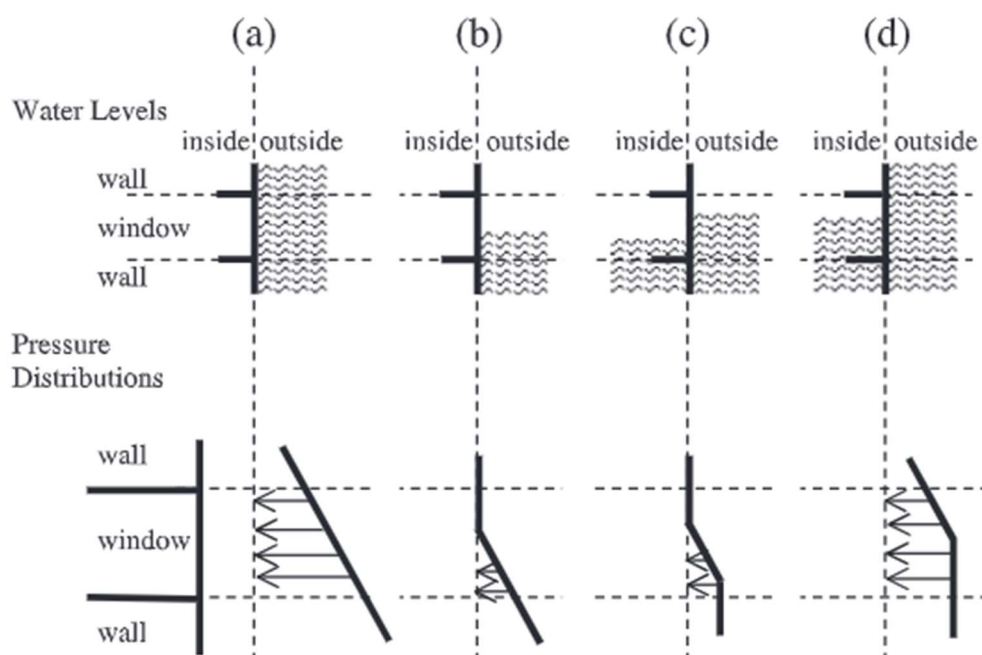


**Figure 15:** Water levels and pressure distribution levels on building component in each situation(Kelman & Spence, 2004)

The hydrostatic pressure refers to the lateral pressure generated by the difference in water depth on either side of a vertical component(Fig. 15), calculated using the method provided by Kelman and Spence(Kelman & Spence, 2004).

$$\Delta P = \rho_w g (f_{\text{diff}} - y) = \Delta P_{\text{hydrostatic at } y=0} - \rho_w g y$$

for  $h \leq y \leq f_{\text{diff}}$

(where  $y = 0$  is the base of the building)

$$\Delta P = 0 \text{ for } y > f_{\text{diff}}$$
(1)

(a) Water covers the entire window on one side yielding a linear pressure. (b) Water rises partway up the window on one side. (c) Water rises partway up the window on both sides, but to different y-values on each side. (d) Water entirely covers the window on one side and rises partway up the other side.

On the other hand, hydrodynamic pressure is the lateral pressure generated by flowing water, depending on the direction of flow. It may be positive, pushing the component inward, or negative, creating suction. The determining factor is the direction of the flow velocity vector perpendicular to the surface of the building component, which can be calculated using the method proposed by FEMA (Conrad et al., 2012). Additionally, the duration of the flood determines the contact time between water and building components, reflecting the damage caused to water-sensitive building elements due to exposure time, which is also a key factor in determining the extent of damage.

### 3.2.2 Damage assessment methods

#### HAZUS-MH Flood model

HAZUS-MH is a nationally standardized methodology and risk assessment software program containing three models for estimating potential losses from natural hazards (i.e., earthquakes, hurricanes, and floods). The HAZUS-MH flood model was released by FEMA in 2004. It currently contains methods for assessing losses in rivers and coastal areas. (Nadal et al., 2010)

The depth-damage function expresses the relationship between flood depth and damage percentage. Typically used to estimate the extent and severity of damage to structural elements and contents, the HAZUS flood model employs a similar approach, using "confidence-weighted" depth-damage curves provided by the FIA, as well as selected curves developed by various USACE districts to estimate damage to the general building stock. (Scawthorn et al., 2006)

More than 900 curves for structures, contents, and facilities are provided, as described in the Flood Modeling Technical Manual. An example is list below.

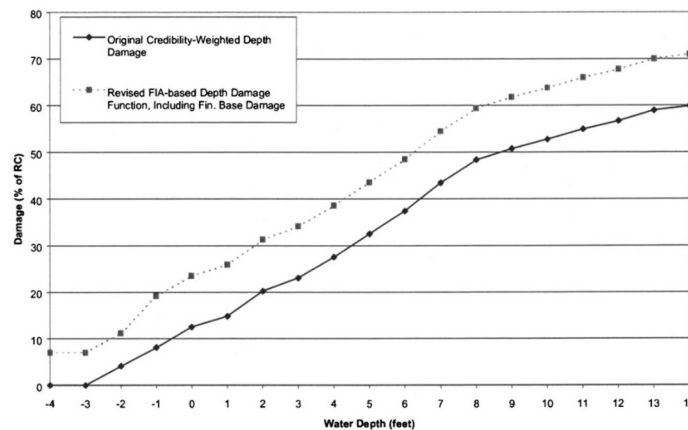


Figure 16: FIA-based structure depth-damage curve, two or more stories, basement-modified (Scawthorn et al., 2006)

### Alternative Flood Damage Assessment Methods

In order to study the hydrostatic and hydrodynamic forces of floods and the effects of mudslide deposition, Mazzorana created a finite element model for both structure and soil-structure interaction. Nadal considered the different velocity forces of river floods, storm surges, and tsunamis, as well as the effects of sediment impacts, resulting in a depth-velocity-damage 3D image that shows the expected damage for a given water velocity at each depth. (Nadal et al., 2010)

#### 3.2.3 Components fragility analysis

##### 3.2.3.1 Fragility quantification analysis

Fragility is a conditional probability that describes the probability that a building component will exceed a specified level of damage for a given level of hazard intensity. (Nofal et al., 2020) In order to capture the impact of flooding on building structural components, detailed parameters of each building component need to be evaluated in addition to the building location, planned area and height required for a general vulnerability assessment. Each component is described by a number of parameters such as: geometry, layout position in the building, materials, openings, etc. These parameters make the vulnerability of each component change with the parameters at the same location. In this section, a methodology is proposed to predict the vulnerability of the components and the results are shown in terms of failure probability-water depth curves.

In addition to exceeding the specified damage level Eq.(2), vulnerability is also a way of expressing the probability of failure in terms of whether the intensity of flooding exceeds the resistance to flooding. Eq.(3)

$$P(DS) = \sum P(DS|D = x) \cdot P(D = x) \quad (2)$$

$$F_r(x) = P[D(x) > R|IM(x)] \quad (3)$$

where  $P(DS)$  = probability of being in a DS,  $P(D = x)$  = probability that demand have certain value  $x$ ,  $P(DS|D = x)$  = conditional probability of being in DS condition on demand  $D = x$ ,  $F_r(x)$  = fragility function,  $D(x)$  = System or component demand,  $R$  = system or component resistance, and  $IM(x)$  is the intensity measure. (Nofal et al., 2020)

For a good statistical fit, structural systems and component fragilities usually are expressed in terms of a lognormal cumulative distribution function ( $\lambda_r$ ,  $\xi_r$ ) as shown in Eq. (4) (Nofal et al., 2020)

$$F_r(x) = \Phi \left[ \frac{\ln(x) - \lambda_r}{\xi_r} \right] \quad (4)$$

At the component level, each component is differently sensitive to depth, e.g. for structures, masonry is not as resistant to water as cement, and for contents, appliances are completely damaged at the first contact with water. Also the location of the component affects the level of damage, for example a window with a higher elevation than the wall will be much less damaged at the same depth of water. Considering the diversity of parameters of building elements increases the complexity of analyzing flood damage.

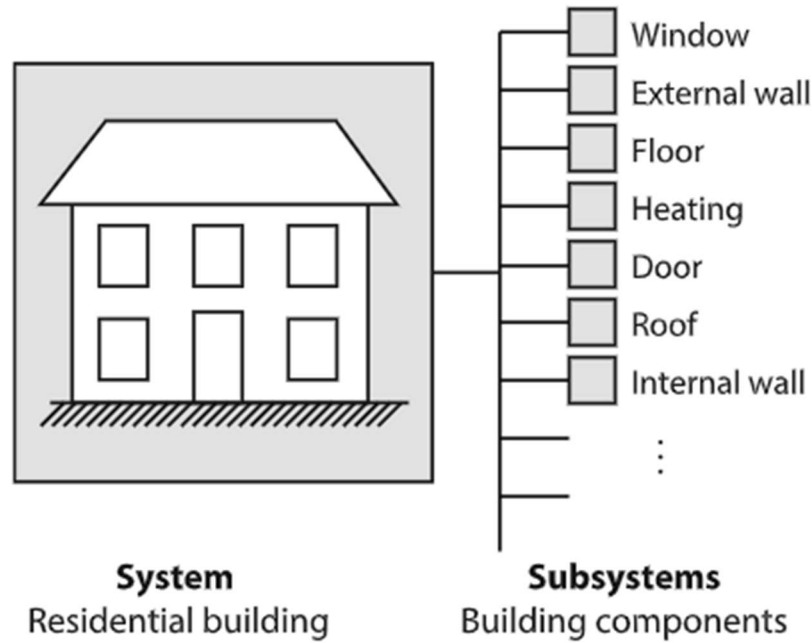


**Figure 17.** Hierarchical representation of a building as a collection of components (Custer & Nishijima, 2015)

Custer and Nishijima (2015) propose a layered approach, dividing the building by characteristics (material) into different layers and analyzing the fragility of each layer. When only the structural elements of the outer skin of the building are analyzed, the material and elevation among the multitude of parameters become determinants of the degree of damage. In the case of structural elements of the building, the material and elevation often point to the same characteristics, e.g., facade: rammed earth with an elevation of 0, window: glass with an elevation of 0.9 m. Thus, the fragility of the building skin system is transformed into the fragility of the different characteristics of elements characterized by different depths of the water.

The following assumptions are made in order to obtain the fragility curves for each components:

1. The probability of failure - depth curve is cumulative distributed.
2. The range is four times the standard deviation.
3. The damaging water depth – probability density is normally distributed between these ranges.
4. Each component is affected by flooding independently of each other.
5. Hydrodynamic effects due to differences in neighboring water depths are not considered.

Based on these principles, and the mean depth and standard deviation depth of capability can be found in the table 6. Finally, the fragile curves (Fig. 17) can be generated in python (Fig. 16).

Component	DS0		DS1		DS2		DS3		DS4	
	Crawspace Insulation	Flooring Insulation	AC Unit/ Heater	Wood Flooring	Washer/ Dryer	Lower Cabinets	Drywall (DS3)	Upper Cabinets	Wood Framing	Decking Flooring
Min depth (m)	-1.25	-0.3	-1.2	0	0.05	0	0.8	1.3	0.5	2
Max depth (m)	-0.85	0.1	0.6	1	0.25	0.9	1.5	2	4.5	4
Mean depth (m)	-1.05	-0.1	-0.3	0.5	0.15	0.45	1.15	1.65	2.5	3
Stan. Dev. of depth(m)	0.1	0.1	0.45	0.25	0.05	0.225	0.175	0.175	1	0.5
Min duration (hr)	0	0	0	48	0	24	24	24	144	144
Max duration (hr)	10	10	1	96	0.5	48	48	48	240	240
Mean duration (hr)	5	5	0.5	72	0.25	36	36	36	192	192
Stan. Dev. of duration (hr)	2.5	2.5	0.25	12	0.125	6	6	6	24	24
Min Rep. Cost (USD \$)	1420	710	3700	3720	350	9000	1167	6000	7100	14200
Max Rep. Cost (USD \$)	4260	2130	7200	6820	1500	18000	3501	12000	18460	35500
Mean Rep. Cost (USD \$)	2840	1420	5450	5270	925	13500	2334	9000	12780	24850
Stan. Dev. of Rep. Cost (\$)	710	355	875	775	287	2250	583	1500	2840	5325

**Table 6:** Extreme water depths and durations that different materials can withstand(Nofal et al., 2020)

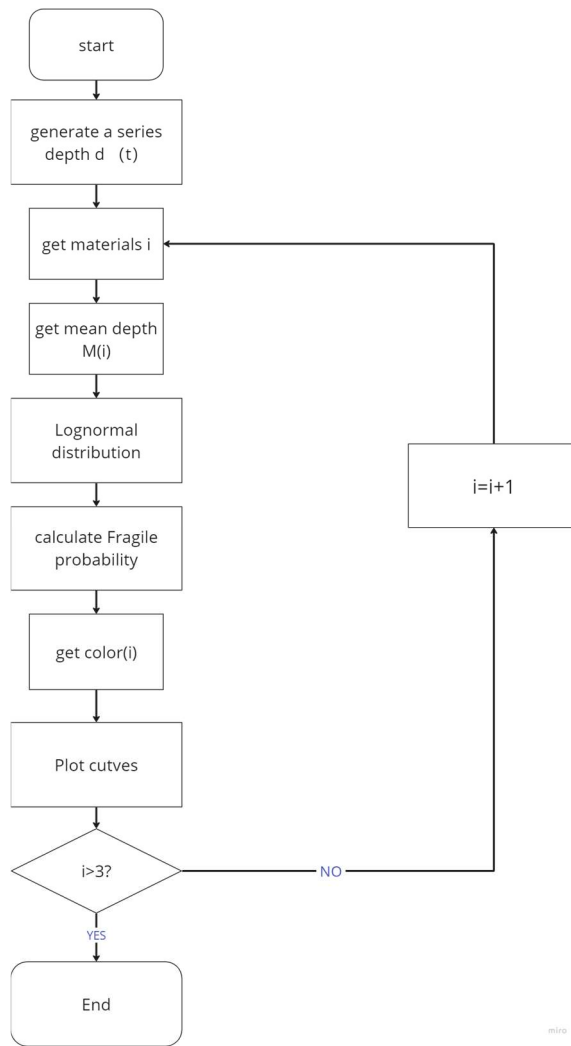


**Figure 18:** Flowchart of scripting fragile curves graph.

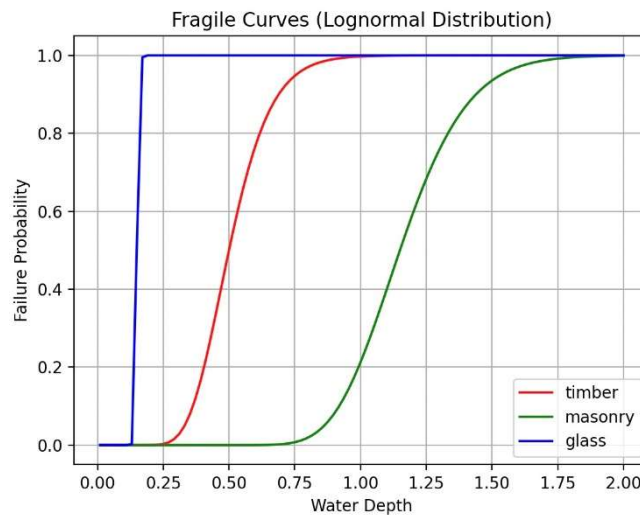


**Figure 19:** Fragile curves with different materials for individual components of a one-story residential building on a slab-on-grade foundation. Timber for door(RED); Masonry for wall(GREEN); Glass for window(BLUE)

From the above table, it can be concluded that the fragile probability of a member at a specific location can be directly assessed based on the water level obtained from the simulation software.

"Fragile probability" typically refers to situations or systems where the likelihood of certain outcomes is highly sensitive to small changes in initial conditions or inputs. This concept urges caution in predicting and managing risks, emphasizing the need for robust and adaptable strategies.

### 3.2.3.2 Damage level classification

There are no clear quantitative indicators for damage ratings at the building component level, and the table here references damage ratings for buildings in the HAZUS model (fema\_hazus-flood-model-technical-manual-5-1), which defines the rating metric as brittleness and provides a description of the impact of different damage ratings on the interior and exterior of the building. Since the model evaluates the impact rating on the whole building when the structure is damaged by empirical statistics and does not directly generalize to the component level, this paper proposes a customized component damage rating.

DS Level	Description	Damage Scale	Damage Ratio
DS0	Insignificant damage to components below first-floor elevation. Water enters crawlspace/basement and touches foundation (crawlspace or slab on grade). Damage to components within the crawlspace/basement including base insulation and stored inventory. Minor damage to garage interiors including drywall, cabinets, electrical outlets, wall insulation (Garage is below the FFE). No sewer backup into the living area.	Insignificant	0.0-0.03
DS1	Water touches floor joists up to minor water enters the building. Damage to carpets, pads, baseboards, flooring. Damage to the external AC unit (if the AC unit is not elevated) and the attached ductworks (if ductworks are in the crawlspace). Complete damage to the garage interior (if the garage is below FFE). No drywall damages with the potential of some mold on the subfloor above the crawlspace. Could have a minor sewer backup and/or minor mold issue.	Slight	0.03-0.15
DS2	Partial damage to drywalls along with damage to electrical components (base-outlets), water heater and furnace. Complete damage to major equipment, appliances, and furniture on the first floor. Damage to the lower bathroom and kitchen cabinets. Doors and windows may need replacement. Could have a major sewer backup and major mold issues.	Moderate	0.15-0.5
DS3	Damage to the non-structural components and interiors within the whole building including (but not limited) drywall damage to upper stories for multi-story buildings (e.g., attic, second story, etc.). Electrical switches and mid-outlets are destroyed. Damage to bathroom/kitchen upper cabinets, lighting fixtures on walls are destroyed with potential damage to ceiling lighting fixtures. Studs reusable; some may be damaged. Major sewer backup will happen along with major mold issues. Equipment, appliances, and furniture on the upper floors are also damaged (e.g., attic, second floor, etc.).	Extensive	0.5-0.7
DS4	Significant structural damage present (e.g., studs, trusses, joists, etc.). Non-structural components and interiors are destroyed including all drywall, appliances, cabinets, furniture, etc. Damage to rooftop units/components including roof insulation, sheathing and electro-mechanical systems (rooftop AC units, electrical systems, cable railing, sound system, etc.). Foundation could be floated off. The building must be demolished or potentially replaced.	Complete	0.7-1.0

**Table 7:** Damage states description along with their damage scale and damage ratio as a percentage of the total building replacement cost.(Nofal et al., 2020)

Damage State	0	1	2	3	4	
Interior Damage Assessment		Water enters the foundation but no contact or no visible damage to electrical, plumbing, or floor joists.	Water enters house; damage to carpets, pads, baseboards, flooring, but no drywall damage. Touches joists. Could have some mold on subfloor above crawlspace.	Drywall damage up to 2 feet and electrical damage, heater and furnace and other major equipment on floor damaged; Lower bathroom and kitchen cabinets damaged. Doors need replacement.	Substantial drywall damage, electrical panel destroyed, bathroom/kitchen cabinets and appliances damaged; lighting fixtures on wall destroyed; ceiling lighting may be ok.	All drywall, ceiling lights, appliances, cabinets etc. destroyed and need replacement.
	Attachments or Detached Structures	Water touches exterior of garage or porch but no visible damage.	Visible damage or water marks/mud.	Minor damage to garage door/ minor damage on decks.	Major damage on garage door or on decks (i.e. garage door needs replacement).	Major or significant structural damage present; floated away or destroyed.
	Walls	Water may or may not touch walls but no visible damage.	Water touches walls but no damage on the wall or cladding or insulation, just aesthetic marks/mud.	Need to clean and dry the wall out. Slight damage on insulation or cladding which need partial replacement.	Water penetration through holes or cracks on the walls. Or water penetration through broken windows. Studs reusable when dried.	Significant structural damage present or collapse; majority of walls damaged beyond the point of reuse.
Foundation	Water enters crawlspace or touches foundation but no visible damage.	Water enters crawlspaces but not any significant damage. Just water marks/ mud.	Minor cracks on foundation stem walls.	Cracks or holes on foundation stem walls.	Major structural damage on foundation. Differential settlement or the structure floated off the foundation.	

**Table 8:** Damage descriptions for external and internal building components.(van de Lindt et al., 2018)

This paper customizes a damage grading approach designed to facilitate the visualization and assessment of overall building damage (Figure 20). The method categorizes the percentage of damage for each material into five categories, ranging from minor to severe damage. The definitions of the grades refer to the descriptions in the HAZUS model, and the five grades are color-coded from light to heavy magnitude in light to dark colors. (Table 9)

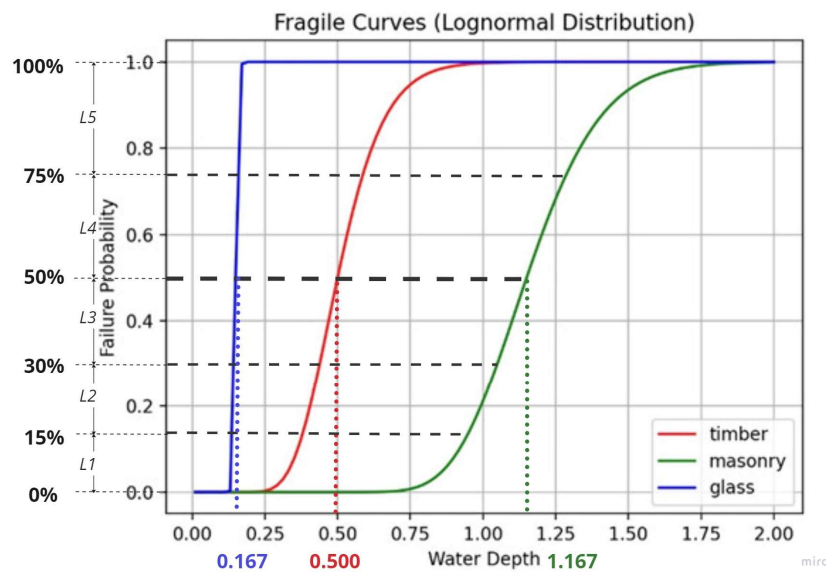


**Figure 20:** Fragile curves with different materials for individual components of a one-story residential building on a slab-on-grade foundation. Timber for door(RED); Masonry for wall(GREEN); Glass for window(BLUE)

Fragile class	Functionality	Damage Scale	Fragility probability	Color coding
<b>L1</b>	Operational	Insignificant	0-15%	Light yellow
<b>L2</b>	Limited Occupancy	Slight	15%-30%	Light orange
<b>L3</b>	Restricted Occupancy	Moderate	30%-50%	Orange
<b>L4</b>	Restricted Use	Extensive	50%-75%	Red
<b>L5</b>	Restricted Entry	Complete	75%-100%	Dark red

**Table 9:** Definition of fragile level

The upper limit of water depth corresponding to the fragility level of different materials can be obtained by reading the fragility curves. (Table 10) It should be noted that since the window has a height above the ground, it is necessary to add the height above the ground of the window to the original water depth to get the water depth capacity.

Materials	L1(m)	L2(m)	L3(m)	L4(m)	L5(m)
<b>Timber</b>	0.370	0.440	0.500	0.600	1.000
<b>Glass</b>	0.125	0.140	0.167	0.180	0.200
<b>Masonry</b>	0.900	1.150	1.167	1.300	2.000

**Table 10:** Definition of fragile level

### 3.2.4 Loss analysis approach

This subsection presents an alternative loss analysis method to compare building-level loss estimates and propagate uncertainties across all building formations. The analysis uses the probability of failure of building assemblies to calculate flood losses. Initially, the component failure probability is assessed to determine whether a component can continue to be used. The average total building replacement cost is then calculated by summing the number of components that lose functionality, each multiplied by the average simulated replacement cost per component. (Figure 21) This relationship is illustrated in equation (5-7).

$$L_k(IM = x) = P[D(x) > R_k | IM = x] \cdot \begin{pmatrix} Lr_k^1 \\ Lr_k^2 \\ \vdots \\ Lr_k^n \end{pmatrix} = \begin{pmatrix} L_k^1 \\ L_k^2 \\ \vdots \\ L_k^n \end{pmatrix} \quad (5)$$

$$L_t(IM = x) = \begin{pmatrix} L_1^1 \\ L_1^2 \\ \vdots \\ L_1^n \end{pmatrix} + \begin{pmatrix} L_2^1 \\ L_2^2 \\ \vdots \\ L_2^n \end{pmatrix} + \begin{pmatrix} L_3^1 \\ L_3^2 \\ \vdots \\ L_3^n \end{pmatrix} + \dots + \begin{pmatrix} L_N^1 \\ L_N^2 \\ \vdots \\ L_N^n \end{pmatrix} = \begin{pmatrix} L_t^1 \\ L_t^2 \\ \vdots \\ L_t^n \end{pmatrix} \quad (6)$$

$$\mu_{L_t}(IM = x) = \sum_{k=1}^N \mu_{L_k}(IM = x) = \sum_{k=1}^N \frac{\sum_{i=1}^n L_k^i}{n} \quad (7)$$

where  $L_k$  = a generated replacement cost vector for component  $k$  at a specified intensity measure ( $IM=x$ ),  $L_k^i$  = an  $i^{\text{th}}$  Flood Simulations simulated total replacement cost of component  $k$ , and  $L_k^i$  = an  $i^{\text{th}}$  Flood Simulations simulated replacement cost for component  $k$  at a specified intensity measure ( $IM=x$ ).  $L_t$  = a randomly generated total building replacement cost vector at a specified intensity measure ( $IM=x$ ),  $L_t$  = an  $i^{\text{th}}$  Flood Simulation simulated total building replacement cost, and  $P[D(x) > R_k | IM=x]$  = failure probability conditioned on the value of the intensity measure (depth) for component  $k$ .  $\mu_{L_k}$  = mean total building replacement cost at a specified intensity measure ( $IM=x$ ), and  $\mu_{L_k}$  = mean replacement cost of component  $k$  at a specified intensity measure ( $IM=x$ ).

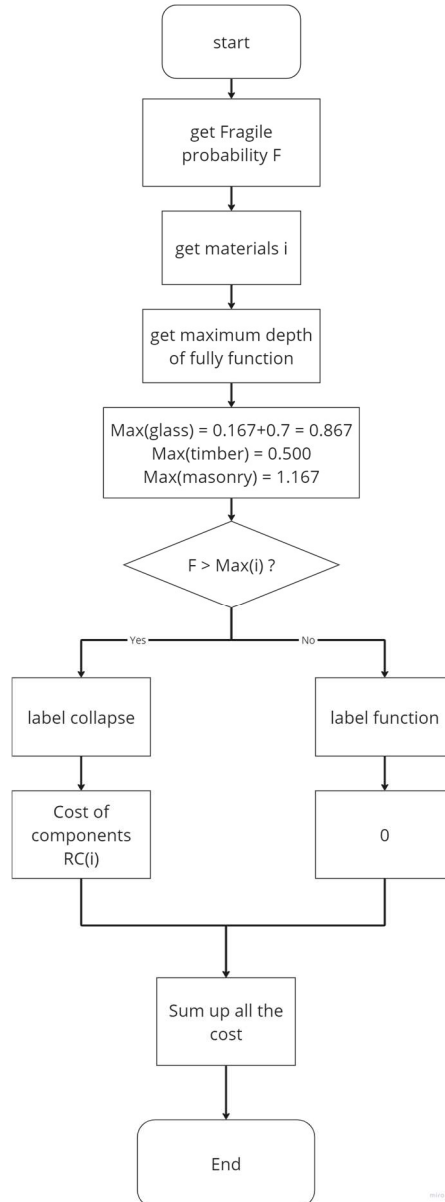


Figure 21: Flowchart of evaluating the damage state of building

The analysis assumes that the damage of any component is statistically independent from the damage of other components. From a practical standpoint, this assumption is necessary due to the lack of data correlating component damage to structural systems. Component replacement costs vary spatially (with

geographic price variability) and temporally (with market circulation timeliness). Therefore, these cost data were extensively collected using Home Advisor's online published costing methodology. Expert-provided data were based on selected areas of the building, and the price data included both the cost of building materials and the combined cost of labor to derive an average cost per component. (Table 11)

Component	DS0		DS1		DS2		DS3		DS4	
	Crawlspace Insulation	Flooring Insulation	AC Unit/ Heater	Wood Flooring	Washer/ Dryer	Lower Cabinets	Drywall (DS3)	Upper Cabinets	Wood Framing	Decking Flooring
Min depth (m)	-1.25	-0.3	-1.2	0	0.05	0	0.8	1.3	0.5	2
Max depth (m)	-0.85	0.1	0.6	1	0.25	0.9	1.5	2	4.5	4
Mean depth (m)	-1.05	-0.1	-0.3	0.5	0.15	0.45	1.15	1.65	2.5	3
Stan. Dev. of depth(m)	0.1	0.1	0.45	0.25	0.05	0.225	0.175	0.175	1	0.5
Min duration (hr)	0	0	0	48	0	24	24	24	144	144
Max duration (hr)	10	10	1	96	0.5	48	48	48	240	240
Mean duration (hr)	5	5	0.5	72	0.25	36	36	36	192	192
Stan. Dev. of duration (hr)	2.5	2.5	0.25	12	0.125	6	6	6	24	24
Min Rep. Cost (USD \$)	1420	710	3700	3720	350	9000	1167	6000	7100	14200
Max Rep. Cost (USD \$)	4260	2130	7200	6820	1500	18000	3501	12000	18460	35500
Mean Rep. Cost (USD \$)	2840	1420	5450	5270	925	13500	2334	9000	12780	24850
Stan. Dev. of Rep. Cost (\$)	710	355	875	775	287	2250	583	1500	2840	5325

**Table 11:** Average cost for each material

### 3.3 Digitalization

Interest in smart city development is surging among major ICT companies and governments worldwide responsible for urban innovation. This momentum, coupled with the proliferation of affordable and efficient sensors, has propelled the concept of urban spaces and digital twins. Urban digital twins necessitate the representation of cities as three-dimensional models, often with datasets too vast for conventional platforms to handle directly. Thanks to the swift advancements in Internet technology and computer hardware, leveraging web services for visualizing flow field simulations is now feasible. Visualization techniques can effectively portray intricate flow data and patterns, while BIM-GIS integrated method enable automated analysis of structural damage extent, with results accessible directly on ArcGIS platforms. This convergence facilitates collaborative decision-making among engineers, designers, and water regulators to enhance building resilience against flooding.

Building damage resulting from flooding is predominantly influenced by both flood dynamics and building attributes which correspond to two datasets: flood parameters (depth, duration, flow velocity) contributing to building damage, and the structural components of the target building that withstand flooding impacts. Geographic Information Systems (GIS) excel at providing large-scale characterization, offering data such as elevations, road networks, and building contours. Conversely, Building Information Modeling (BIM) supplements information regarding building geometry and material properties. Micro-level Flood Damage Analysis (FDA) necessitates a blend of both tools to achieve precise and specific risk assessments. Hence, a solution integrating BIM with GIS is imperative to fulfil the requirements of micro-level assessment and 3D visualization for potential building damage due to flooding. This assessment provides intuitive insights to support decision-making processes for designers, engineers, and other stakeholders.

#### 3.3.1 Three methods of BIM-GIS integration

BIM-GIS integration in the data collection of urban flood disaster has several groups of data sources, which are hazard data group, geographic information data group, building data group, and component data group. There are multiple data within each group, meaning that more format types need to be integrated in one digital tool, which is not simple. Therefore, issues in terms of spatial scales, granularity levels, differences in collection representations, storage and access methods, and semantic mismatches are discussed by Karimi et al. (Akinci et al., 2009; El-Mekawy, 2010; Karimi & Akinci, 2009)

(Amirebrahimi et al., 2015a) categorizes three types of integration:

- a) Application level; b) Process level; c) Data level.

### 3.3.1.1 Application level

For the application level, the integration approach uses central configuration or rebuild (Karimi & Akinci, 2009), where for GIS and BIM the application side is either modified by patching or rebuilt from scratch. This approach is costly and difficult to build and is not applicable to this project.

### 3.3.1.2 Process level

For process integration approaches, such as OGC's OWS-4 project (Zhu et al., 2019), an open source approach (OSA) is used to lubricate the exchange of information between BIM (IFC) and GIS (shapefile). The IFC-Tree is used on the BIM to identify the graphical information in the digital model, which is converted into a GIS-readable document using the algorithmic framework of Automated Multi-patch Generation (AMG). This approach links BIM and GIS information through semantic mapping and then completes the integration on a third-party platform, which is more flexible compared to application-based approaches. However, the underlying data layer integration also needs to be addressed and accomplishing interoperability is a major challenge for process integration.

### Implementation of flood damage visualization

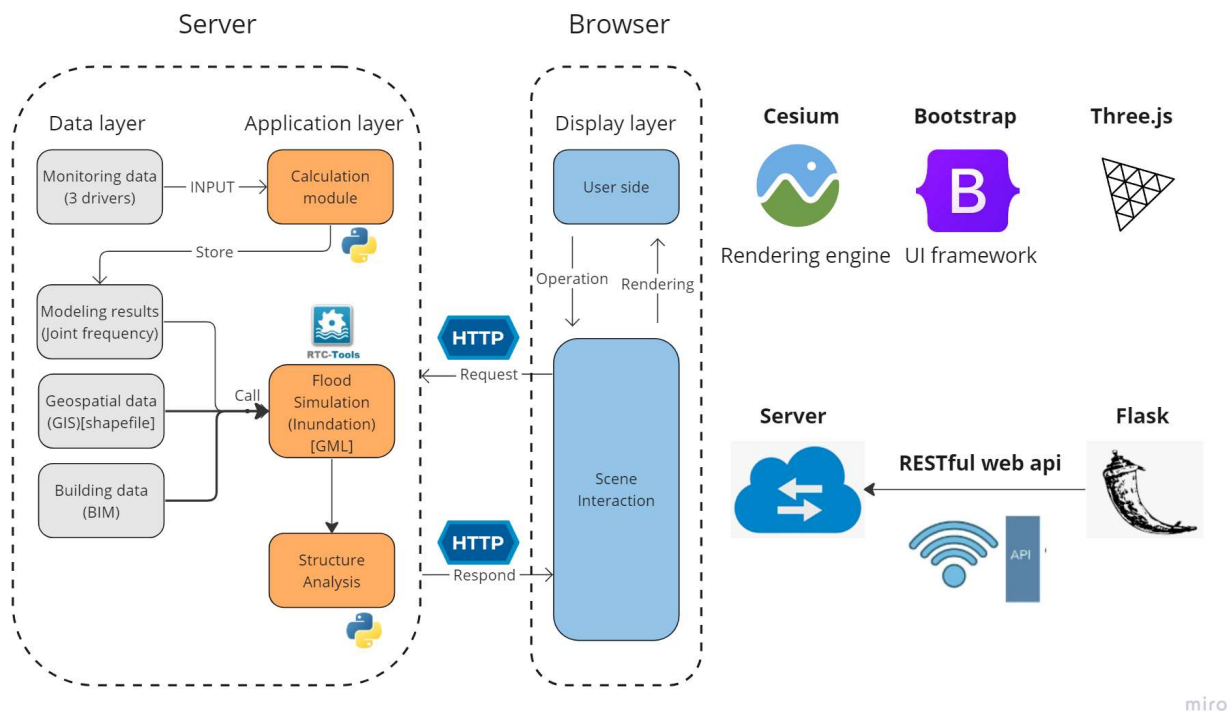


Figure 22: Research methodology for 3D visualization at process level

This study introduces the development of a watershed visualization platform based on the B/S architecture, designed specifically for water flow visualization. According to the logical relationships of business processing, the platform is divided into three layers: the data layer, the application layer, and the presentation layer. The overall framework of the platform is shown in Figure 22.

The data layer is managed by a database server for data storage and retrieval. In this study, the data layer stores monitoring data, water flow simulation results, and geographic spatial data. Monitoring data primarily originates from hydrological stations, including water level and flow rate data, which are transmitted in real-time to the data server via communication networks. Hydrodynamic models are used to simulate water flow and generate output results based on monitoring station data. Geographic spatial data (including images,

terrain, vector layers, and scalar layer data) are processed and loaded to create a three-dimensional environment within the watershed.

The application layer serves as the intermediary between the data layer and the presentation layer, facilitating data processing, transformation, and implementation of the platform's business logic. It comprises three modules: the flow calculation module, the flow visualization module, and the 3D visualization module.

The flow calculation module initializes the 2D hydrodynamic model using station monitoring data from the data layer, simulates river flow information, and stores the simulation results in the database based on different attributes.

The water flow visualization module is a crucial component of the platform. It offers three types of flow field data visualization methods—vector field visualization, scalar field visualization, and dynamic field visualization—depending on the input water flow data types. The model calculation results are transformed into colored texture information using shader technology.

In the 3D visualization module, the digital elevation model (DEM) data are rendered into a terrain grid by a graphic rendering engine. Additionally, images, annotations, and model data are loaded to construct a virtual environment of the watershed.

The display layer serves as the user interface where interactive commands and rendering results from the client are handled. The client-side display is rendered in the browser. When the user sends an interactive request to the server side through the operator interface, the application server responds to the request, calls the relevant module, and returns the result to the client display.

The platform follows a front-end and back-end separation model, employing languages and toolkits with open-source permissions. Bootstrap serves as the foundational UI framework for the front-end, while CesiumJS acts as the rendering engine for water flow and 3D visualization (Müller et al., 2016). Graphics shader operations are based on OpenGL ES version 2.0.

On the backend, Flask is utilized as the web server framework for monitoring and responding to requests. Function modules are deployed on the server side to provide calling interfaces, and data is stored in a MySQL database. Access to large, unstructured data such as high-precision images and videos is facilitated through a file server.

### **Challenge of Web GIS based visualization**

Using web-based visualization for this project presented several challenges:

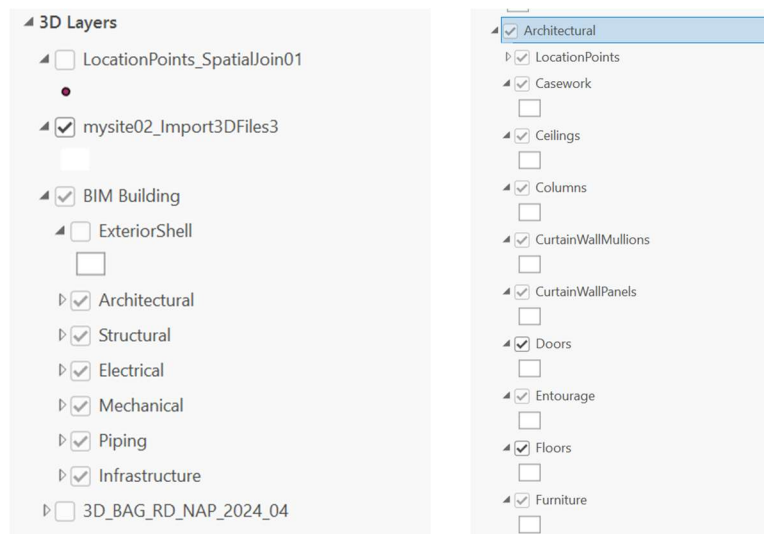
1. **Data Migration:** The simulation software needs to retrieve data online, perform simulations in the cloud, and export results via API. This necessitates a high degree of openness in the simulation software. Many open-source professional simulation tools are commercial and have limited usage periods. Additionally, when exporting BIM Revit models, even using the Wavefront OBJ format, significant model information is lost, which is critical for disaster analysis that relies on model attributes.
2. **High Computational Skills Required:** Implementing web-based visualization involves both front-end and back-end interactions, requiring the setup of a framework. The back-end typically uses Python and the Flask framework, while the front-end involves JavaScript and JSON, using the Vue framework. Even though Cesium has its own CesiumJS library, understanding, modifying, and integrating these different code formats demands high-level computer programming skills.

### 3.3.1.3 Data level

However, the challenges can be addressed effectively at the data level by using solutions provided by ESRI and ArcSDE. These platforms facilitate BIM and GIS data transfer through their application programming interfaces (APIs). For instance, the work by (Nagel et al., n.d.) demonstrates that GIS's commonly used format, CityGML, and BIM's commonly used format, IFC, can be directly converted within these systems, allowing the integration of models from both domains. In addition, tools such as ifcexplorer, BIMserver, FME(“FME Workshop on Formal Methods in Software Engineering FormaliSE 2013,” 2013), etc. export BIM model data directly to GIS and avoid loss of semantics. Patel et al. (2013) proposed a coupled semantic and geometric conversion method from IFC to CityGML. The IFC FOR GIS project aims to expand IFC models to include geospatial information.

In practical application, when importing BIM-based Revit models into ArcGIS Pro, it was found that the commonly used VRT format in Revit not only retains model attribute information in ArcGIS Pro but also displays different component categories in separate layers. This offers several advantages:

- A) It becomes easier to hide and show components, such as hiding the roof to better view interior damage.
- B) During data analysis, it allows for the differentiation of material properties and the assignment of corresponding vulnerability curves.
- C) Filters can be used to view damage levels within the same group or different components with the same damage level.



## 3.3.2 Methodology of computational analysis

### Data communication

To visualize the impact of compound flooding on building components, enabling stakeholders to clearly understand the location, extent, and cost of damage, simulation-derived results must be analyzed and visualized alongside building component properties. This section outlines the methodology for communicating data between applications and analyzes the changes in data structure relationships when Building Information Modeling (BIM) and Geographic Information Systems (GIS) are combined.

The figure 23 illustrates the path of data communication in the three components of data preparation, damage assessment, and visualization.

In the visualization part:

1. The color coding is obtained from the damage classification of each component by spatially combining the simulated flood data with the component vulnerability curves. The data are spatially combined by searching for the nearest value within a certain range in the "Spatial Join" function, which connects the raster data to the sensitivity of the material to flooding.
2. Multiple Climatic Environments is a combination of the results of flood simulations in different climatic environments with the attributes of the building materials. Three simulations are performed under three different regression cycles, and the results of each of them are repeated in part 1 to obtain the damage scenarios under the three climatic environments.
3. The data of the pop-up window is derived from the filtering of the BIM model attributes to obtain the component ID, class, and material.

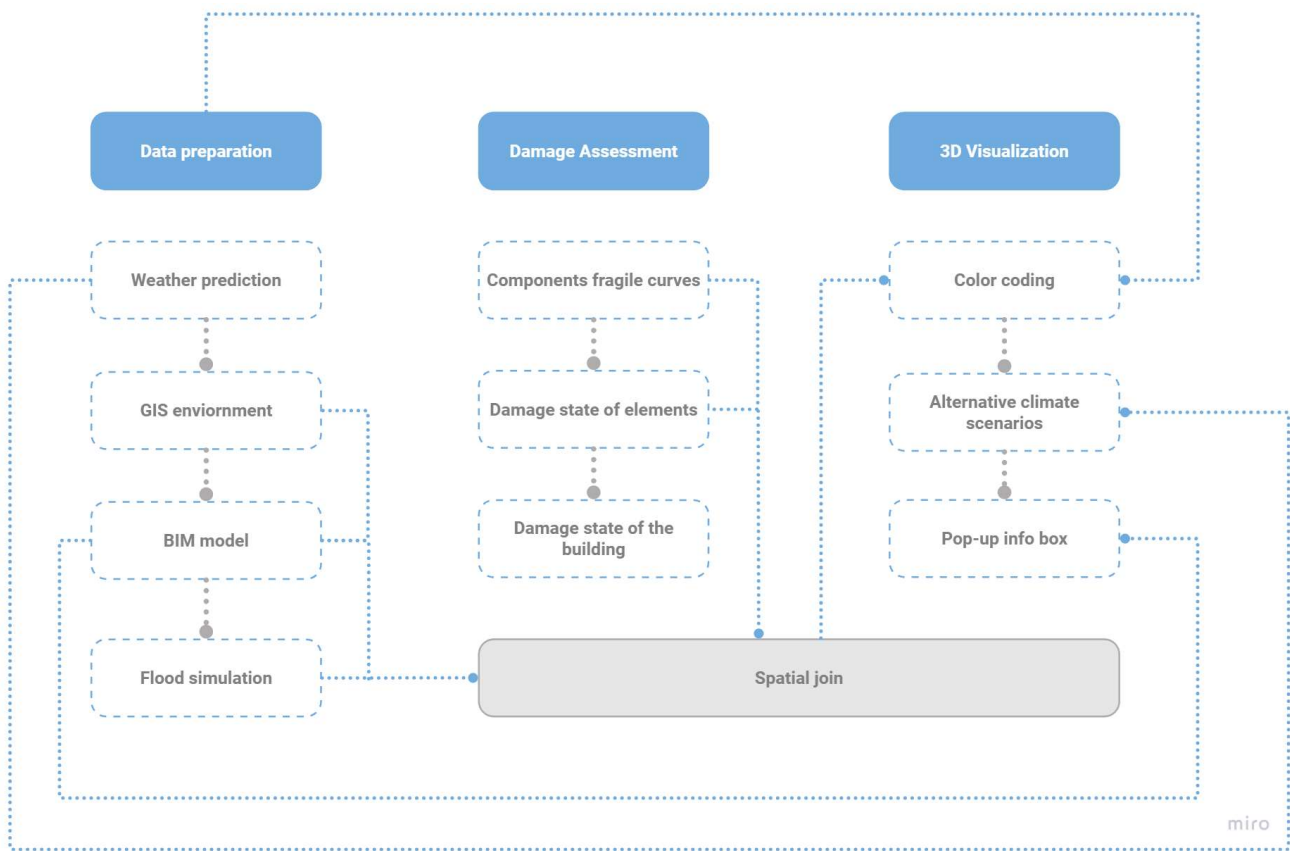


Figure 23: Overall workflow and conceptual data flow graph

The computational workflow involves the following steps:

1. **Data Extraction:** Extract the properties data of the building from the BIM model and construct the data structure using the hierarchical relationship of RVT.
2. **Modeling Environment Setup:** Build the modeling environment in ArcGIS Pro by importing the topography, coordinate system, and the CityGML format file of the 3D BAG, which contains the community-scale building contours and heights.
3. **Flood Map Integration:** Read the raster data from the flood map (spatial distribution of water depth) and fit it to the map.

- Water Depth and Vulnerability Analysis:** Analyze the water depth and vulnerability curves at the same location using "Spatial Join" to read the probability of component failure.
- Probability Classification:** Classify the probability by "Symbology" to mark the failure probability with different colors.
- Component Replacement and Cost Calculation:** Using the "Calculate Field" tool, count the number of components that need to be replaced (with a probability of failure greater than 50%) and calculate the cost of repairing the entire building.

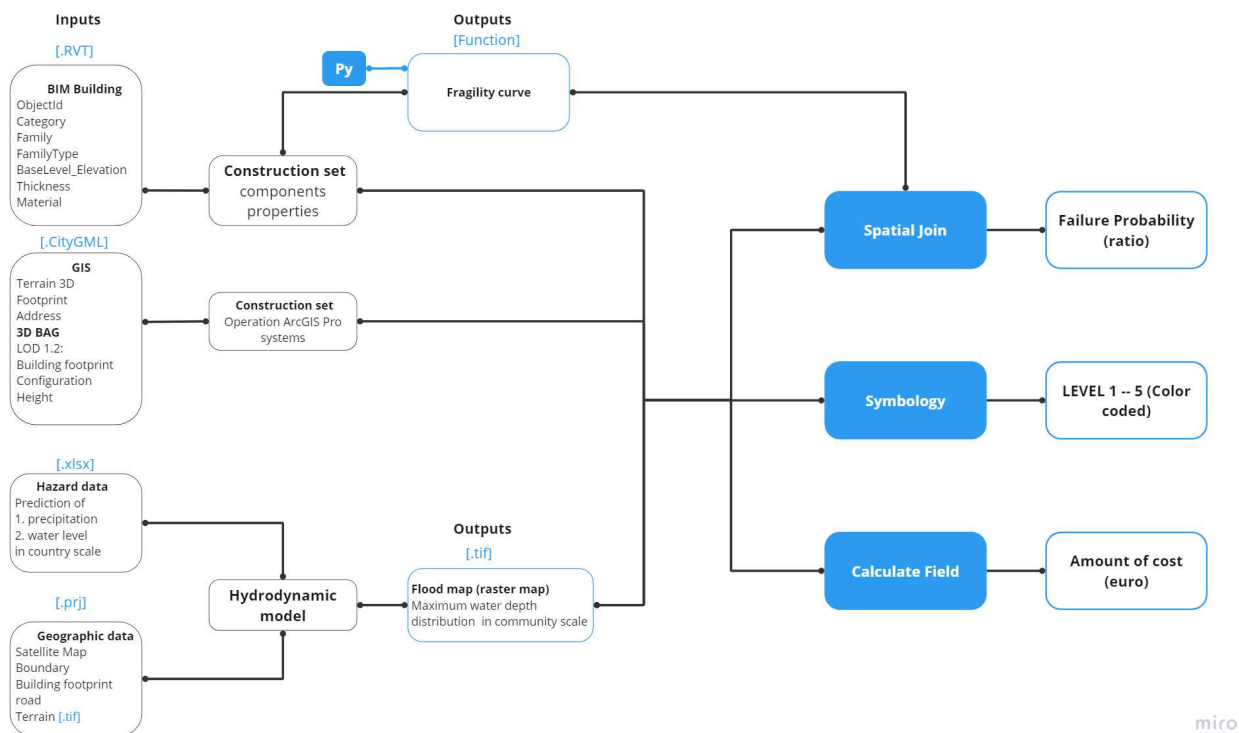
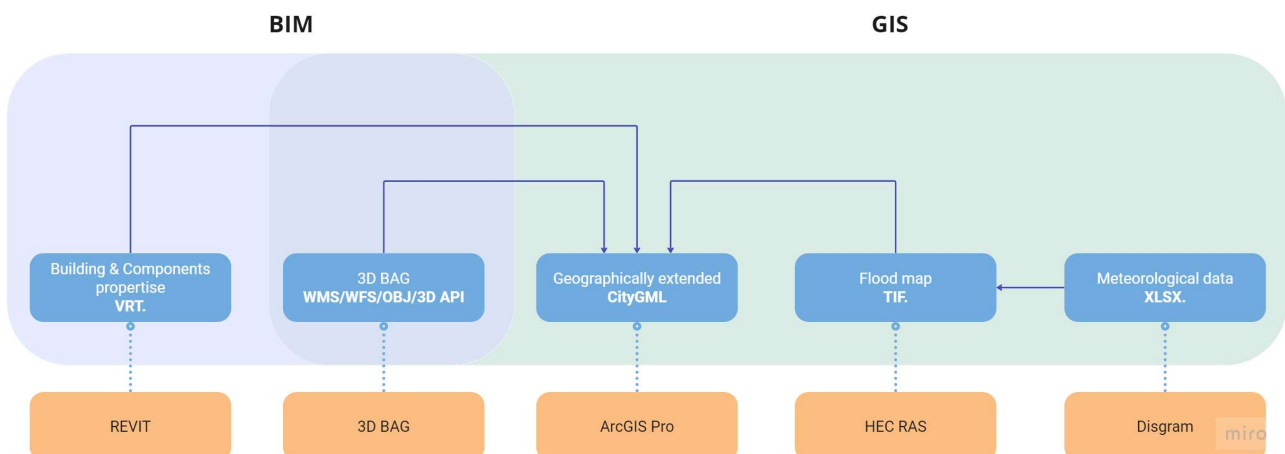


Figure 24: Computational workflow detailed program

### Data Utilization and Analysis



**Figure 25:** Collaboration between the database of BIM and GIS (including software and data format)

BIM-GIS based scenario analysis and demonstration is the essential feature for urban flood hazard assessment. GIS is designed to provide a visual representation of the topography, elevation, and intensity of the hazard in the affected area. BIM can reflect the detailed properties of the affected buildings and components. In addition, some studies have used VR AR technology (Padilha et al., 2019) for immersive disaster demonstration to visually identify the damage and impact factors caused by the disaster.

When converting between the two, it is particularly important to pay attention to the issue of changes in data attributes with loss of semantics, and doors are given as an example in the figure 26 to demonstrate such changes.

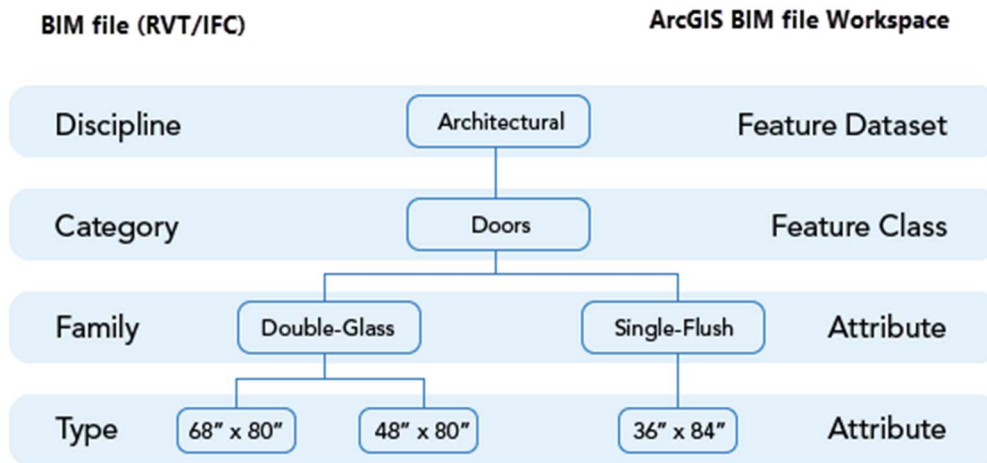


**Figure 26:** Correspondence between BIM, GIS model data features

On the other hand, the integration of these datasets allows the results to be presented on a GIS platform. Table 12 lists the type, components, representations, and data sources of the datasets. When selecting data sources, comparisons can be made to choose the one that is more general, contains more details, and is easier to communicate with.

Main type	Component	Representation	Potential data source	Data format
<b>Hazard</b>	Flood depth	Raster map	GIS (CityGML or WaterML)	Tif./ vrt.
	Flood velocity	Raster map	GIS (WaterML)	Tif./ vrt.
	Duration	Raster map	GIS (CityGML or WaterML)	Tif./ vrt.
	Maximum extent	2D polygon	GIS (CityGML or WaterML)	Tif./ vrt.
<b>Geographically info</b>	Address	Coordination	GIS	Xy.
	Footprint	2D polygon	GIS	XML

	Terrain	2D point with Z values	GIS	DEM/SDTS
<b>Building level</b>	Footprint	2D polygon	BIM	Vrt.
	Storeys & Spaces	3D surfaces	BIM	Vrt.
	Floor height	Z value	BIM	Vrt.
	Wall, Floor, Window, Beam, Column, Openings, Ceiling	3D representation by multi-surface and solid geometrics	BIM	Vrt.
<b>Components level</b>	Location	Centre point	BIM	Vrt.
	Elevation	2D point with Z value	BIM	Vrt.
	Materials	Textual description	BIM	Vrt.

**Table 12:** The data requirements analysis

### 3.3.3 Interactive map attempts

To enable interactive map functions, commands need to be issued from ArcGIS Pro to call the flood simulation software, ensuring real-time dynamic data updates. Specifically, invoking HEC-RAS within ArcGIS Pro can be attempted by applying external extension code. However, this approach requires a high proficiency in R language, and the extension code package is compatible only with ArcGIS, not with the higher version of ArcGIS Pro.

An alternative plug-in that supports similar data conversion is HEC-GeoRAS. HEC-GeoRAS is a GIS extension that provides users with a set of procedures, tools, and utilities for preparing GIS data for import into HEC-RAS and generating GIS data from RAS output. Nonetheless, this plug-in is supported only in ArcGIS version 10.2. Therefore, its applicability to ArcGIS Pro still needs to be expanded.

Another alternative is to share all relevant layers to ArcGIS Online. ArcGIS Online is a cloud-based geographic information system (GIS) platform that allows users to create, share, and analyze maps and spatial data. It provides a comprehensive suite of tools for mapping, data analysis, and collaboration, making it an essential resource for organizations and individuals involved in spatial data management.

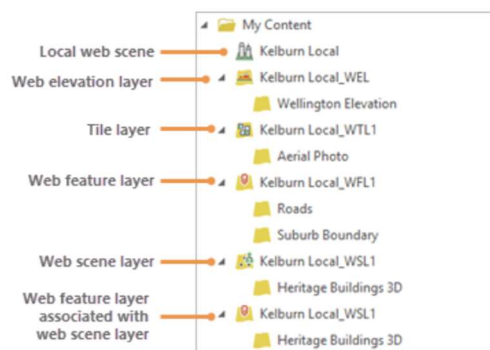
Developed by Esri, ArcGIS Online integrates seamlessly with ArcGIS Pro, ensuring that data transfer does not result in semantic loss. By using the "Share a Web Scene" feature, users can share scenes from ArcGIS Pro to their active portal. Web scenes are interactive geographic information presentations that enable the visualization and spatial analysis of data in 3D.

Note that due to different roles within the organization, there may be issues with sharing all layers of the entire scene in its entirety. (The screenshot on the left side below shows the type of layers in one scene.) This will require contacting the responsible person in the organization to change the privileges. Loading 2D data such as feature layers is commonly permitted; however, the sharing of tile layers has been restricted due to the limitations of a student license. (The graph on the right side below indicates the student license privileges, which the tile layer isn't allowed to published.) Due to time constraints, the organizers could not be contacted to resolve this issue. As a result, the online page only shows the extent of the damage to

representative points of the components. This limitation contradicts the purpose of the visualization. Therefore, in this paper, visualization was performed solely on the local ArcGIS Pro software.

For future web-based interactive maps, there are two potential solutions:

1. Switch to ArcGIS software and call the HEC-RAS simulation results in ArcGIS through the HEC-GeoRAS extension.
2. Request the "Publish Hosted Tile Layers" permission from the organizer of the ArcGIS Online group and store the data in the cloud.



**Role Privileges:**

- Edit features
- Publish hosted feature layers
- Publish hosted scene layers
- Add members from other organizations
- Create, update, and delete groups
- Create, update, and delete content
- Join organization groups
- Join external groups
- Share content with groups
- Share content with organization
- Share content with public
- View groups shared with organization
- View content shared with organization
- View organization members
- Demographics
- Feature report
- GeoEnrichment

Finally, to make the map interactive, ArcGIS Pro software utilizes the combination of different layers. This includes displaying the damage level of various components under the same disaster scenario and the response of the same component to different disaster levels. By toggling layers on and off, a certain degree of interactivity is achieved. The specific workflow is illustrated in the accompanying figure 27.

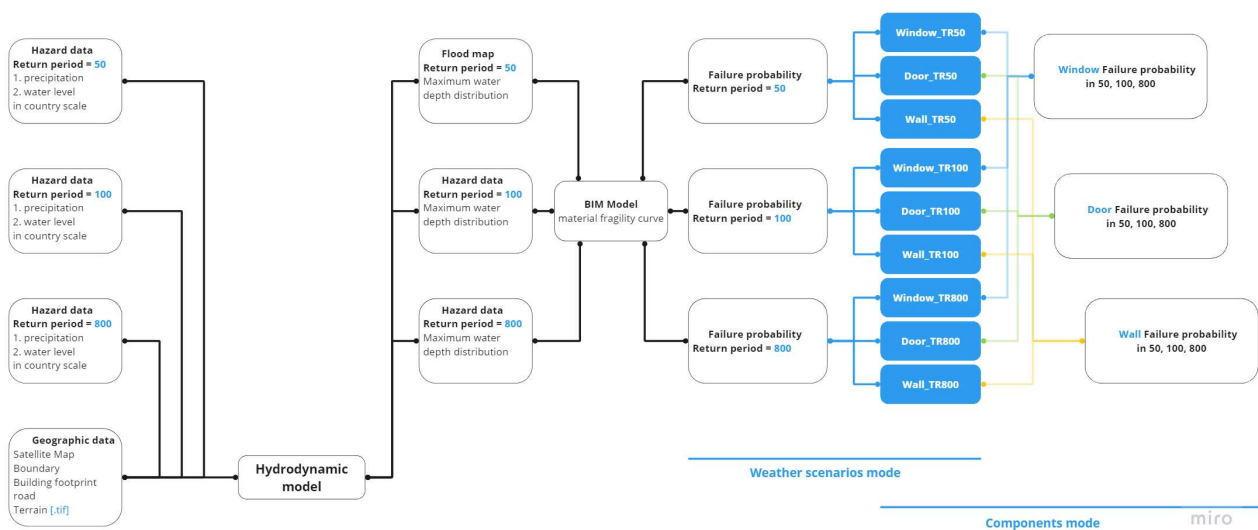


**Figure 27:** Different modes in visualization

## 4 Case study

The study site is a residential area located next to the coastline of The Hague, with a perimeter of about 900 meters and an area of about 42,833 square meters. The coordinates of the four vertices are 52.066758, 4.210271; 582960.61, 5769154.40; 52.090993, 4.245268; 585313.25, 5771890.31; and are enclosed in the red box in the figure 28. In this residential neighbourhood, the buildings are two- to three-story, hip-roofed masonry structures with wood doors and glass windows. The address of Tortellaan 37, 2566 CE Den Haag (Fig. 26) is highly similar to the improved building department house in terms of structure, material floor height, area, and building profile.

The area is also a coastal neighborhood. From the Figure 29, it is understood that this area is a disaster-prone risk zone. If extreme weather occurs, the risk is high and the potential for loss of human life is significant. Therefore, it should be emphasized as a priority area for risk control design. Selecting this area as a research object holds high value for methodological justification.



Figure 28: Satellite map of the site, red line is the coastline, red box is the site area



**Figure 29:** Target replaced building located in Tortellaan 37, 2566 CE Den Haag



**Figure 30:** Flood heatmap to highlight this community is vulnerable to flooding

The selected BIM model is a two-story residential building with a basement. The building dimensions are 62.31 meters in length, 10.61 meters in width, and 17.8 meters in height (excluding the basement). The structure is supported by shear walls, and it primarily consists of three types of materials: masonry for the walls, glass for the windows, and wood for the doors. The exact method of obtaining this model is detailed in Section 4.2: Data Preparation.



## 4.1 Methodology and workflow

The framework outlined in this chapter consists of three main sections (Figure 31): data preparation, flood damage analysis, and 3D visualization. In the initial phase, Flood Damage Analysis (FDA) integrates flood, building, and geographic data into a cohesive metadata framework. Based on this, structural fragility curves are drawn from the water resistance of the materials. Subsequently, the flood data are spatially integrated with the vulnerability curves, which means that the probability of failure of each component depends on the water depth (distribution location) and the material (water resistance). Finally, the probabilities are derived with damage classes and color-coded to indicate the degree of damage (DS). And more user-friendly features are proposed, such as selecting climate scenarios to compare damage results (with weather data), selecting the same component to see the DS distribution. Or selecting levels of DS to see the type of components with the same DS, etc., and finally there is a pop-up window to display more details intuitively. Each of these sections will be further elaborated in subsequent subsections.

The communication of data is also represented in the figure by dashed lines. Because the assemblies are in the same meta-model, inputs and outputs are straightforward. The spatial join tool in ArcGIS Pro is the key to connecting flood, building, and geographic information. All data are attributes with corresponding spatial relationships, which is the basis for integrating all data. Simply use the spatial location as a clue, and each variable can be overlaid on that spot.

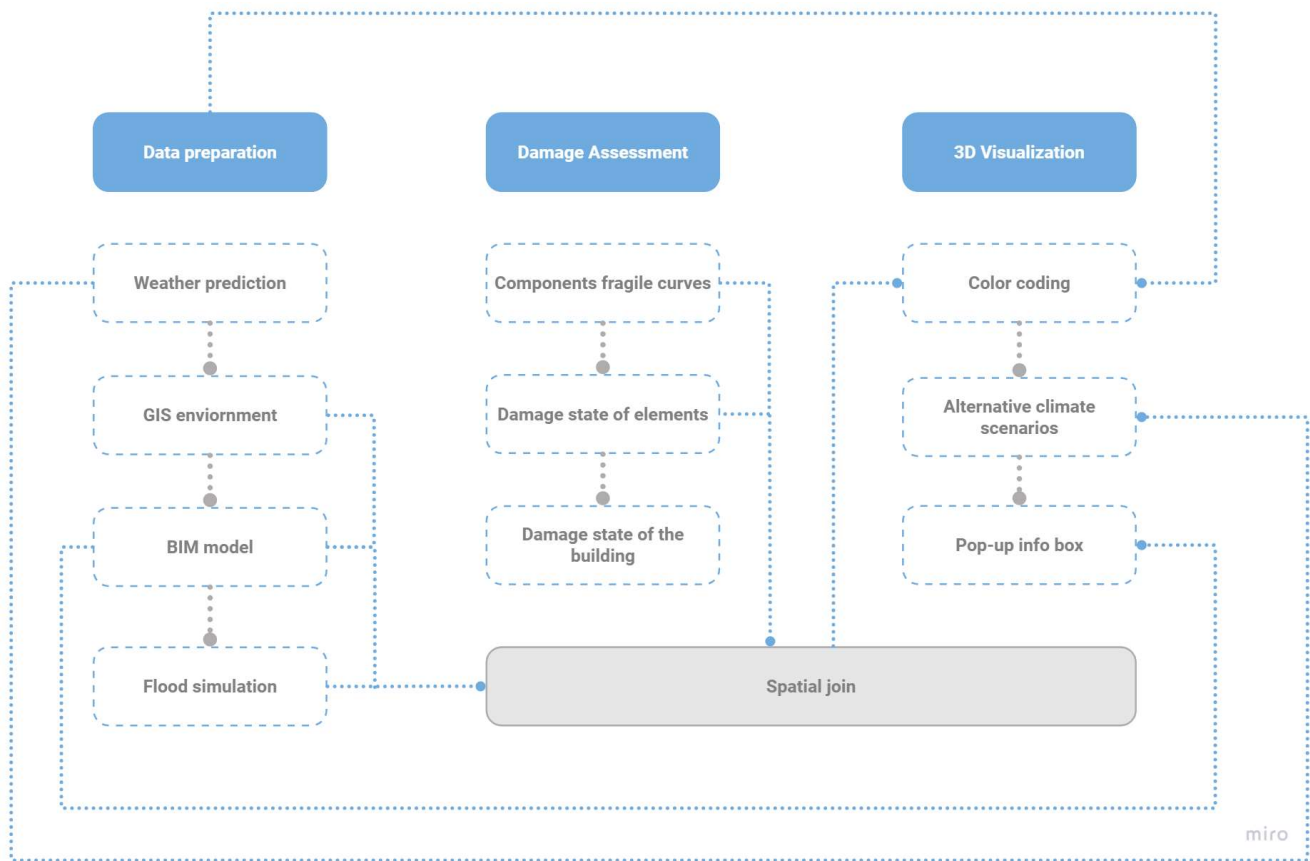


**Figure 31:** Methodology workflow diagram in case study.

## 4.2 Data preparation

The data preparation phase comprises the acquisition and integration of information from diverse sources, divided into two key steps. The first step involves forecasting future flood parameters—such as water depth, velocity, and duration corresponding to the spatial distribution—derived from the drivers of compound flooding. The second step entails modelling information, encompassing building attributes and geographic data.

Regarding flood parameters, which inherently involve 3D spatial and temporal considerations, statistical models are commonly employed to characterize the composite time and estimate its probability of occurrence. Several examples of such statistical models are documented in the literature, utilizing methodologies such as Copula (Lian et al., 2013), Bayesian networks (Gutierrez et al., 2011), bivariate extreme value models (Zheng et al., 2013), or physical modelling (Kew et al., 2013). However, accurately assessing extreme events and predicting their future likelihoods based on limited observational data pose significant challenges. Strategies to address this challenge include leveraging results from multiple sites or employing large ensembles of physical models. While bivariate models are sometimes utilized in idealized settings, they are often constrained by the choice of distribution functions. In contrast, regional climate-based models (RCM) tend to offer a better fit to real-world events (Kew et al., 2013).

### Flood data

In January 2012, a series of active low-pressure systems passed through the North Sea from west to east, accumulating more than 60 mm of rainfall in five days and five consecutive tidal storm surges without any gravity drainage (van den Hurk et al., 2015). This was due to higher than normal rainfall in the preceding weeks and saturated soils across the region. Inland high water levels exceeded the +7 cm Normal Amsterdam Level

(NAP) warning level, leading to precautionary measures such as evacuation and the use of emergency overflow areas.

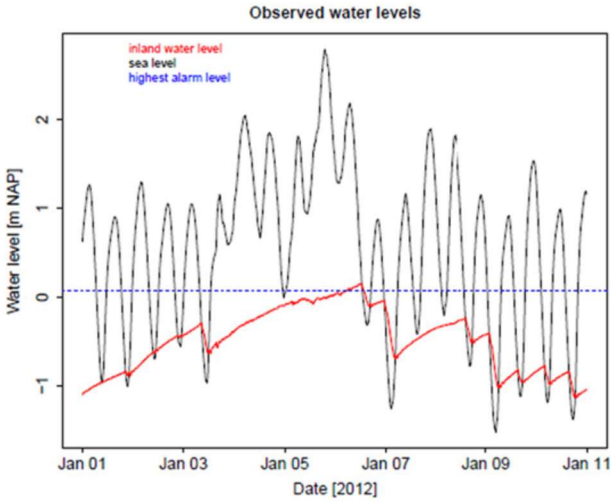


Figure 32: Observed water level in the North Sea (black line) and inland water level close to the Lauwersmeer outlet to the North Sea (red line) during the first 3 weeks of January 2012.(van den Hurk et al., 2015)

In order to perform a reliable analysis of this event, Santos et al. (2021) uses the RCM simulation ensemble to simulate the above event. RCM (regional climate model) is a statistical model used to simulate climate conditions over a specific region of the Earth. They take into account finer spatial details compared to global climate models, making them suitable for assessing regional climate impacts, including temperature, precipitation, and extreme weather events. RCMs are essential for understanding the localized effects of climate change and flood prediction.

By perturbing the initial atmospheric state of the EC Earth in 1850 and assuming historical greenhouse gas concentrations, running each member up to the year 2000 generates an ensemble that gives  $16 \times 50 = 800$  years of weather representative of present-day climate conditions. These regional simulations were then used to drive RTC-Tools, which is a hydrological management simulator generating the corresponding IWL time series at hourly resolution.

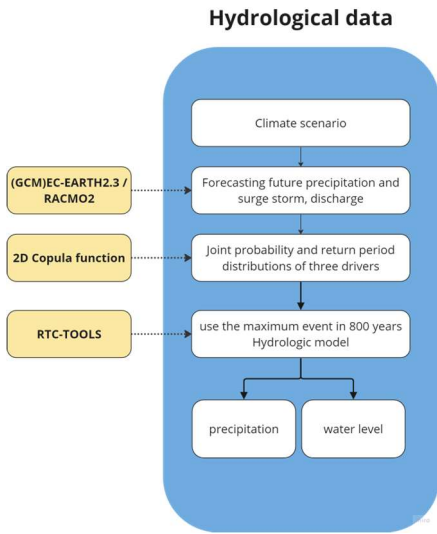
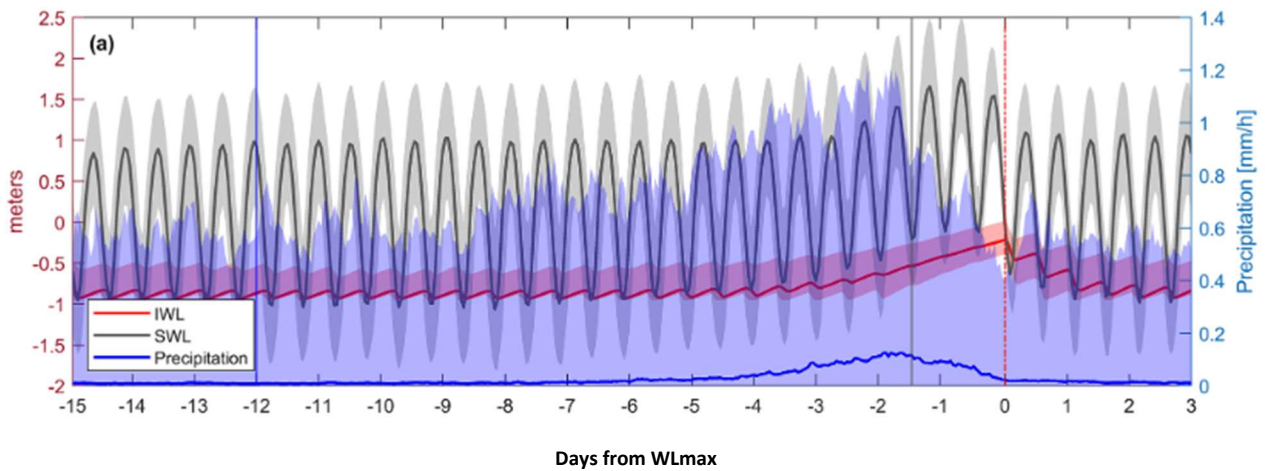


Figure 33: Framework of prediction future flood scenarios



**Figure 34:** Presenting the flood drivers and associated IWL (inland water level), which are computed use all 800 annual maximum events. Solid lines represent the median of all values at a given time, whereas the shaded areas depict the values between the 5th and 95th percentiles. Vertical lines indicate the time windows used for the selected predictors. (Santos et al., 2021)

The source of the weather data for this paper is taken from the 24-h window in which the peak water level is located in this figure. Weather data reads inland water levels and rainfall over a series of time steps during the day.

### Three flood scenarios

As the return period increases, the disaster level intensifies, leading to more severe damage to building components. Understanding the damage status of components across different return periods and the total loss cost of the building is crucial for accurately assessing the disaster-resistant performance of the building throughout its service life and determining when maintenance of specific components is required.

Based on Santos et al. (2021)'s study, a bivariate copula model was applied to fit the effects of rainfall and water level on the Inundation Water Level (IWL). This model helps estimate the impact of changes in the return period on the IWL return level, providing valuable insights into how varying disaster levels affect building damage and loss estimation.

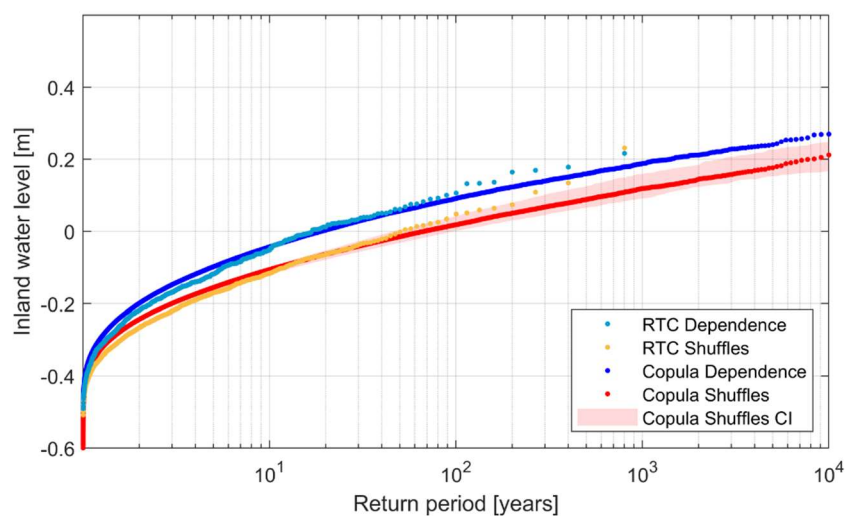


**Figure 35.** IWL return level against estimated return period using a bivariate copula model (2D case). (Santos et al., 2021)

The maximum water depths for which the regression periods are 50, 100, and 800 years are selected as meteorological data, and the water levels and rainfall for the three flood scenarios can be obtained by isometrically scaling the data for the 24-hour window period in Fig. 30, as shown in Table below.

Precipitation [mm/h]:

Hour	TR = 800	TR = 100	TR = 50
1	0	0	0
2	0	0	0
3	8	4.488	1.336
4	15	8.415	2.505
5	10	5.61	1.67
6	60	33.66	10.02
7	50	28.05	8.35
8	6	3.366	1.002
9	3	1.683	0.501
10	2	1.122	0.334
11	6	3.366	1.002
12	10	5.61	1.67
13	16	8.976	2.672
14	70	39.27	11.69
15	30	16.83	5.01
16	10	5.61	1.67
17	5	2.805	0.835
18	3	1.683	0.501
19	2	1.122	0.334
20	5	2.805	0.835
21	30	16.83	5.01
22	50	28.05	8.35
23	25	14.025	4.175
24	0	0	0

Water level [m]:

Hour	TR = 800	TR = 100	TR = 50
1	0.127717	0.071649	0.021329
2	0.054348	0.030489	0.009076
3	0.029891	0.016769	0.004992
4	0.201087	0.11281	0.033582
5	0.665761	0.373492	0.111182
6	0.861413	0.483253	0.143856
7	1.22826	0.689054	0.205119
8	1.57065	0.881135	0.262299
9	1.62573	0.912035	0.271497
10	1.74185	0.977178	0.290889
11	1.57065	0.881135	0.262299
12	1.15489	0.647893	0.192867
13	0.665761	0.373492	0.111182

14	0.347826	0.19513	0.058087
15	0.10361	0.058125	0.017303
16	0.543478	0.304891	0.090761
17	1.03261	0.579294	0.172446
18	1.2038	0.675332	0.201035
19	1.52174	0.853696	0.254131
20	1.30163	0.730214	0.217372
21	1.08152	0.606733	0.180614
22	0.88587	0.496973	0.14794
23	0.592391	0.332331	0.098929
24	0.523651	0.296584	0.078564

## BIM data

BIM model originates from the Faculty of Architecture at Delft University of Technology. The file was too complex and large and did not fit the residential footprint of the selected site. Therefore the original model was modified and simplified as shown in the figure 36. In addition, in order to locate the damage to the walls of each classroom more accurately, the masonry walls were assumed to be separate walls separated by room boundaries, and a simplified one- storey BIM model was created as shown in the figure 36.



**Figure 36:** Simplified BIM Model and separated wall with one-storey (referred to faculty of Architecture in TUDelft)

The BIM data of the surrounding community of the target building was downloaded from the 3D BAG developed by TUDelft. To make the metamodel more lightweight, the LoD1.3 version of the OBJ format model was selected.

Although the 3D BAG can be directly utilized in ArcGIS using built-in tools without needing to download the OBJ model separately, it is necessary to replace an existing BIM building on the site with another building. Since the community model imported directly through ArcGIS tools is a non-editable entity, the community model is loaded manually. (Figure 37)

**3D BAG:** The 3D BAG is a 3D model dataset developed by TUDelft that represents buildings and addresses across the Netherlands. BAG stands for "Basisregistraties Adressen en Gebouwen," which translates to "Basic Registration Addresses and Buildings." The 3D BAG dataset provides detailed and standardized 3D representations of buildings, which can be used for various applications, including urban planning, architecture, and disaster management.



**Figure 37:** Load 3D BAG package in ArcGIS pro automatically and load obj. file downloaded from 3D BAG web site in LoD1.3 version

**LoD (Level of Detail):** Level of Detail refers to the degree of detail in a 3D model. LoD1.3 indicates a specific level of detail in the 3D model. Generally, LoD levels range from LoD0 to LoD4, with higher numbers indicating more detailed models. (Fig. 33) For instance:

- LoD0: A basic representation with simple building footprints.
- LoD1: Simplified block models representing building shapes and heights (LoD1.3 implies a slightly more detailed version within this category).
- LoD2: Models with differentiated roof structures.
- LoD3: Detailed architectural models with windows, doors, and facade structures.
- LoD4: Models that include interior details as well.

Selecting LoD1.3 ensures a balance between model detail and computational efficiency, making it suitable for applications requiring lightweight yet sufficiently detailed models.

#### Data layers

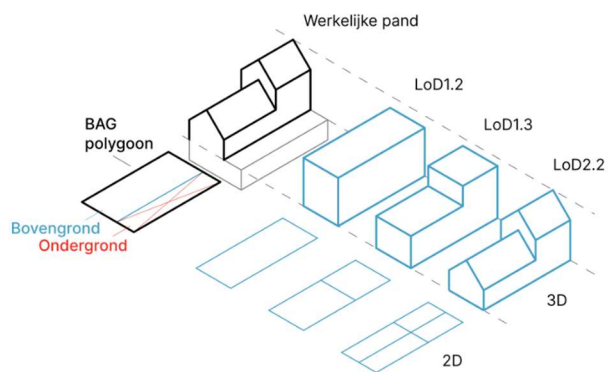


**Figure 38:** Illustration of LoD diagrams with different accuracies

#### GIS

Data in ArcGIS Pro:

The GIS data comes from the map and elevation data that comes with ArcGIS pro.

Data in HEC RAS (Table 13):

Type	Format	Description	Source
Georeferenced projection files	.prj		Spatial Reference <a href="https://spatialreference.org/">https://spatialreference.org/</a>
DEM(Digital elevation model)	.tif	16-level resolution Hi-Res Terrain Corrected	USGS <a href="https://earthexplorer.usgs.gov/">https://earthexplorer.usgs.gov/</a>
Satellite imagery	.tif	16 level	SAS planet <a href="http://www.sasgis.org/download/">http://www.sasgis.org/download/</a>

**Table 13:** Data collection for simulation

### 4.3 Flood simulation

#### Tool selection

Due to the need for consistency between the detailedness and scale of the predictive models for disasters and subsequent structural damage simulation, to ensure the transmission and reception of flood parameter data, it is preferable to accomplish this within the same system. Recent advancements in flood modeling, such as 3D Smoothed Particle Hydrodynamics, and some commercial tools (Delft3D, VISDOM, MIKE 21, TUFLOW, HEC-RAS, GeoHECRAS ) are available for this purpose. The most widely used HEC RAS and MIKE 21 hydraulic models were simulated, and the differences between the results and historical observation data were compared.

Software	Advantage	Disadvantage	Application on flood
HEC-RAS	<ul style="list-style-type: none"> <li>• User-friendly graphical interface for creating and visualizing models.</li> <li>• Widely used and recognized in the engineering community.</li> <li>• Capable of simulating both steady-state and unsteady flows.</li> </ul>	<ul style="list-style-type: none"> <li>• Limited ability to depict complex geometries and boundary constraints.</li> <li>• Computationally intensive for large models or complicated simulations.</li> <li>• Limited in managing interactions between water and the environment, such as sediment transport.</li> </ul>	<ul style="list-style-type: none"> <li>• Riverine floodplain modeling and study.</li> <li>• Assessment of various floodplain management methods.</li> <li>• Evaluation of the effects of planned developments on floodplain conditions.</li> </ul>
MIKE FLOOD	<ul style="list-style-type: none"> <li>• Comprehensive and versatile flood study and prediction tool.</li> <li>• Handles a broad range of hydraulic and hydrological processes.</li> <li>• Integrates with other MIKE software tools for a</li> </ul>	<ul style="list-style-type: none"> <li>• Steep learning curve for new users.</li> <li>• Computationally intensive for large models or complex simulations.</li> <li>• Requires a high level of technical expertise to use effectively.</li> </ul>	<ul style="list-style-type: none"> <li>• Riverine and coastal floodplain modeling and analysis.</li> <li>• Evaluation of different floodplain management strategies.</li> <li>• Assessment of the impacts of proposed</li> </ul>

	more comprehensive solution.		developments on floodplain conditions.
<b>TUFLOW</b>	<ul style="list-style-type: none"> <li>• User-friendly interface with graphical tools for building and visualizing models.</li> <li>• Handles a wide range of hydraulic and hydrological processes.</li> <li>• Flexible and adaptable to unique modeling requirements.</li> </ul>	<ul style="list-style-type: none"> <li>• Limited in handling large-scale models or complex simulations.</li> <li>• Steep learning curve for new users.</li> <li>• Requires a high level of technical expertise to use effectively.</li> </ul>	<ul style="list-style-type: none"> <li>• Riverine and coastal floodplain modeling and analysis.</li> <li>• Evaluation of different floodplain management strategies.</li> <li>• Assessment of the impacts of proposed developments on floodplain conditions.</li> </ul>

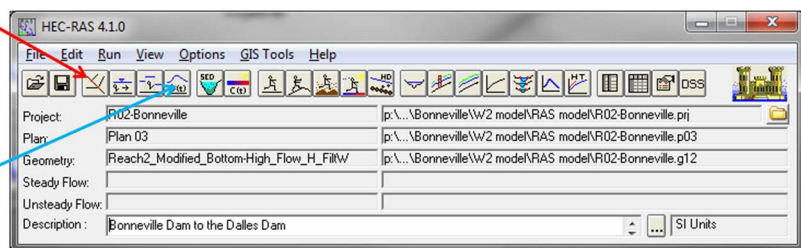
**Table 14:** Comparison of three simulation software (HEC-RAS, MIKE FLOOD, TUFLOW)

Due to the relationship between computational load and data accuracy, the HEC RAS software, which is lighter and faster and requires less input data, was finally selected.

### Data input

The inputs to the HEC RAS are divided into two types of data: geometric data, and hydrologic data. The geometric data are the simulated area, boundary conditions, barrier buildings and their heights. The hydrological data is obtained by Santos et al. (2021) predicted extreme flood data where the rainfall and water level heights can be intercepted for 24 hours during the peak period.

- Geometry
  - Cross Section
  - Scope
  - Buildings
- Flows
  - Precipitation
  - Flow speed
  - Inland water level





# Data output

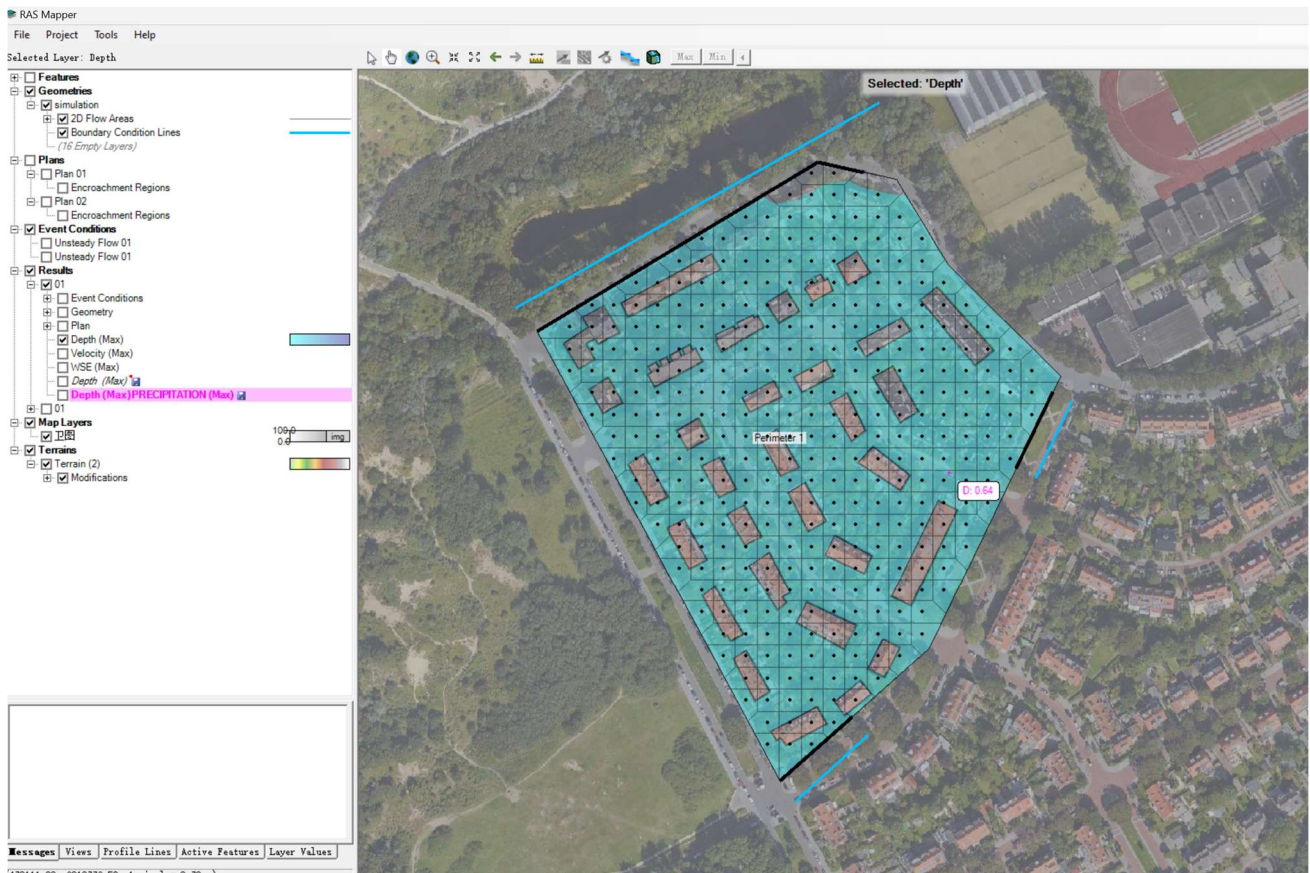


Figure 40: Water depth distribution map

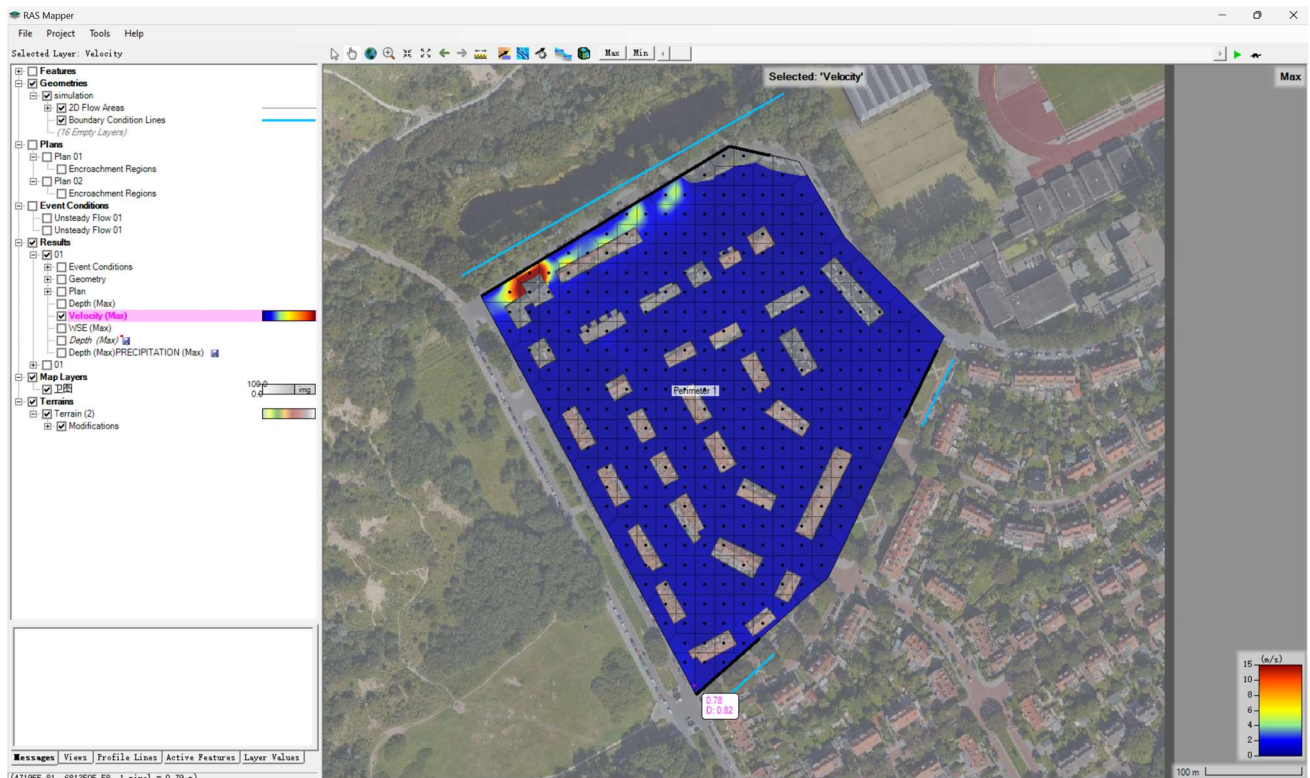


Figure 41: Flow velocity distribution map

## Result display in python

HECRAS Controller is a part of the HEC-RAS application programming interface (API). When trying to fetch data with this function as shown in the figure 42, the output is in the bottom right corner, the first column is the node ID and the last column is the water depth.

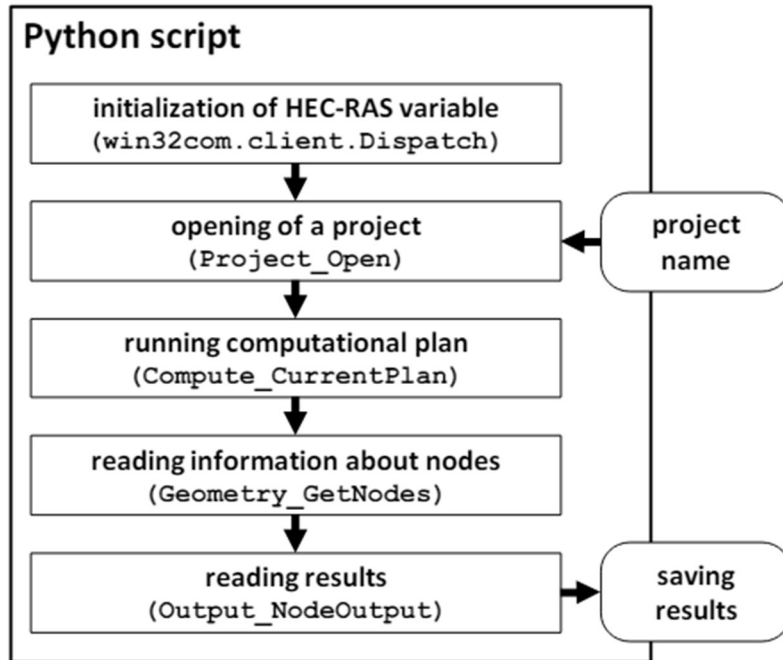


Figure 42: The flowchart that calls the HEC RAS controller and reads the results

```

# create HEC-RAS controller
hec = win32com.client.Dispatch("RAS641.HECRASController")
hec.ShowRas() #show HEC-RAS windows
# open HEC-RAS
RASProject = os.path.join(os.getcwd(),r'E:\TUD_BT\Graduation topics\P3\statistic\URBAN.prj')
hec.Project_Open(RASProject)
# to be populated: number and list of messages, blocking mode
NMsg,TabMsg,block = None,None,True
# computations of the current plan
v1,NMsg,TabMsg,v2 = hec.Compute_Currentplan(NMsg,TabMsg,block)
#ID numbers of the river and the reach
RivID,RchID =1,1
#to be populated: number of nodes, list of RS and node types
NNod,TabRS,TabNTyp = None,None,None
# reading project nodes: cross-sections, bridges, culverts, etc.
v1,v2,NNod,TabRs,TabNTyp =hec.Geometry_GetNodes(RivID, RchID,NNod,TabRS,TabNTyp)
# ID of output variables: WSE, ave velocity
WSE_id,AvVel_id = 2,23

TabWSE= numpy.empty([NNod],dtype=float) # NumPy array for WSE
TabVel = numpy.empty([NNod],dtype=float) # NumPy array for velocities
for i in range(0,NNod): # reading over nodes
    if TabNTyp[i]=="": # simple cross-section
        # reading single water surface elevation
        TabWSE[i],v1,v2,v3,v4,v5,v6 =hec.Output_NodeOutput(RivID,RchID, i+1,0,1,WSE_id)
        # reading single velocity
        TabVel[i],v1,v2,v3,v4,v5,v6 =hec.Output_NodeOutput(RivID,RchID,i+1,0,1,AvVel_id)
hec.QuitRas() # cose HEC-RAS
del hec # delete HEC-RAS controller

sc1_ShowNodes( NNod, TabRs, TabNTyp, TabWSE, TabVel )

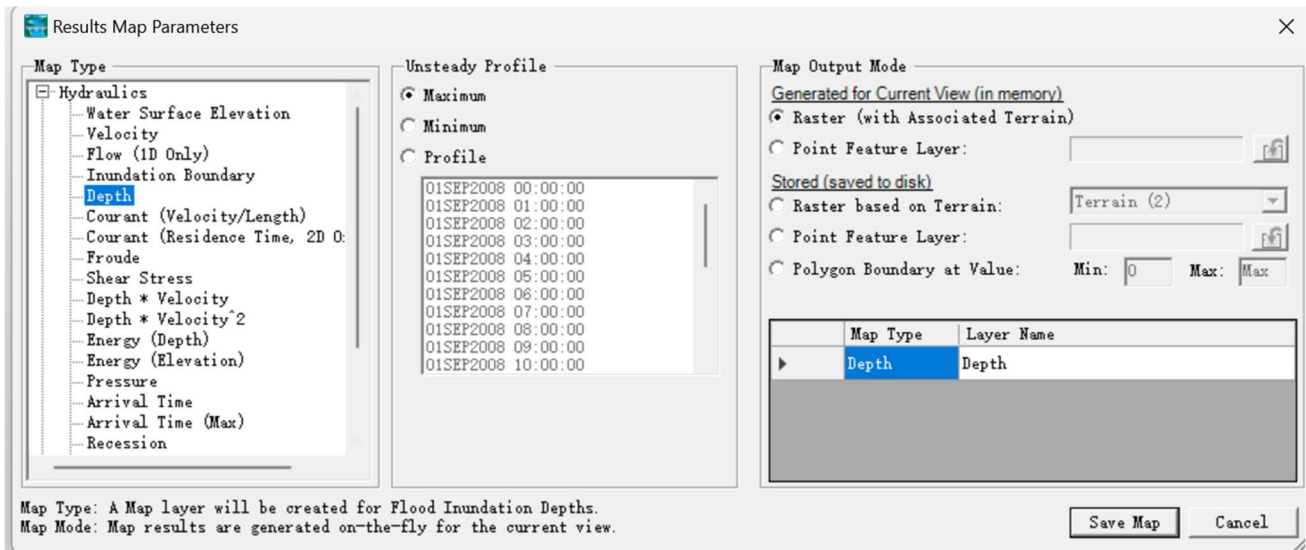
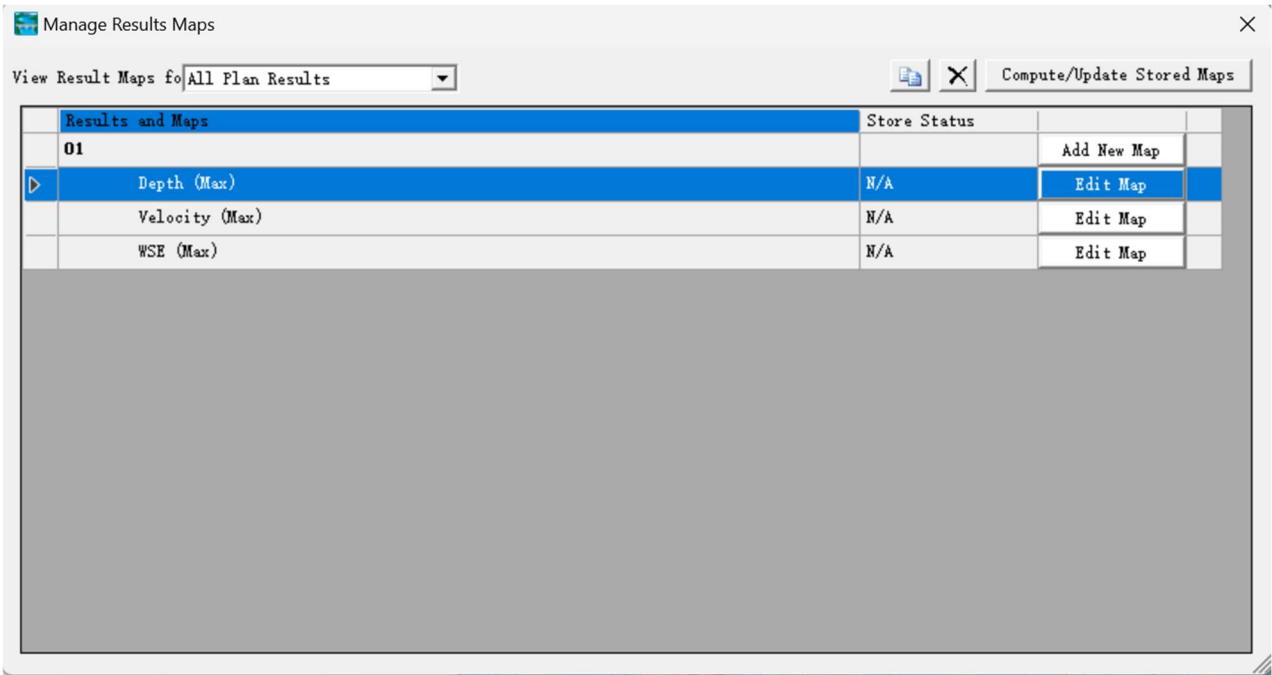
```

507081.6	122.51	1.43
506929.5	122.44	1.44
506814.5	122.38	1.46
506682.9	122.37	0.64
506580.3	122.38	0.34
506351.3	122.35	0.34
506239.4	122.33	0.47
506171.8	122.24	1.36
506171.5	BR	
506114	122.20	1.30

Figure 43: The code that calls the HEC RAS controller and reads the results

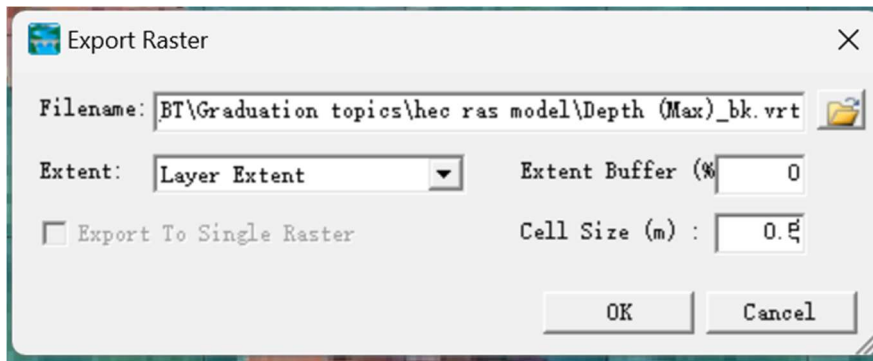
## Result exported with raster map

Once a Results Map has been created, it is listed by Plan in the management dialog. The Manage Results Map dialog is available by right-click on the Results group. It organizes data by Plan and identifies which maps are dynamic or stored and provides a message on the status of the map.



Raster data is made up of pixels (also referred to as grid cells). They are usually regularly-spaced and square. Raster often look pixelated because each pixel has its own value or class.

To save map results as a raster dataset in GeoTiff file format, it's possible to resample the raster data to the desired cell size. So I chose to export with a resolution of 0.5m for the cells to better composite the parameters of the BIM model.



## 4.4 Damage assessment

### 4.4.1 Fragile curves

The maximum, minimum, and average water depths resisted by the different materials, as well as the standard deviation, were read according to the methods mentioned in Section 3.2.3.1. Based on the pre-definition that the fragility curves satisfy the lognormal distribution, the fragility curves for masonry, wood, and glass are plotted through the code.(Fig. 44)

```

1 import numpy as np
2 import matplotlib.pyplot as plt
3 from scipy.stats import lognorm
4
5 # mean depth
6 midpoint_depths = [0.5, 1.15, 0.15] # mean depth
7 sigmas = [0.25, 0.175, 0.05] # stan.Dev of depth
8 colors = ['red', 'green', 'blue'] # color represent
9 materials = ['timber', 'masonry', 'glass'] # materials name
10
11 # a series of water depth
12 depths = np.linspace(0.01, 2, 100) # a series of depth, from 0 to 10
13
14 plt.figure()
15
16 # plot fragile curve
17 for i in range(len(midpoint_depths)):
18     mean = np.log(midpoint_depths[i]) # mean log
19     # according to log normal distributio, get failure probabilities
20     failure_probabilities = lognorm.cdf(depths, sigmas[i], scale=np.exp(mean))
21     plt.plot(depths, failure_probabilities, color=colors[i], label=materials[i])
22
23 # add title and label
24 plt.title('Fragile Curves (Lognormal Distribution)')
25 plt.xlabel('Water Depth')
26 plt.ylabel('Failure Probability')
27
28
29 plt.legend()
30
31 # present
32 plt.grid(True)
33 plt.show()
34

```

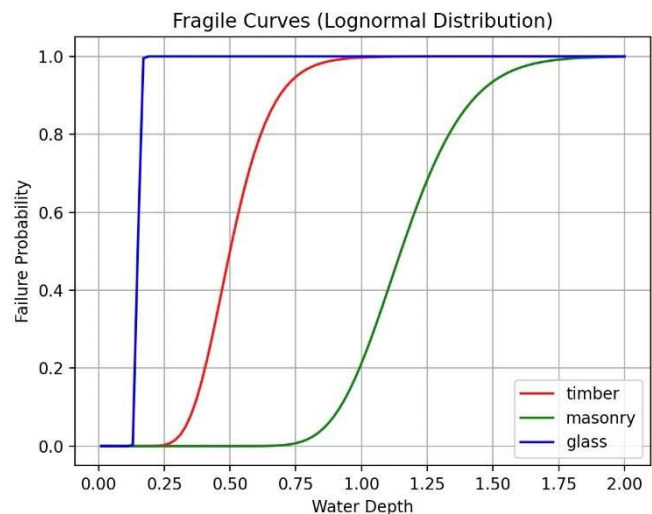


Figure 44: Script(left) of plotting fragility curves(right) and the result.

### 4.4.2 Damage classification

Fragile class	Functionality	Damage Scale	Fragility probability	Color coding
L1	Operational	Insignificant	0-15%	Light yellow
L2	Limited Occupancy	Slight	15%-30%	Light orange
L3	Restricted Occupancy	Moderate	30%-50%	Orange
L4	Restricted Use	Extensive	50%-75%	Red

<b>L5</b>	Restricted Entry	Complete	75%-100%	Dark red
-----------	------------------	----------	----------	----------

**Table 15:** Definition of damage level

According to the grading method mentioned in section 3.2.3.2, the vulnerability ratio, also known as the probability of failure, can be determined by referencing Table 15 when the damage class is known. The upper and lower limits corresponding to the water depth can be identified from the figure. Consequently, for each material, a table can be derived that shows the correlation between water depth and damage class. (Table 16)

Materials	L1(m)	L2(m)	L3(m)	L4(m)	L5(m)
<b>Timber</b>	0.370	0.440	0.500	0.600	1.000
<b>Glass</b>	0.125	0.140	0.167	0.180	0.200
<b>Masonry</b>	0.900	1.150	1.167	1.300	2.000

**Table 16:** Correspondence between damage class and water depth capacity for different materials

#### 4.4.3 Overall damage cost

The filter can be used to filter out all the building blocks that satisfy a failure probability of 50% or more and add a collapse parameter term with a value of 1 to them. By calculating this field the number of collapses for each type of component can be obtained, multiplied by the average replacement cost for each component (according to section 3.2.4)(Eq.5), and calculating the sum of the replacement costs for all types of components, the total building repair cost can be obtained.(Table 17)

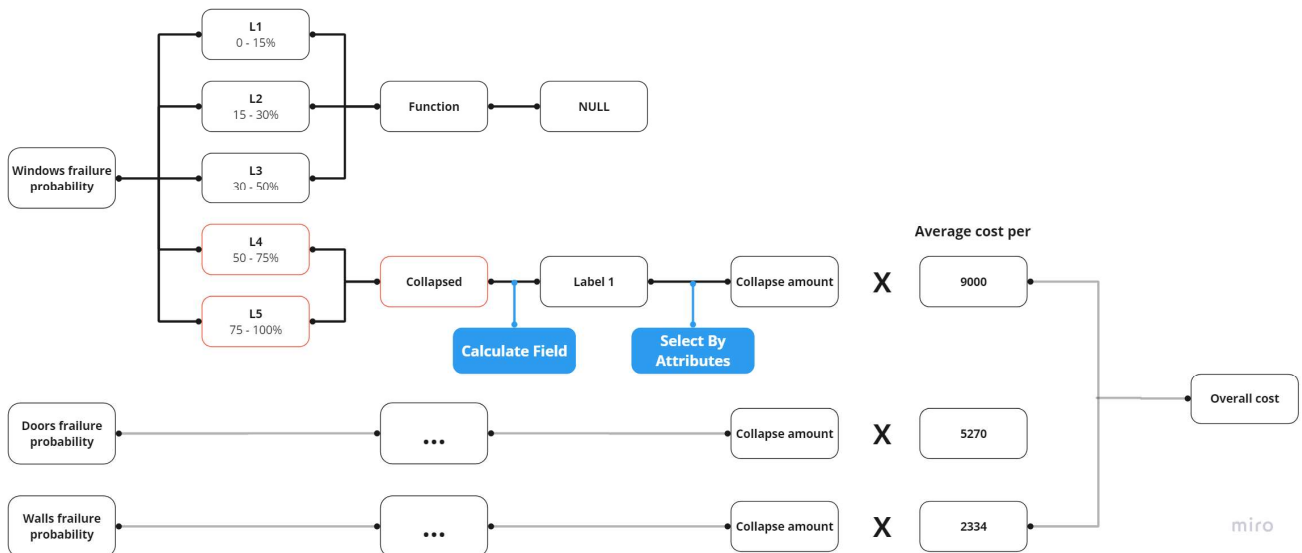


**Figure 45:** Workflow of overall cost calculation

$$\mu_{L_i}(IM = x) = \sum_{k=1}^N \mu_{L_k}(IM = x) = \sum_{k=1}^N \frac{\sum_{i=1}^n L_k^i}{n} \quad (5)$$

	Window cost	Door cost	Wall cost	Overall cost
TR = 50	0	2*5270	0	10540
TR = 100	0	10*5270	0	52700
TR = 800	9*9000	10*5270	0	133700

**Table 17:** Damage cost from components and overall

## 4.5 3D Visualization

After the assessment and valuation of the damage, a report regarding the damage to the components is generated. Such reports should contain the number, type and details of damaged components, their damage state, and the cost of the required treatment option. In addition to the report, the geometry of the individual building elements can be colour coded in a 3D model by their damage states to visualize their damage. Depending on the visualization requirements of the user, a desktop or web visualization tool can be developed or adopted. This tool should allow for functionalities such as show/hide component category (e.g. doors or walls), camera movement at an object zoom level as well as selection and inquiry about the details of a particular component. In this way, susceptible assemblies and their locations in the building can be visually inspected and queried to assist the decision-making.

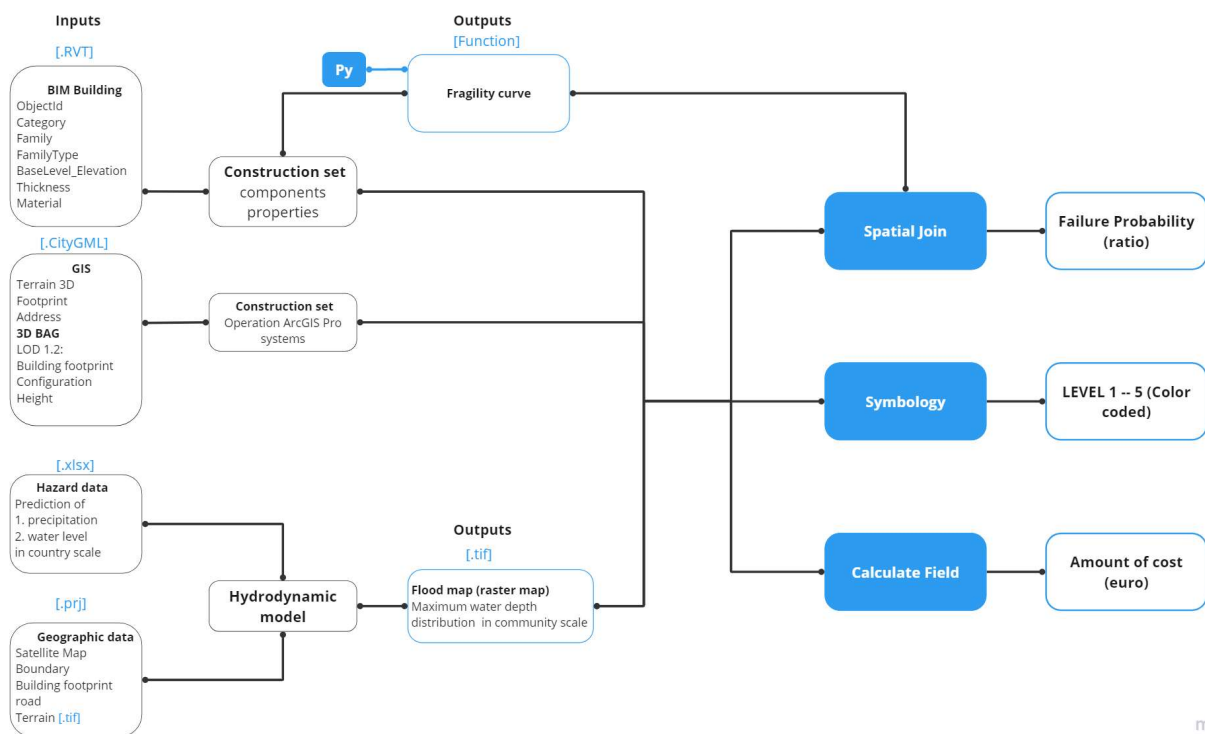


**Figure 46:** Computational workflow detailed program

### 4.5.1 Building an "integrated model"

The integrated model combines three main data sources: BIM, GIS, and Flood Hazard Maps, using ArcGIS Pro as the data platform. The components are as follows:

- **BIM Model:** The original Revit 3D model is loaded directly into ArcGIS Pro. The "Georeference" tool is used to align the model coordinates accurately.
- **GIS Data:** This includes geographic data such as elevation, building outlines, and road networks, along with the city model from 3D BAG. The Level of Detail (LOD) 1.3 file of the 3D BAG, downloaded

in OBJ format from the official 3D BAG website, is processed using Blender. In Blender, the original building model of the study area is deleted, and the coordinate position is aligned.

- **Flood Hazard Data:** Hazard raster data are obtained from flood hydrodynamic model simulations under different disaster scenarios. These images are loaded into the integrated model in TIF file format.

This integration enables comprehensive analysis and visualization of flood impacts on building components and the surrounding environment.

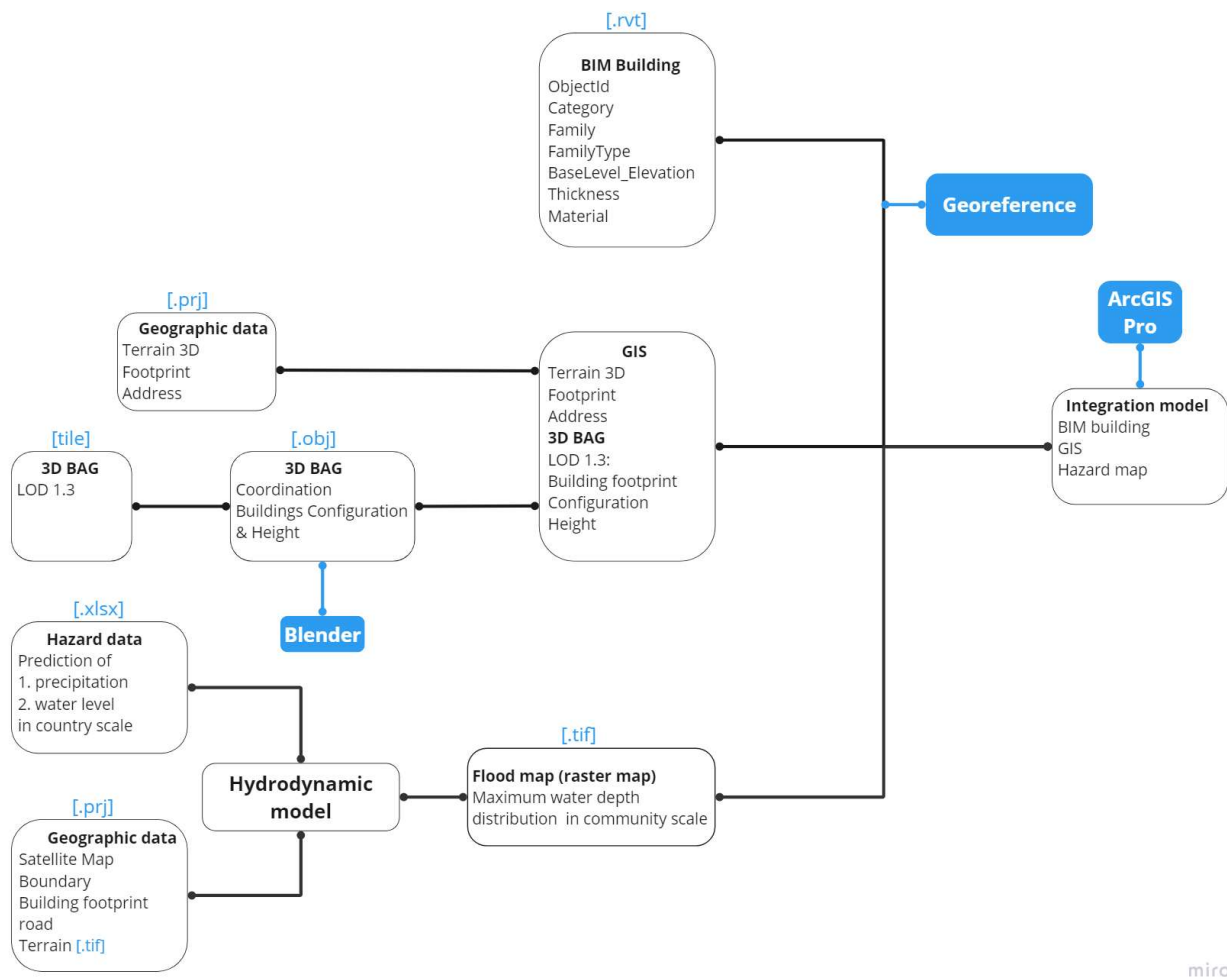


Figure 47: Data flowchart of creating integration model

## 4.5.2 Spatial join

### Spatial analysis

Joins attributes from one feature to another based on the spatial relationship. A spatial join matches rows from the Join Features values to the Target Features values based on their relative spatial locations. By default, all attributes of the join features are appended to the attributes of the target features and copied to the output feature class. Figure 41 abstractly explains the intersection principle that depends on positional relationships. Figure 42 shows the conceptual diagram of another methods using point cloud calculation which is similar to spatial join as applied to flood risk assessment.

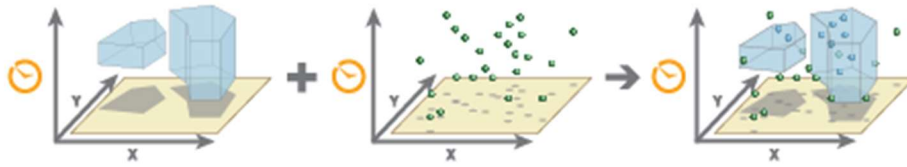


Fig 48. Illustration of spatial join

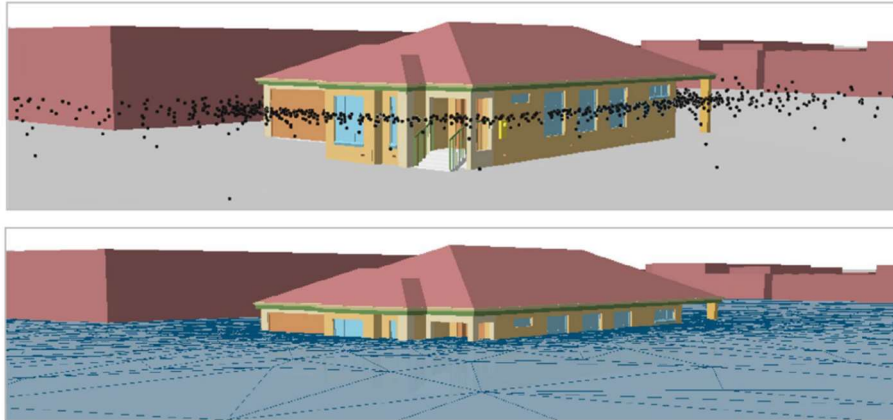
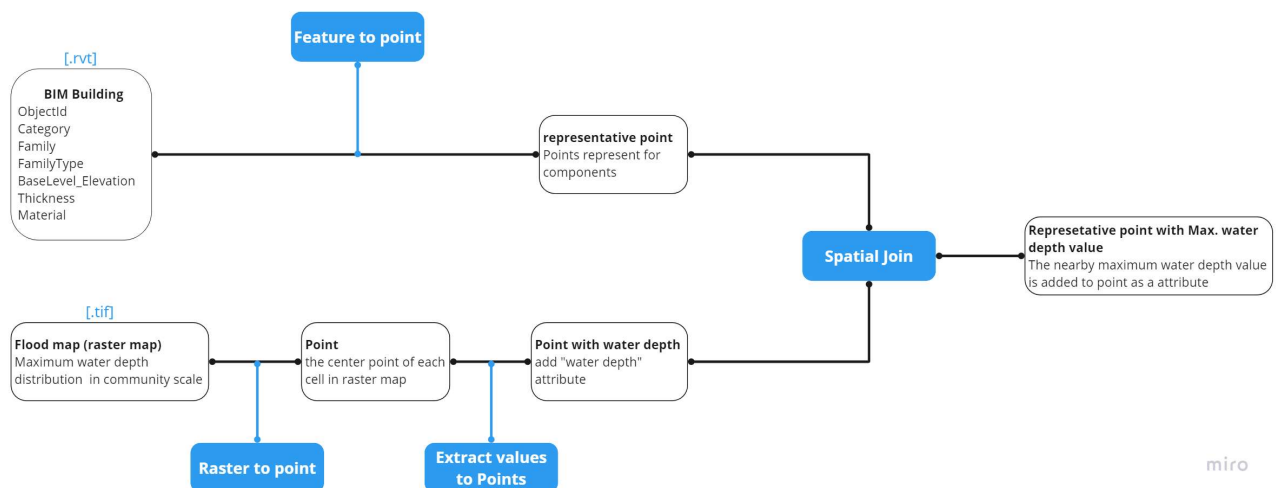


Figure 49: Point cloud join in flood scenario

To visualize the results of the simulation data, the water depth and fragility curves of each component need to be imported as parameters into the model properties. However, spatial aggregation can only occur between points and points, points and lines, and points and polygons. Since the 3D tile format data of the components cannot be used directly for spatial analysis, the following steps were taken: (Figure 51)

1. **Feature to Point Conversion:** The "Feature to Point" tool was used to find the point located at the center of each component, ensuring that it landed on the ground.
2. **Raster Transformation:** The raster data results from the flood simulation were transformed so that each raster cell's value was assigned to its centroid. The depth of water parameter was then added to the centroid's attributes.
3. **Data Aggregation:** Using the representative point of the component as the center, a search radius of 1 meter was established. The depth of water data from the centroids of the surrounding raster cells was screened, and the maximum value was added to the parameter of the representative point.



miro

Figure 50: Data flowchart of spatial analysis

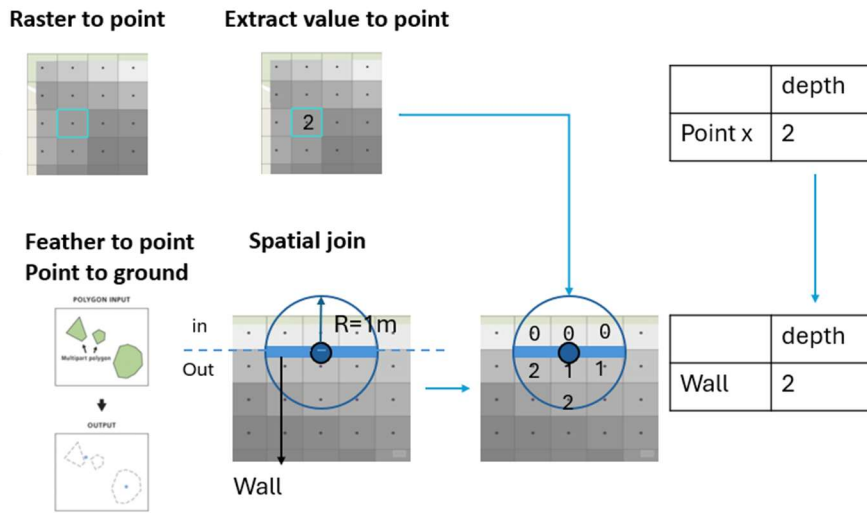


Figure 51: Conceptual workflow of spatial analysis

### 4.5.3 Colour coded

The color coding of the component points provides a hierarchical display of the probability of failure. The process involves the following steps:

1. **Material-Based Color Coding:** Component points are color-coded based on their physical property, specifically the material type.
2. **Failure Probability Curves:** In Python, the water depth-failure probability curves for the three materials are plotted. The failure probability for each component is calculated based on the water depth data at individual points.
3. **Classification Using Symbology:** The calculated failure probabilities are classified into five classes using the "Symbology" tool. The color coding is applied to the component points, ranging from the lightest to the darkest color, to represent increasing levels of failure probability.

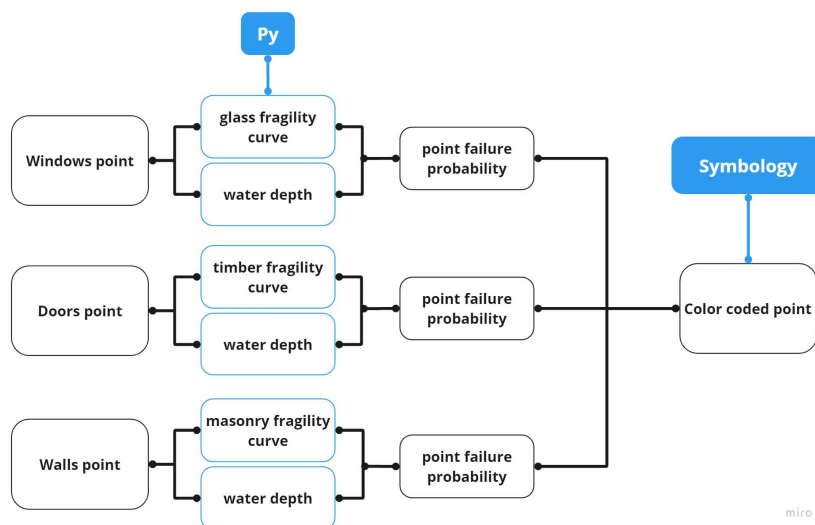


Figure 52: Data flowchart of color coded

#### 4.5.4 Display modes

Section 3.3.3 explains the methodology for presenting disaster scenarios for different return periods. By combining data from the same set of component damage results, two display modes can be obtained:

1. **Different Component Performances Under the Same Return Period:** This mode displays how various components perform under a specific return period.
2. **Impact of Different Flood Levels on Components Within the Same Category:** This mode shows the effect of varying flood levels on components of the same category, allowing for a comparative analysis of component vulnerability.

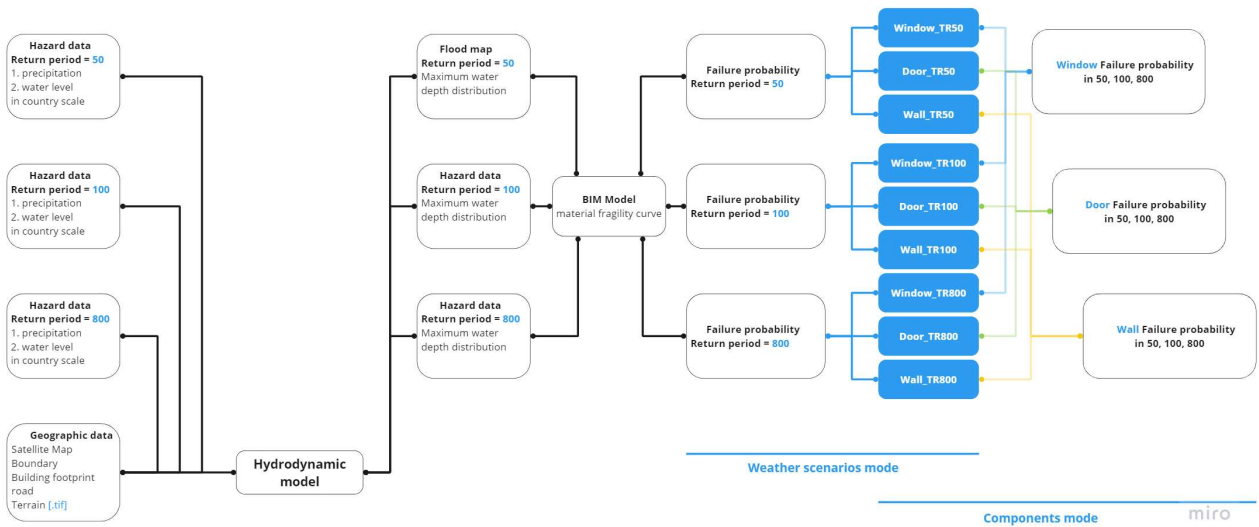


Figure 53: Data flowchart in Different modes

#### 4.6 Result and discussion

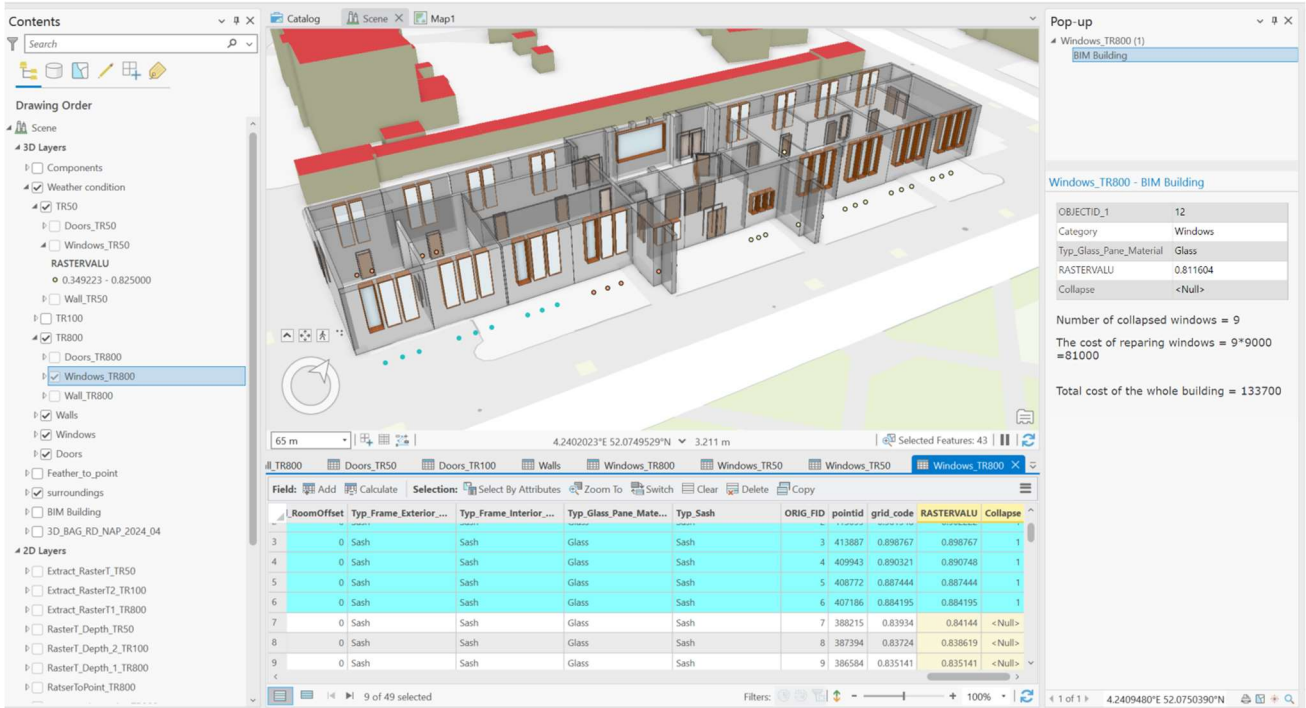
The final result is shown in Figure below. The following features are available:

1. when clicking on the corresponding point, the point is highlighted and a prompt box pops up, showing the water depth specific water depth data and failure probability
2. The color represents the state of damage, dark red is the highest value
3. irrelevant components can be filtered out by displaying and hiding the layers, and the 3D component model is semi-transparent in order to view the final result more clearly
4. Collapsed members are highlighted to show their location, making it easier to target replacement members.
5. Displays component-level damage and calculates total building repair costs in pops up box for flood scenarios with different return periods

and some shortcomings that still need to be improved:

1. the colors are not directly displayed on the model and the visualization results are not intuitive. It is because in spatial analysis, only the value of a point can be assigned to another point. Therefore only the window representative point has a water depth value that can be further marked by the color. How to make the water depth a variable of the window component itself, or to map the color of the representative point to the window (one-to-one relationship) is the next key step.

- All operations run locally. Web-based interactive maps allow you to send commands from the web without opening simulation and GIS software and retrieve simulation data through an extended interface. This approach allows the entire process to be automated and updated in real time, with more freedom to make adjustments.



## Result validation

As we can see from the graph, the windows on the left have more damage, presumably due to the greater distance from the coast. Additionally, at the same distance, the windows adjacent to the street are more damaged than the windows facing the paths in the neighborhood, presumably due to the fact that there is more screening around the inner street, and the surrounding buildings share the pressure of the water flow so that the windows are not overly exposed to the water flow.

This result is in line with the general perception of flood damage to buildings, and to some extent validates the feasibility of the method.

The screenshot displays a BIM software interface with a 3D model of a building. The interface includes a 'Contents' panel on the left, a central 3D view, and a 'Pop-up' window on the right. The 'Pop-up' window shows the following data:

**Windows\_TR800 - BIM Building**

OBJECTID_1	12
Category	Windows
Typ_Glass_Pane_Material	Glass
RASTERVALU	0.811604
Collapse	<Null>

Number of collapsed windows = 9  
The cost of repairing windows = 9\*9000 = 81000  
Total cost of the whole building = 133700

The table below shows the data for the selected features:

Field:	Add	Calculate	Selection:	Select By Attributes	Zoom To	Switch	Clear	Delete	Copy
#_RoomOffset	Typ_Frame_Exterior...	Typ_Frame_Interior...	Typ_Sash	ORIG.FID	pointid	grid_code	Typ_Glass_Pane_Mate...	RASTERVALU	Collapse
1	0	Sash	Sash	1	391456	0.550577	Glass	0.553843	<Null>
2	0	Sash	Sash	2	390239	0.545623	Glass	0.547251	<Null>
3	0	Sash	Sash	3	389027	0.531723	Glass	0.531723	<Null>
4	0	Sash	Sash	4	385083	0.486721	Glass	0.490875	<Null>
5	0	Sash	Sash	5	383912	0.473739	Glass	0.473739	<Null>
6	0	Sash	Sash	6	382326	0.457232	Glass	0.457232	<Null>
7	0	Sash	Sash	7	363355	0.35299	Glass	0.354934	<Null>

## Result comparison

### In flood scenarios mode

Door\_TR800:



Window\_TR800:



### Wall\_TR800:



Using the maximum flood return period of 800 years as an example, a longer return period represents a higher intensity of flooding. In this scenario, highlighting indicates that a component is completely damaged and labeled as collapsed. All representative points of the doors are highlighted, nine window points are highlighted, while no wall components are highlighted. This indicates that complete damage varies widely among different components.

Even though windows (glass) exhibit the highest sensitivity to flooding effects according to the vulnerability curves, they sustain less damage compared to wooden doors. This is because the elevation of windows above ground level reduces the hydrostatic pressure difference between internal and external water levels.

Brick walls, on the other hand, did not experience any component collapse under the highest intensity disaster. This suggests that the walls remained structurally sound throughout the building's service life and did not require any replacement measures.

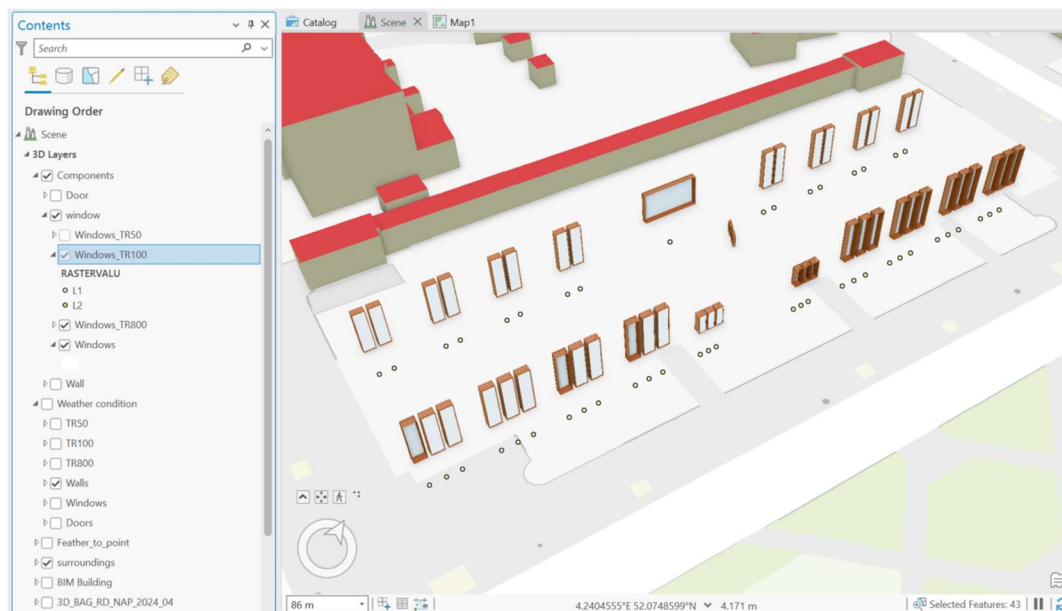
This analysis highlights the differential impact of flooding on various building components and underscores the importance of component-specific resilience strategies.

### In components mode

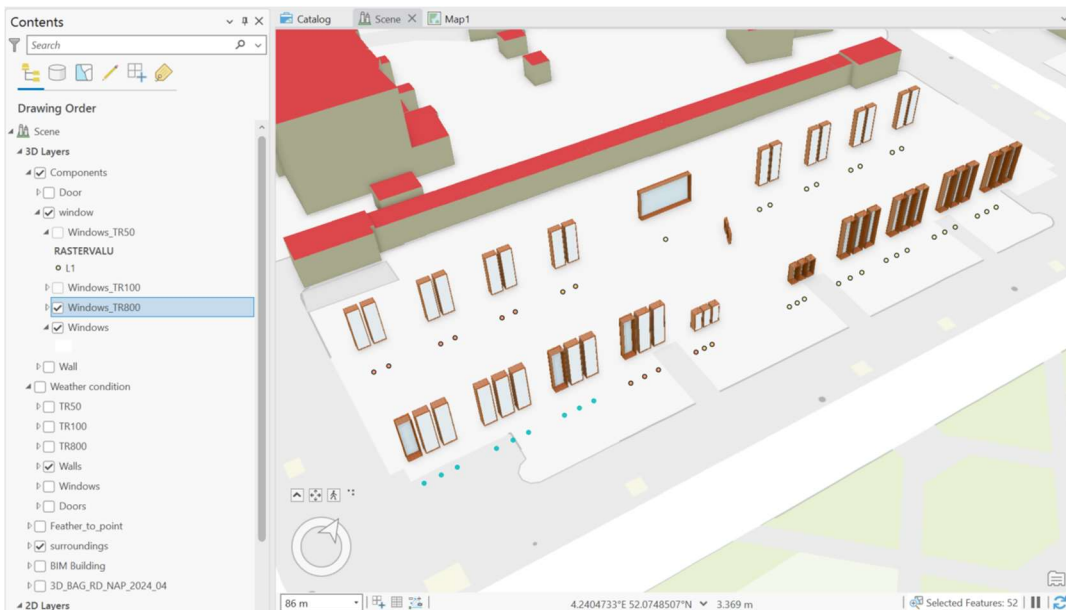
Window\_TR50:



Window\_TR100:



Window\_TR800:

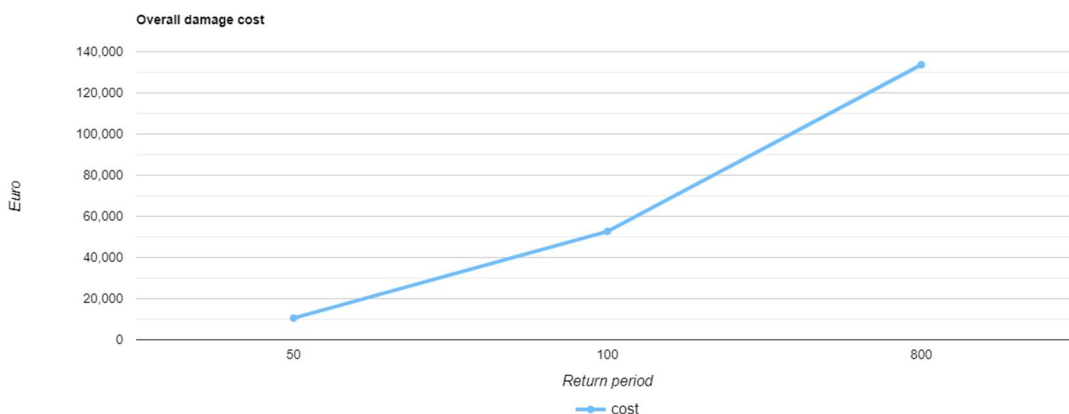


In the component display mode, the same component's response to flooding for different return periods is presented. For example, in the case of windows:

- 50-Year Scenario: All windows have a damage level of 1.
- 100-Year Scenario: The damage level remains unchanged at 1, although the probability of failure increases.
- 800-Year Scenario: The damage level for nine windows increases steeply to 5, with damage levels distributed across levels 1 to 4.

This analysis shows that flood levels below the 100-year return period have minimal impact on the windows. However, due to the high sensitivity of windows to flooding, they can rapidly collapse under more intense flood conditions. To achieve a more accurate prediction of the critical point where window collapse begins, increasing the resolution of the return period may be considered where appropriate.

## Damage cost



Plot the regression cycle-loss money line graph from the table total loss(Section 4.4.3). This shows that below 100 years, the loss comes from the failure of the wooden doors; above 100 years, the loss of windows increases. Since windows are more expensive, the greater the rate of increase in overall losses.

## 5 Conclusion

### 5.1 Response to the questions

#### Main research question

How We Built a BIM-GIS Based Viewer to Quantify the Risk of Structures components When Facing Compound Flooding Scenarios?

This paper presents an innovative approach to flood assessment that integrates models at the data level, addressing the limitations of traditional flood assessments which often fail to achieve micro-evaluation at the component level. The powerful data storage capabilities of BIM models, compared to GIS, compensate for these shortcomings and support detailed vulnerability analysis of building components. However, case studies have shown that semantic loss can significantly impact the data advantages of BIM models. Thus, developing an accessible and integrated "meta-model" is crucial for solving this problem.

To address this, two approaches—process level and data level—were explored. It was found that process-level data migration faces numerous licensing issues, whereas flood assessment functionalities are more easily and rapidly implemented using a data-level model. Importing BIM into ArcGIS without any format conversion preserves the information integrity during the transfer. This method ensures that the data hierarchy of BIM is well integrated into GIS, and with ArcGIS Pro's robust spatial analysis, data editing, and information integration capabilities, all data can be spatially linked and edited within a unified model for visualization purposes.

Another significant contribution of this work is the quantitative analysis of structural damage at a micro level. Leveraging the data accuracy of professional flood simulation software and BIM models, it is possible to precisely determine the impact of floods on individual components and the characteristics of each component's attributes. This precision is essential for quantification. Unlike traditional quantitative analyses such as HAZUS, this study employs the distribution characteristics of vulnerability curves to map corresponding vulnerability curves of materials, specifically water depth-failure probability curves. This approach provides a method to derive the probability of failure based on the quantification of water depth, enhancing the accuracy and reliability of flood damage assessments.

#### Sub-questions

1. How to assess multi-hazards risk for compound flooding in quantitative manner in urban scale, to consider of hazard inter-dependency?

There are three approaches in total, which are statistic modeling, numerical modeling and empirical modeling. In this paper, the numerical model is used i.e. by physically simulating the complex water movement and using the flood drivers as variables to finally get the flood map.

2. How to construct a hydrodynamic model to simulate urban flooding during compound flood outbreaks?

Hydrodynamic simulation of the study area was performed by inputting geometric data: topography, channel, elevation, building contours, as well as hydrological data such as: rainfall, sea level, inland water level, and flow velocity.

3. What intensity indexes and performance indicators should be used to analyse failure behaviour of structure.

Intensity indexes: water depth, velocity, duration, hydrodynamic pressure, debris impact

Performance indicators: water resistance, fragility curve

4. How to integrate simulation models in a viewer for their efficient performance on building structures, to interactively display the hazard index of each component?

Integrating BIM (RVT.) and GIS(SHP.) and Flood(tif.) data into ArcGIS Pro. With the Spatial Join Tool, the intensity value will be added to the components. Classification of the value using Symbology function, the components will be color coded.

## 5.2 Recommendation for future work

### 1. **Comprehensive Structural Analysis:**

- **Interior and Exterior Evaluation:** Analyze not only the building's exterior but also account for water penetration due to osmotic pressure, and evaluate the internal structural elements concurrently.
- **Multifactor Analysis:** Consider not only the effect of water depth but also the effects of water velocity and duration on building components.

### 2. **Advanced Flood Simulations:**

- **Complex Flood Scenarios:** Simulate not only single extreme events but also complex floods with varying levels of damage. These scenarios can be presented separately using filters for detailed analysis.
- **Future-Oriented Analysis:** Analyze not only historical extreme events but also consider the potential impact of floods over the next 100 years (or one building lifecycle).

### 3. **Open-Source Data Integration:**

- **Data Storage and Retrieval:** Utilize both local and cloud-based storage solutions. The process can be open-sourced, with data retrieved from sources like Copernicus. Use the HEC-RAS controller for automatic flood map generation, and store data in the cloud with 3D BAG and Revit Cloud.
- **Web-Based Visualization:** ArcGIS Online retrieves all the information, connects it to Cesium, and displays it on the web. This integration ensures comprehensive and accessible flood risk data visualization.

### 4. **Enhanced Real-Time Forecasting:**

- **Integration of Real-Time Data:** Incorporate real-time data, data-driven modeling, and digital visualization tools to significantly improve real-time flood forecasting.
- **Stakeholder and Public Benefits:** Enhance early warning systems, preparedness, and flood prevention capabilities. This integration leads to more effective flood risk management and reduced impacts on communities, benefiting stakeholders and the public.

## 6 Reflection

In this project, I aim to develop a visualization tool designed to intuitively and efficiently illustrate the extent of damage to building components caused by flooding induced by extreme compound flood. This tool will not only account for the impacts of such flooding but also precisely identify damage to building elements, enabling designers to assess building robustness early in the design stage. It will assist engineers in planning critical structural reinforcements before the structural design phase and help operators implement precautionary measures to protect vulnerable parts of the building before a disaster strikes. By catering to multiple stakeholders, this tool seeks to provide a cost-effective solution to minimize the loss of life and property.

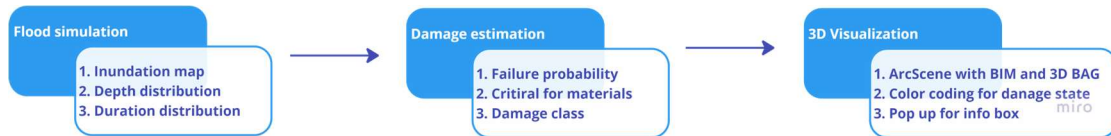


**Figure 53:** A brief workflow for implementation

### Compound Flood simulation

The product design process is illustrated in the figure above. (Fig.53) The first step involves deriving the flood base parameters required for hydraulic model simulation, such as base level, rainfall, and flow speed, based on compound flood events that have occurred in the Netherlands. The second step is to quantitatively analyze the impact of the flood on the building element (with various materials) and to rate the level of damage based on the obtained fragile curves. The third step was to visualize the data results using ArcGIS Pro and mark the damage rating with colors.



**Figure 54.** Interface of hydrodynamic simulation results in Hec Ras

### Compound Flood simulation

The first step involved using hydraulic modeling to simulate inundation scenarios under real extreme flood conditions. This step aimed to generate maps of urban building inundation. Utilizing parameters for extreme weather conditions ensures comprehensive coverage of all possible flood scenarios. These parameters were sourced from literature (van den Hurk et al., 2015), which documents the most similar composite event to a flood hazard that has occurred in the Netherlands in recent years.

Given that water depth and velocity in urban centers can be influenced by surrounding buildings, simulating community-scale flooding scenarios allows for both the consideration of these influences and achieving sufficient accuracy in analyzing building component levels.

The focus of this phase was on using specialized hydrodynamic software to obtain maps showing the geographic distribution of water depth. (Fig.44) At the project's outset, a thesis study was conducted to select

appropriate software. This involved reviewing and analyzing ten papers that summarized various hydrodynamic software, models, and their parameters. Additionally, the study organized information on formula methods, open sources, and the input and output parameters of twenty different hydraulic engineering software currently in use. Ultimately, two software packages were selected for this project: MIKE FLOOD and HEC-RAS.

The project process involved researching and studying both MIKE FLOOD and HEC-RAS software separately, followed by conducting simulation tests. Ultimately, HEC-RAS was chosen as the simulation software for several reasons:

#### **MIKE FLOOD:**

**1. Specialization and Input Parameters:** MIKE FLOOD requires many specialized input parameters, such as details of the underground pipe network and land permeability, which were not readily available. The absence of these parameters made the simulation challenging to execute.

**2. Complexity and Sub-packages:** The MIKE series includes a wide range of sub-packages, and coupling the models of several subsystems (like MIKE21 1D/2D and MIKE FLOOD) during the simulation increases both the complexity and the difficulty of adjustments.

**3. Licensing Issues:** The API port of MIKE FLOOD is commercially licensed, requiring substantial fees. Although initial software selection considered open-source options, the practical application revealed prohibitive costs associated with the API.

#### **HEC-RAS:**

**1. Balance of Professionalism and Ease of Use:** HEC-RAS strikes a good balance between professionalism and user-friendliness. It supports composite flood drivers, such as rainfall, runoff, and water levels, and is highly compatible with various data formats.

**2. Visualization Capabilities:** HEC-RAS offers a high degree of visualization, allowing intuitive viewing of results in different layers. Users can also directly modify data geometry within the view, facilitating easier debugging.

**3. Direct Export to Raster Map File:** HEC-RAS can export results directly to raster map files without requiring additional conversion, making it a straightforward source for subsequent spatial data analysis.

Ultimately, HEC-RAS features its own open-source API port (HEC-RAS Controller), which can be accessed using Python code to automate running the software and outputting results. And also stands out for its' flexibility (allowing for easier adjustment of model sets with hydraulic data).

During the testing process, Simona is responsible for ensuring the rigor and reliability of the simulation. To accurately reproduce recent extreme compound disasters, she suggested using rainfall and runoff parameters from the peak hours of these extreme events as model inputs. Utilizing known parameters from actual composite events provides a more realistic simulation compared to using extreme theoretical values.

Azarakhsh guided the project's digitalization efforts, placing significant emphasis on the feasibility of API integration. She recommended creating an API request demo to evaluate the interface response time. This suggestion is very sufficient, highlighting that it was unnecessary to wait until all simulation modeling is complete to perform this step. By testing the API call with a completed example early in the process, potential issues with the API could be identified and addressed promptly, allowing for quick adoption of alternatives if needed.

## Damage quantification and classification

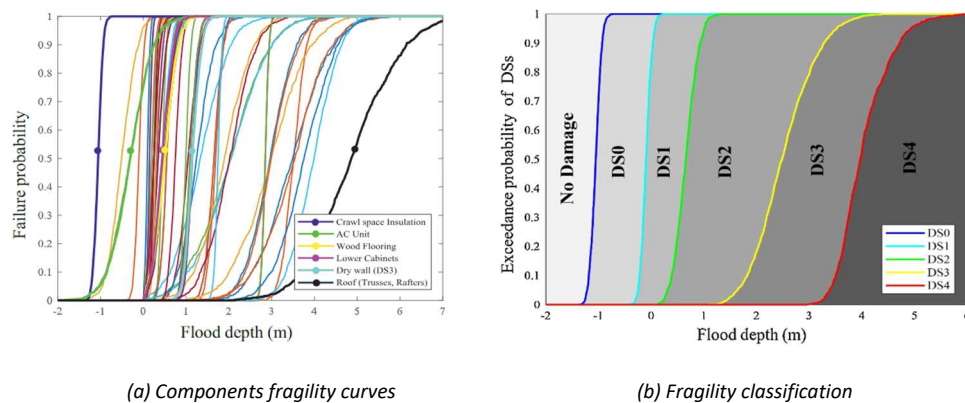


**Fig.45:** Identification damage levels (Nofal et al., 2020)

The second step is damage assessment. This involves translating the simulation results, specifically the water depth, into damage levels for building components and then grading this damage. This step is crucial for transitioning from an urban scale to a building scale, aiming to derive a practical assessment system and criteria. The primary contribution of this work is the development of flood vulnerability curves for buildings without relying on empirical field data.

In our literature review, we used keywords such as "vulnerability analysis," "fragile analysis," "damage assessment," and "risk map," which led us to 17 relevant articles. These articles helped us organize widely used assessment methods, formula models, and parameters. Faced with the choice between performing a finite element analysis of a building structure and defining damage in five levels of severity through the Monte Carlo framework, I conducted separate tests for each approach.

### Finite Element Analysis (FEA):

- 1. Software Requirements:** This method required using specialized ANSYS software.
- 2. Data Transfer:** The process involved transferring simulation data from HEC-RAS to ANSYS.
- 3. Visualization:** The results then needed to be visualized in ArcGIS Pro.
- 4. Complexity and Time Consumption:** The data transfer between these platforms was complex and time-consuming, adding significant overhead to the process.

### Monte Carlo Framework:

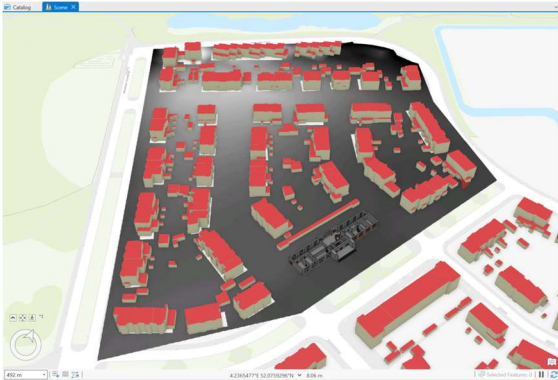
- 1. Damage Assessment Method:** This approach defines damage in five levels of severity using a Monte Carlo framework.
- 2. Component-based Analysis:** The framework divides the building into separate components, assigning each to one of five predefined damage states.
- 3. Efficiency:** This method utilizes expert-based data obtained from online sources, making it more straightforward and less time-consuming compared to the FEA process.

Based on these tests, the Monte Carlo framework proved to be more efficient and feasible for the project, given the complexity and time constraints associated with the finite element analysis approach.

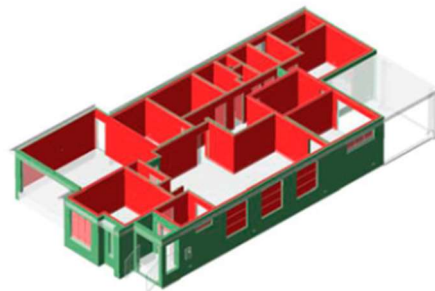
After thorough analysis and comparison, Simona suggested employing the univariate and multivariate component flood vulnerability method.(Nofal et al., 2020) This method uses expert-based data sourced from online resources and applies them within a Monte Carlo framework. It divides the building into separate

components, assigning each to one of five predefined damage states that collectively characterize the damage to the entire building. (Fig.45)

### 3D Visualization



(a) BIM-GIS Integration in ArcGIS



(b) color coding elements(Amirebrahimi et al., 2016)

**Fig.46:** Visualization of data results

The last step involves using FDA (Flood Damage Assessment) alongside ArcGIS Pro and Scene visualization to create a comprehensive framework for BIM-GIS integrated 3D visualization. This framework is designed to depict a building's unique behavior against floods. To achieve this, it combines two essential types of information:

**Building Information:** Complete building information is represented through Building Information Modeling (BIM). BIM provides detailed, accurate, and comprehensive data about the building's components, materials, and structural characteristics. (fig.46)

**Flood Information:** Flood-related data, typically managed by hydrodynamic software, is outputted to a Geographic Information System (GIS). GIS manages spatial data and provides a platform for visualizing flood extents, depths, and other hydrodynamic results. (fig.46)

The integration of BIM and GIS is crucial because neither can independently fulfill the project's requirements. BIM excels in detailed building information, while GIS specializes in spatial and flood data management. By integrating these systems, the framework can effectively visualize and assess flood damage in a 3D environment, offering a holistic view of the building's vulnerability and behavior during flood events.

However, in the initial stages, my aim was to develop a fully open-source web-based platform utilizing a B/S architecture for 3D geospatial data visualization, enabling dynamic and high-performance renderings of geographic data within a web browser. But, despite my architectural background, diving into web GIS proved challenging.

**1. Extensive computer background to acquire and apply.** While my undergraduate studies provided me with skills in Python editing through Grasshopper's interface and exposure to basic smart navigation projects using Python for data analysis during graduate school, the scope of this project demanded a deeper understanding of front-end visualization and back-end simulation, necessitating proficiency in Python, JavaScript, JSON, CesiumJS, Vue, Flask, and API requests. Despite investing significant time and effort in expanding my knowledge base, I encountered substantial hurdles during implementation. Even basic tasks, such as importing a BIM model into the Cesium platform, proved time-consuming and arduous, taking nearly half a month to accomplish.

2. **Api for simulation software.** The requirement for open-source simulation software posed additional challenges, particularly with the HEC-RAS controller, which, although open-source, differed significantly in its API call methods, resulting in further delays.

3. **Build a fully functional front-end framework.** Despite substantial progress in exporting hydrodynamic simulation results using the HEC-RAS controller and integrating detailed 3D representations of buildings and addresses from the 3D BAG dataset into Cesium, challenges persisted in developing a fully functional front-end framework using Vue and Flask, particularly in introducing clickable BIM models of each component. Consequently, despite diligent efforts, the intended fully functional B/S system remains unrealized. As it stands, the achieved milestones include exporting hydrodynamic simulation results, importing 3D BAG data into Cesium, and constructing the front-end framework using Vue.

The challenging journey of this project was made manageable and ultimately successful thanks to the unwavering patience and invaluable support of my mentor, Azarakhsh. From the outset, she played a crucial role in helping me organize the pipeline for integrating simulation data into Cesium, providing guidance and encouragement every step of the way. Recognizing the importance of practical feasibility, she wisely advised me to create a small demo to test the viability of our approach, setting a solid foundation for subsequent development.

When I encountered obstacles, particularly in loading city model data, Azarakhsh's resourcefulness shone through. She directed me to consult the 3D BAG documentation and facilitated a productive meeting with Ping Mao, a fellow GIS student who had faced similar challenges. Their collaborative efforts and shared experiences proved invaluable, enabling me to overcome hurdles and successfully load the model.

Throughout the project, Azarakhsh's unwavering support extended beyond technical assistance. She consistently demonstrated patience and understanding, even during moments of frustration or anxiety stemming from my limited coding skills. Her calm demeanor and empathetic approach not only alleviated my concerns but also inspired me to explore alternative solutions and persevere through challenges.

When I sought her opinion on alternative approaches after extensive research and contemplation, she graciously affirmed my considerations and offered insightful suggestions for implementation. This enabled me to pivot swiftly and confidently realign my project direction. Her encouragement and guidance were instrumental in fostering a sense of empowerment and motivation, ultimately contributing to the project's progress and success.

Above all, both of my mentors' mentorship has left a lasting impact, prompting me to reflect on the power of patience, collaboration, and resilience in overcoming obstacles. Her guidance has not only enriched my technical skills but also fostered a deeper appreciation for the importance of mentorship and support in navigating complex endeavors.

For the final phase of the project, the following objectives have been outlined:

**1. Simulation of Composite Flooding Events:** Expand the simulation scope to include various levels of composite flooding, requiring an increased number of samples for simulation and hierarchical display of exported results in ArcGIS. Utilizing filters, the damage grading can be visualized separately for each event.

**2. Incorporating Duration in Damage Assessment:** Explore the impact of both water depth and duration on building components' damage. This entails creating a graph to illustrate the resistance of different materials to duration and correlating it with the damage grading based on the water depth approach.(Fig.47)

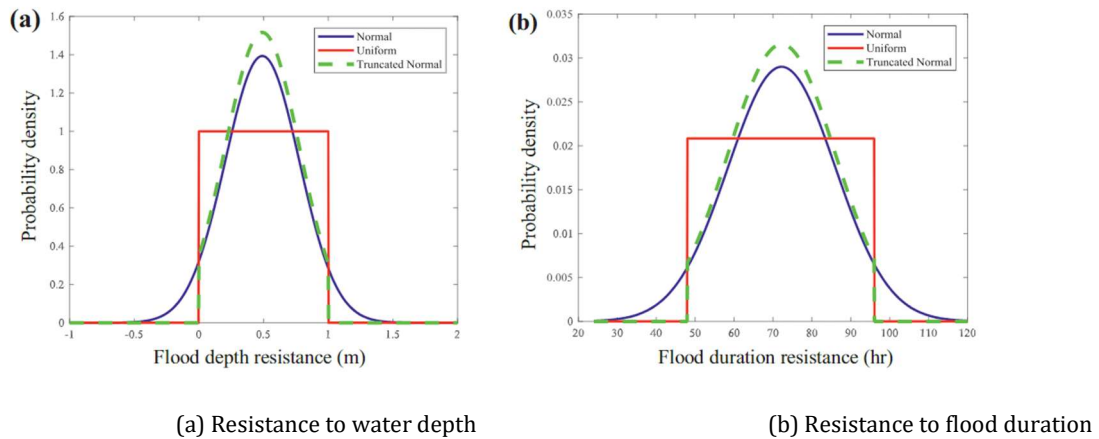


**Figure 55:** Flood resistance for specific material (Nofal et al., 2020)

**3. Integration of Cesium and ArcGIS:** Investigate methods to connect Cesium and ArcGIS, enabling the visualization of results through the web interface. This involves exploring ArcGIS documentation to understand its API capabilities and learning the requirements of the Cesium call interface to facilitate seamless communication between the two platforms.

1. What is the relation between your graduation project topic, your master track (A, U, BT, LA, MBE), and your master programme (MSc AUBS)?

The topic of this project is "A Design Tool to Analyze and Visualize the Risk of Building Structures under Compound Flood Hazards." Digital tools to aid in decision-making are among the most crucial concerns in the building technology profession.

This tool is designed not only for optimizing building design during the early stages but also for use in civil engineering by combining hydraulic and structural aspects to measure and mitigate the risk of building structures under compound flood hazards. Moreover, it can contribute to structural optimization, making it a versatile and valuable resource across various stages of building and infrastructure development. This idea is in line with the concept of building technology to make up for building and civil engineering technology.

2. How did your research influence your design/recommendations and how did the design/recommendations influence your research?

My research influenced the final design in three key ways: through a comparative study of hydraulic models, a dissertation study of evaluation systems, and a study of visualization systems. These studies provided robust arguments for data reliability, methodological rigor, and application feasibility.

My design identified problems that arise when synthesizing and applying research from different fields. For instance, when quantifying damage, calculating the bending moment and shear force of the structure using finite element analysis posed a challenge because the analysis software could not be effectively linked with ArcGIS. Although finite element analysis offers specialized and accurate assessments of vulnerability, its incompatibility with the overall framework necessitated a change in the research strategy.

3. How do you assess the value of your way of working (your approach, your used methods, used methodology)?

To assess the value of my approach, methods, and methodology, I consider several key factors:

1. Effectiveness in Meeting Objectives: My approach was designed to meet specific project objectives, such as integrating hydraulic simulations with structural analysis and visualizing flood risks in a user-friendly manner. By evaluating how well these objectives were met, I can determine the effectiveness of my methods.

2. Interdisciplinary Integration: The value of my methodology lies in its ability to integrate insights from different disciplines, such as civil engineering, hydraulic modeling, and geospatial analysis. This interdisciplinary approach ensures a comprehensive assessment of building vulnerabilities to compound flood hazards.

3. Stakeholder Engagement and Feedback: Regular engagement with mentors, peers, and other stakeholders provided valuable feedback that informed and improved my methodology. This iterative process of refinement ensured that the final design was aligned with the needs and expectations of its users.

By evaluating these factors, I can confidently assess that my approach, methods, and methodology were valuable and effective in achieving the project's goals and providing practical, reliable solutions for assessing building vulnerabilities to compound flood hazards.

4. How do you assess the academic and societal value, scope and implication of your graduation project, including ethical aspects?

The social relevance of this modeling approach lies in its potential to significantly enhance community resilience and safety in the face of climate change-induced flood hazards. By accurately assessing flood vulnerability at both the structural and component levels, the approach enables proactive measures to be taken to reinforce buildings and infrastructure, thereby reducing the risk of damage and loss of life during flooding events.

Furthermore, the utilization of a web-based interface for data visualization promotes greater accessibility and transparency, allowing for widespread dissemination of critical information to stakeholders, including community members, local authorities, and emergency responders. This empowers communities to make informed decisions, develop effective evacuation plans, and allocate resources efficiently in preparation for flood events.

Overall, by addressing the pressing issue of flood risk management with advanced modeling techniques and accessible data visualization tools, this approach contributes to building more resilient and adaptive communities, ultimately enhancing societal well-being and safety.

5. How do you assess the value of the transferability of your project results?

From a scientific perspective, this modeling approach contributes to advancing our understanding of the complex dynamics of flood hazards in the context of climate change. By incorporating comprehensive assessments of flood hazard triggers and probabilities, the approach provides valuable insights into the multifaceted factors influencing flood risk.

Moreover, the integration of precise component-level analyses represents a significant advancement in flood vulnerability assessment methodologies. This detailed examination allows for a more nuanced understanding of structural vulnerabilities and the potential effectiveness of mitigation measures, thereby informing future research and engineering practices aimed at enhancing resilience to flood hazards.

Additionally, the utilization of a web-based ArcGIS Pro interface for data visualization not only facilitates collaboration among stakeholders but also presents opportunities for further scientific inquiry. The

accessibility of data through such platforms enables researchers to explore new avenues of analysis, validate modeling assumptions, and refine predictive models, ultimately advancing the state of the art in flood risk assessment and management.

Overall, this modeling approach contributes to the scientific community by expanding our knowledge of flood risk dynamics, improving the accuracy of vulnerability assessments, and providing tools for collaborative research and decision-making in the field of flood hazard mitigation and adaptation.

6. How could the tools I used in the project be further developed?

**1. Integration with More Data Sources:** Future iterations could integrate additional data sources, such as real-time weather data, to enhance the accuracy and timeliness of flood risk assessments. This integration could enable more proactive and responsive planning and decision-making.

**2. Advanced Analytical Tools:** Incorporating advanced analytical tools and machine learning algorithms could further refine the damage assessment process. These tools could analyze patterns and predict vulnerabilities more accurately, providing deeper insights into flood risks.

7. what strategies did you employ to overcome these obstacles, and how did this experience shape your approach to interdisciplinary collaboration in future projects?

**1. Regular group exchanges:** Simona arrange group meeting each month. In these exchanges, cross-cutting topics serve as conduits for sharing literature, data sources, and tools, enriching our collective understanding. Moreover, exposure to diverse topics inspires fresh ideas, encourages thinking outside conventional boundaries, and fosters a deeper appreciation for varied research methods. By leveraging this interdisciplinary synergy, we not only enhance our individual projects but also cultivate a collaborative environment that propels innovative research forward.

**2. Flexibility and Adaptability:** Remaining flexible and adaptable to changing circumstances and unforeseen challenges was key. Being open to alternative approaches and willing to adjust strategies as needed allowed for more effective problem-solving.

**3. Learning from Mistakes:** Going fast, failing fast, and learning fast from bad experiences is the most useful thing I've learned. Because ignorance of other fields is sure to be accompanied by misinterpretation, the fastest way to correct it is to learn from the experience of trying and to refine your knowledge of other subjects even more.

## 7 Bibliography

- Akinci, B., Karimi, H., Pradhan, A., Wu, C.-C., & Fichtl, G. (2009). CAD and gis interoperability through semantic web services. In *CAD and GIS Integration* (pp. 199–222). Auerbach Publications. <https://doi.org/10.1201/9781420068061-c9>
- Amirebrahimi, S., Rajabifard, A., Mendis, P., & Ngo, T. (2015a). A data model for integrating gis and bim for assessment and 3d visualisation of flood damage to building. ..
- Amirebrahimi, S., Rajabifard, A., Mendis, P., & Ngo, T. (2015b). A framework for a microscale flood damage assessment and visualization for a building using bim–gis integration. *International Journal of Digital Earth*, 9(4), 363–386. <https://doi.org/10.1080/17538947.2015.1034201>
- Apel, H., Aronica, G. T., Kreibich, H., & Thielen, A. H. (2008). Flood risk analyses—how detailed do we need to be? *Natural Hazards*, 49(1), 79–98. <https://doi.org/10.1007/s11069-008-9277-8>
- Bevacqua, E., Maraun, D., Vousdoukas, M. I., Voukouvalas, E., Vrac, M., Mentaschi, L., & Widmann, M. (2019). Higher probability of compound flooding from precipitation and storm surge in europe under anthropogenic climate change. *Science Advances*, 5(9), eaaw5531. <https://doi.org/10.1126/sciadv.aaw5531>
- Bevacqua, E., Vousdoukas, M. I., Zappa, G., Hodges, K., Shepherd, T. G., Maraun, D., Mentaschi, L., & Feyen, L. (2020). More meteorological events that drive compound coastal flooding are projected under climate change. *Communications Earth & Environment*, 1(1). <https://doi.org/10.1038/s43247-020-00044-z>
- Conrad, D., Kapur, O., & Mahadevia, A. (2012). FEMA\_2012. ..
- Couasnon, A., Eilander, D., Muis, S., Veldkamp, T. I. E., Haigh, I. D., Wahl, T., Winsemius, H. C., & Ward, P. J. (2020). Measuring compound flood potential from river discharge and storm surge extremes at the global scale. *Natural Hazards and Earth System Sciences*, 20(2), 489–504. <https://doi.org/10.5194/nhess-20-489-2020>
- Custer, R., & Nishijima, K. (2015). Flood vulnerability assessment of residential buildings by explicit damage process modelling. *Natural Hazards*, 78(1), 461–496. <https://doi.org/10.1007/s11069-015-1725-7>
- El-Mekawy, M., & A. Östman. (2010). Semantic mapping: an ontology engineering method for integrating building models in ifc and citygml. ..
- FME workshop on formal methods in software engineering formalise 2013. (2013, May). *2013 1st FME Workshop on Formal Methods in Software Engineering (FormaliSE)*. <https://doi.org/10.1109/formalise.2013.6612269>
- Ge, Y., Dou, W., Gu, Z., Qian, X., Wang, J., Xu, W., Shi, P., Ming, X., Zhou, X., & Chen, Y. (2013). Assessment of social vulnerability to natural hazards in the yangtze river delta, china. *Stochastic Environmental Research and Risk Assessment*, 27(8), 1899–1908. <https://doi.org/10.1007/s00477-013-0725-y>

- Gutierrez, B. T., Plant, N. G., & Thieler, E. R. (2011). A bayesian network to predict coastal vulnerability to sea level rise. *Journal of Geophysical Research: Atmospheres*, 116(F2). <https://doi.org/10.1029/2010jf001891>
- Hasan Tanim, A., & Goharian, E. (2020). Developing a hybrid modeling and multivariate analysis framework for storm surge and runoff interactions in urban coastal flooding. *Journal of Hydrology*, 125670. <https://doi.org/10.1016/j.jhydrol.2020.125670>
- Hatzikyriakou, A., & Lin, N. (2017). Simulating storm surge waves for structural vulnerability estimation and flood hazard mapping. *Natural Hazards*, 89(2), 939–962. <https://doi.org/10.1007/s11069-017-3001-5>
- Hatzikyriakou, A., & Lin, N. (2018). Assessing the vulnerability of structures and residential communities to storm surge: an analysis of flood impact during hurricane sandy. *Frontiers in Built Environment*, 4. <https://doi.org/10.3389/fbuil.2018.00004>
- Hawkes, P. J. (2008). Joint probability analysis for estimation of extremes. *Journal of Hydraulic Research*, 46(sup2), 246–256. <https://doi.org/10.1080/00221686.2008.9521958>
- Heinrich, P., Hagemann, S., Weisse, R., Schrum, C., Daewel, U., & Gaslikova, L. (2023). Compound flood events: analysing the joint occurrence of extreme river discharge events and storm surges in northern and central europe. *Natural Hazards and Earth System Sciences*, 23(5), 1967–1985. <https://doi.org/10.5194/nhess-23-1967-2023>
- Hou, J., Zhou, N., Chen, G., Huang, M., & Bai, G. (2021). Rapid forecasting of urban flood inundation using multiple machine learning models. *Natural Hazards*, 108(2), 2335–2356. <https://doi.org/10.1007/s11069-021-04782-x>
- Karimi, H. A., & Akinci, B. (2009). *CAD and GIS Integration*. Auerbach Publications. <https://doi.org/10.1201/9781420068061>
- Kelman, I. (2002). Physical flood vulnerability of residential properties in coastal, eastern england. ...
- Kelman, I., & Spence, R. (2004). An overview of flood actions on buildings. *Engineering Geology*, 73(3–4), 297–309. <https://doi.org/10.1016/j.enggeo.2004.01.010>
- Kew, S. F., Selten, F. M., Lenderink, G., & Hazeleger, W. (2013). The simultaneous occurrence of surge and discharge extremes for the rhine delta. *Natural Hazards and Earth System Sciences*, 13(8), 2017–2029. <https://doi.org/10.5194/nhess-13-2017-2013>
- Khanal, S., Ridder, N., de Vries, H., Terink, W., & van den Hurk, B. (2019). Storm surge and extreme river discharge: a compound event analysis using ensemble impact modeling. *Frontiers in Earth Science*, 7. <https://doi.org/10.3389/feart.2019.00224>
- Klerk, W. J., Winsemius, H. C., van Verseveld, W. J., Bakker, A. M. R., & Diermanse, F. L. M. (2015). The coincidence of storm surges and extreme discharges within the rhine–meuse delta. *Environmental Research Letters*, 10(3), 035005. <https://doi.org/10.1088/1748-9326/10/3/035005>

- Kumar, V., Sharma, K., Caloiero, T., Mehta, D., & Singh, K. (2023). Comprehensive overview of flood modeling approaches: a review of recent advances. *Hydrology*, *10*(7), 141. <https://doi.org/10.3390/hydrology10070141>
- Kumbier, K., Carvalho, R. C., Vafeidis, A. T., & Woodroffe, C. D. (2018). Investigating compound flooding in an estuary using hydrodynamic modelling: a case study from the shoalhaven river, australia. *Natural Hazards and Earth System Sciences*, *18*(2), 463–477. <https://doi.org/10.5194/nhess-18-463-2018>
- Leal, M., Reis, E., Pereira, S., & Santos, P. P. (2021). Physical vulnerability assessment to flash floods using an indicator-based methodology based on building properties and flow parameters. *Journal of Flood Risk Management*, *14*(3). <https://doi.org/10.1111/jfr3.12712>
- Lian, J. J., Xu, K., & Ma, C. (2013). Joint impact of rainfall and tidal level on flood risk in a coastal city with a complex river network: a case study of fuzhou city, china. *Hydrology and Earth System Sciences*, *17*(2), 679–689. <https://doi.org/10.5194/hess-17-679-2013>
- Loveland, M., Kiaghadi, A., Dawson, C. N., Rifai, H. S., Misra, S., Mosser, H., & Parola, A. (2021). Developing a modeling framework to simulate compound flooding: when storm surge interacts with riverine flow. *Frontiers in Climate*, *2*. <https://doi.org/10.3389/fclim.2020.609610>
- Merz, B., Kreibich, H., Schwarze, R., & Thielen, A. (2010). Review article &quot;assessment of economic flood damage&quot;. *Natural Hazards and Earth System Sciences*, *10*(8), 1697–1724. <https://doi.org/10.5194/nhess-10-1697-2010>
- Nadal, N. C., Zapata, R. E., Pagán, I., López, R., & Agudelo, J. (2010). Building damage due to riverine and coastal floods. *Journal of Water Resources Planning and Management*, *136*(3), 327–336. [https://doi.org/10.1061/\(asce\)wr.1943-5452.0000036](https://doi.org/10.1061/(asce)wr.1943-5452.0000036)
- Nagel, C., Stadler, A., & Kolbe, T. H. (n.d.). CONCEPTUAL requirements for the automatic reconstruction of building information models from uninterpreted 3d models. ..
- Nofal, O. M., van de Lindt, J. W., & Do, T. Q. (2020). Multi-variate and single-variable flood fragility and loss approaches for buildings. *Reliability Engineering & System Safety*, *202*, 106971. <https://doi.org/10.1016/j.res.2020.106971>
- Padilha, V. L., de Oliveira, F. H., Proverbs, D., & Fuchter, S. K. (2019, September). Innovative applications of vr: flash-flood control and monitoring. *2019 IEEE International Symposium on Measurement and Control in Robotics (ISMCR)*. <https://doi.org/10.1109/ismcr47492.2019.8955726>
- Parsapour-moghaddam, P., Rennie, C. D., & Slaney, J. (2018). Hydrodynamic simulation of an irregularly meandering gravel-bed river: comparison of mike 21 fm and delft3d flow models. *E3S Web of Conferences*, *40*, 02004. <https://doi.org/10.1051/e3sconf/20184002004>
- Patel, S., Donkers, S., & Stoter, J. (2013). Automatic generation of citygml lod3 building models from ifc models. ..

Ridder, N., de Vries, H., & Drijfhout, S. (2018). The role of atmospheric rivers in compound events consisting of heavy precipitation and high storm surges along the dutch coast. *Natural Hazards and Earth System Sciences*, 18(12), 3311–3326. <https://doi.org/10.5194/nhess-18-3311-2018>

Santos, V. M., Casas-Prat, M., Poschlod, B., Ragno, E., van den Hurk, B., Hao, Z., Kalmár, T., Zhu, L., & Najafi, H. (2021). Statistical modelling and climate variability of compound surge and precipitation events in a managed water system: a case study in the netherlands. *Hydrology and Earth System Sciences*, 25(6), 3595–3615. <https://doi.org/10.5194/hess-25-3595-2021>

Scawthorn, C., Flores, P., Blais, N., Seligson, H., Tate, E., Chang, S., Mifflin, E., Thomas, W., Murphy, J., Jones, C., & Lawrence, M. (2006). HAZUS-mh flood loss estimation methodology. ii. damage and loss assessment. *Natural Hazards Review*, 7(2), 72–81. [https://doi.org/10.1061/\(asce\)1527-6988\(2006\)7:2\(72\)](https://doi.org/10.1061/(asce)1527-6988(2006)7:2(72))

Sun, H., Zhang, X., Ruan, X., Jiang, H., & Shou, W. (2024). Mapping compound flooding risks for urban resilience in coastal zones: a comprehensive methodological review. *Remote Sensing*, 16(2), 350. <https://doi.org/10.3390/rs16020350>

Svensson, C., & Jones, D. A. (2004a). Dependence between sea surge, river flow and precipitation in south and west britain. *Hydrology and Earth System Sciences*, 8(5), 973–992. <https://doi.org/10.5194/hess-8-973-2004>

Svensson, C., & Jones, D. A. (2004b). Dependence between sea surge, river flow and precipitation in south and west britain. *Hydrology and Earth System Sciences*, 8(5), 973–992. <https://doi.org/10.5194/hess-8-973-2004>

Taramelli, A., Righini, M., Valentini, E., Alfieri, L., Gatti, I., & Gabellani, S. (2022, April 27). *Building-scale flood loss estimation through enhanced vulnerability pattern characterization: application to an urban flood in milano, italy*. Copernicus GmbH. <https://doi.org/10.5194/egusphere-2022-225>

van de Lindt, J. W., Gillis Peacock, W., & Mitrani-Reiser, J. (2018). Community resilience-focused technical investigation of the 2016 lumberton, north carolina flood: .. <https://doi.org/10.6028/nist.sp.1230>

van den Hurk, B., Siegmund, P., & Klein Tank, A. (2016). KNMI'14: climate change scenarios for the 21st century -a netherlands perspective. ..

van den Hurk, B., van Meijgaard, E., de Valk, P., van Heeringen, K.-J., & Gooijer, J. (2015). Analysis of a compounding surge and precipitation event in the netherlands. *Environmental Research Letters*, 10(3), 035001. <https://doi.org/10.1088/1748-9326/10/3/035001>

Vousdoukas, M. I., Mentaschi, L., Voukouvalas, E., Verlaan, M., Jevrejeva, S., Jackson, L. P., & Feyen, L. (2018). Global probabilistic projections of extreme sea levels show intensification of coastal flood hazard. *Nature Communications*, 9(1). <https://doi.org/10.1038/s41467-018-04692-w>

Xia, X., Liang, Q., & Ming, X. (2019). A full-scale fluvial flood modelling framework based on a high-performance integrated hydrodynamic modelling system (hipims). *Advances in Water Resources*, 132, 103392. <https://doi.org/10.1016/j.advwatres.2019.103392>

Xu, K., Wang, C., & Bin, L. (2022). Compound flood models in coastal areas: a review of methods and uncertainty analysis. *Natural Hazards*, 116(1), 469–496. <https://doi.org/10.1007/s11069-022-05683-3>

Zellou, B., & Rahali, H. (2019). Assessment of the joint impact of extreme rainfall and storm surge on the risk of flooding in a coastal area. *Journal of Hydrology*, 569, 647–665. <https://doi.org/10.1016/j.jhydrol.2018.12.028>

Zheng, F., Westra, S., & Sisson, S. A. (2013). Quantifying the dependence between extreme rainfall and storm surge in the coastal zone. *Journal of Hydrology*, 505, 172–187. <https://doi.org/10.1016/j.jhydrol.2013.09.054>

Zhong, M., Xiao, L., Li, X., Mei, Y., Jiang, T., Song, L., & Chen, X. (2024). A study on compound flood prediction and inundation simulation under future scenarios in a coastal city. *Journal of Hydrology*, 628, 130475. <https://doi.org/10.1016/j.jhydrol.2023.130475>

Zhu, J., Wang, X., Wang, P., Wu, Z., & Kim, M. J. (2019). Integration of bim and gis: geometry from ifc to shapefile using open-source technology. *Automation in Construction*, 102, 105–119. <https://doi.org/10.1016/j.autcon.2019.02.014>

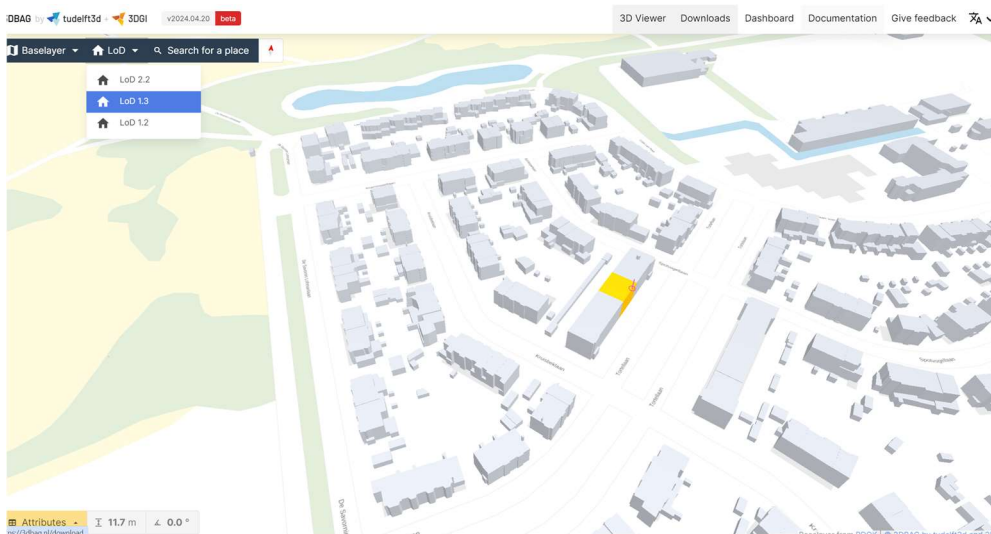
## 8 Appendix

### Visualization process

#### Import 3D BAG to ArcGIS Pro

Due to 1) need to edit and delete individual buildings in 3D BAG 2) don't need a very high precision LoD model as only footprints of surrounding buildings are needed. So manually add OBJ models downloaded from 3D BAG website.

- (1) Find my site on 3D BAG website and select LoD 1.3 (a)
- (2) Pick a tile from the grid and download the OBJ zip file (b)
- (3) Open the OBJ in blender and delete the original building on the site (c)
- (4) Load the modified OBJ model in ArcGIS Pro. (d)



(a)

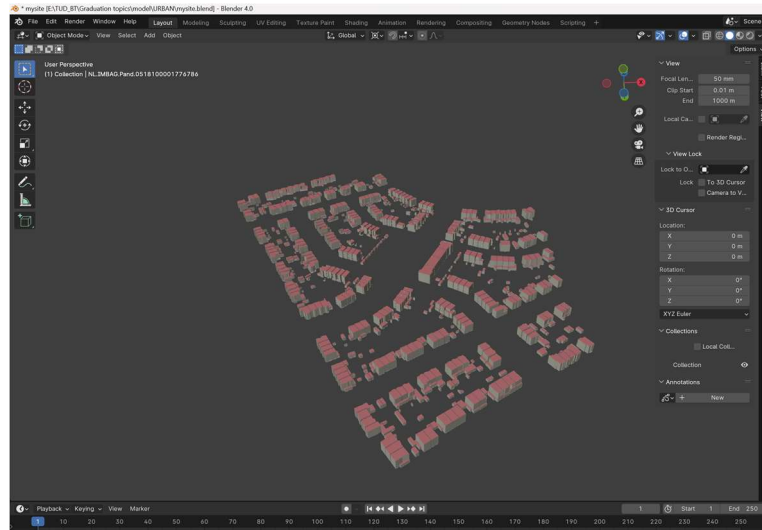
#### Downloads for tile number 9-248-588

To keep filesizes manageable the 3DBAG dataset is subdivided in tiles. For each tile we offer the data in a number of different file formats. Use the button below to select the tile of interest to see the download options.

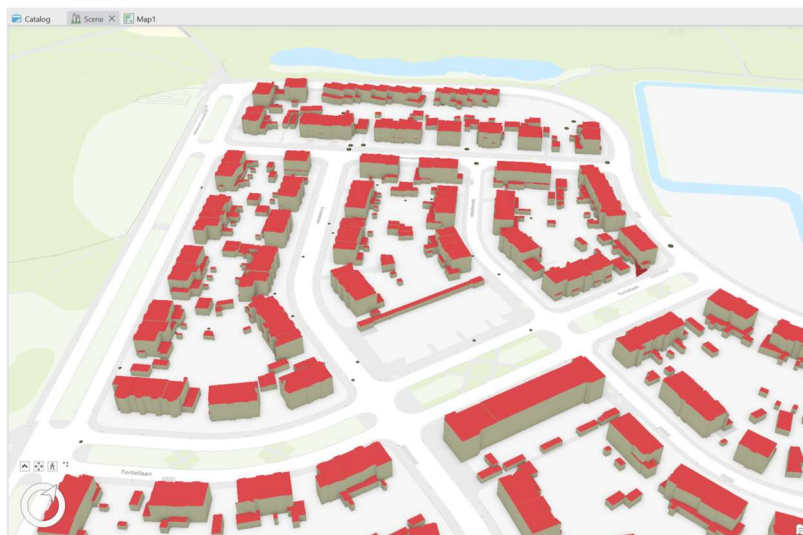
Tile number	Format	File	SHA-256	Version
9-248-588	CityJSON	<a href="#">9-248-588.city.json</a>	eb62745d2a245cbe6c3d6d6e80713ffc3975433add7f070211dce168881fe75	v2024.04.20
9-248-588	OBJ	<a href="#">9-248-588.obj.zip</a>	95b5da23bb4835cd2f8274140f3bf2581b296b3641577d04fedb3340a108c766	v2024.04.20
9-248-588	GPKG	<a href="#">9-248-588.gpkg</a>	dbdc51feb3ab301bd90489f593d16b4c36181a85724a51f31d2b52a9d4455f93	v2024.04.20

[Pick another tile](#)

(b)



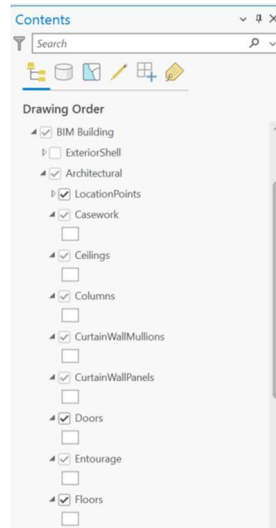
(c)



(d)

### Read and add Revit.rvt (BIM) projects to ArcGIS Pro

- (1) In the Catalog pane, right-click Folders and click Add Folder Connection
- (2) In the Navigation Pane, under Project, expand Folders and Importing-Content. Click the Data\_Files folder and select the Revit folder.
- (3) In the Catalog pane, expand the folder , Revit , and BIM Building .rvt .
- (4) The entire BIM Building .rvt project can be used directly as a data source without conversion.



### Georeferencing a Revit.rvt (BIM) model

Because the model does not yet have a coordinate system defined, it is displayed at the origin of the map's coordinate system, which is a location off the west coast of Africa. A coordinate system is needed for the layer and georeference it to the correct location.

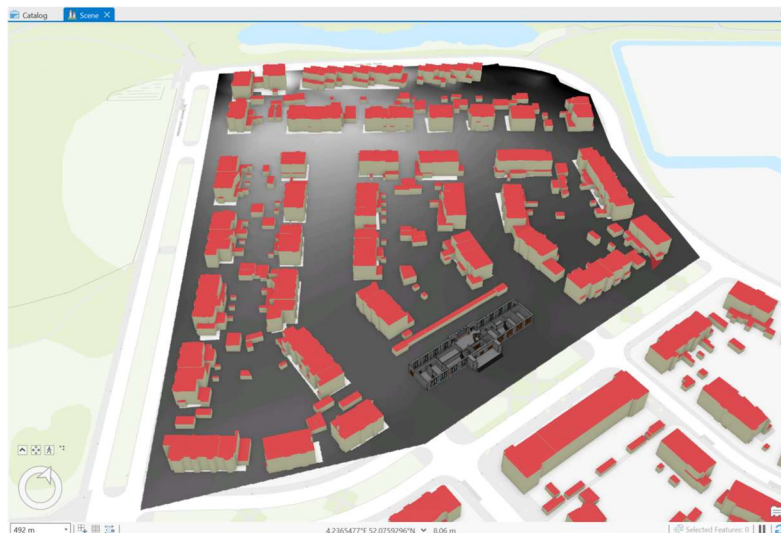
- (1) In the Contents pane, right-click BIM Building and click Zoom To Layer .
- (2) Move the building to the ideal location.
- (3) On the ribbon, click the BIM Data tab. In the Alignment group, click Georeference .
- (4) Elevate To Ground. To elevate the selected feature layer on top of the scene's elevation surface based on the location of an anchor point.
- (5) When the building reappears in its new location, click the Close Georeferencing button to exit the georeferencing process.

### Import Raster map to ArcGIS Pro

- (1) In ArcCatalog or the Catalog window, right-click the geodatabase and click Import > Raster Dataset .
- (2) Select the raster datasets from HEC RAS to import and click Add .
- (3) Since my dataset has already been specified. It shows like this.



Now that the BIM, 3D BAG, and raster maps have been loaded into the original model, they can be spatially analyzed to get the water depth corresponding to each component.



Get point from raster map:

#### Raster to point:

- For each cell of the input raster dataset, a point will be created in the output feature class. The points will be positioned at the centers of cells that they represent. The NoData cells will not be transformed into points. (Table 18)
- The input raster can have any cell size and may be any valid raster dataset.
- The Field parameter allows you to choose which attribute field of the input raster dataset will become an attribute in the output feature class. If a field is not specified, the cell values of the input raster (the VALUE field) will become a column with the heading Grid\_code in the attribute table of the output feature class. (Table 18)

Label	Explanation	Data Type
Input raster	The input raster dataset.  The raster can be integer or floating-point type.	Raster Layer
Output point features	The output feature class that will contain the converted points.	Feature Class
Field (Optional)	The field to assign values from the cells in the input raster to the points in the output dataset.  It can be an integer, floating point, or string field.	Field

Table 18



**Extract values to Points:**

Extracts the cell values of a raster based on a set of point features and records the values in the attribute table of an output feature class. In other words the raster's bathymetry data is given to the raster's center point

**Geoprocessing**

Extract Values to Points

The Extract Multi Values to Points tool provides enhanced functionality or performance.

**Parameters** Environments

Input point features  
Raster\_Depth\_1

Input raster  
:pth (Max)PRECIPITATION.Terrain (2).11.tif

Output point features  
Extract\_RasterT1

Interpolate values at the point locations

Append all the input raster attributes to the output point features

OBJECTID *	Shape *	pointid	grid_code	RASTERVALU
1	Point	451781	0.68259	0.68259
2	Point	451782	0.684684	0.684684
3	Point	451783	0.686781	0.686781
4	Point	451784	0.688879	0.688879
5	Point	451785	0.69098	0.69098
6	Point	451786	0.693086	0.693086
7	Point	451787	0.695193	0.695193
8	Point	451788	0.697304	0.697304

This screenshot shows that the water depth value is given to the Extract\_RasterT1 files. In the end, the point with depth is generated.

Get point from building feature:

**Feature to point:**

Creates a feature class containing points generated from the centroids of the input features or placed within the input features. In my case, I entered three components of three different materials into the function and obtained the location points for each of the three components. Figure presents an example of windows.

**POLYGON INPUT**

**OUTPUT**

**Geoprocessing**

Feature To Point

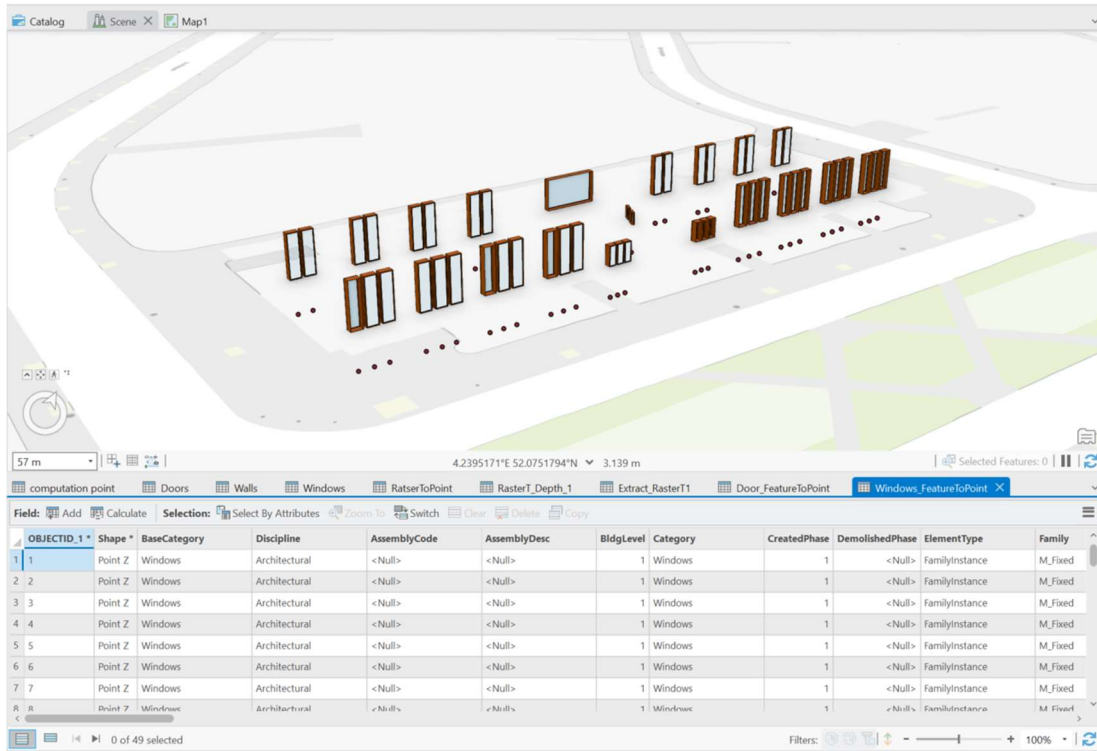
No pending edits.

**Parameters** Environments

Input Features  
Doors

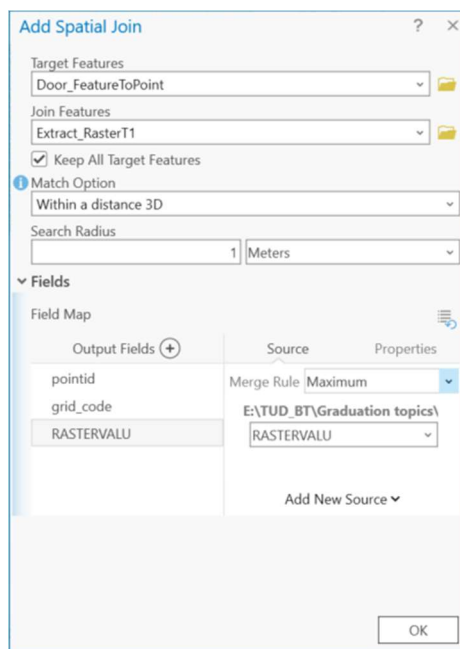
Output Feature Class  
Doors\_FeatureToPoint

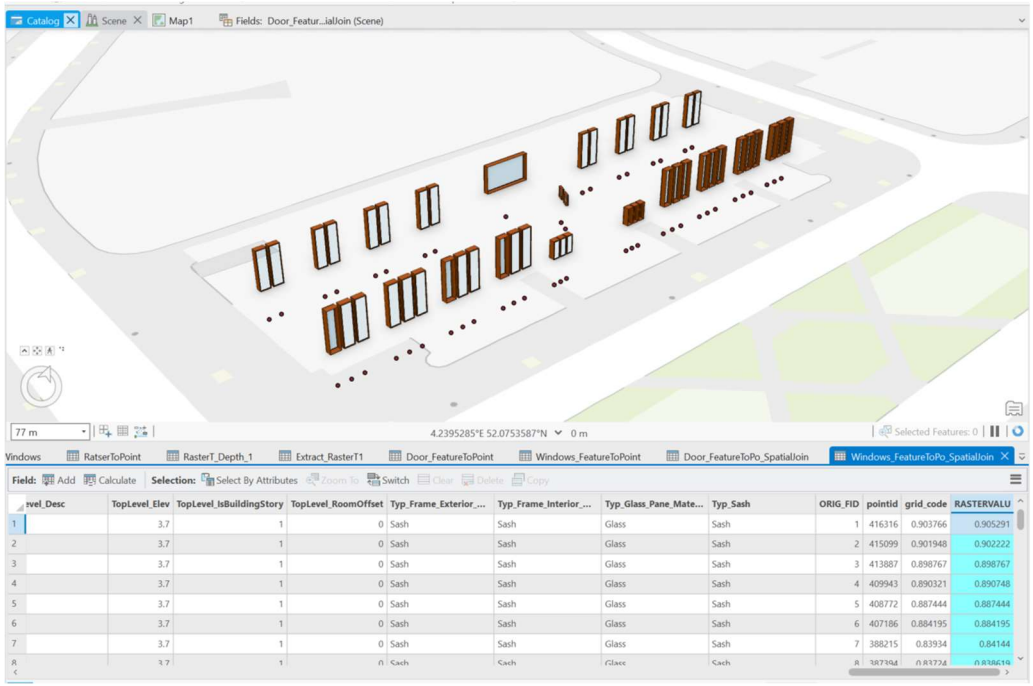
Inside



### Spatial join:

Spatial aggregation is a method of adding attribute data from connected element points to a target point. Here, my goal is to add information about water depth within the raster data to nearby window location points. The search method is changed to a 3D search with a radius of one meter and the attribute to be added is the water depth. Since it may involve a window location searching for more than one raster point, the value of maximum water depth is used to assign to the window point. Finally, window points with water depth data were obtained.





Colour coding for DS:

**Symbology:**

Based on the water depth parameter, each window point is assigned a color symbol. By setting the range for each color (according to the DS evaluation criteria shown in Table 19), color-coded window points can be obtained. It is important to note that due to the height of the windows, the immersion depth equals the water depth minus the height of the window from the ground. Here, since the window heights from the ground are consistent, we can directly apply the DS criteria. However, for buildings with windows at varying heights, the height must be subtracted before evaluation.

